https://ntrs.nasa.gov/search.jsp?R=19670030927 2020-03-16T16:47:53+00:00Z

**HONEYWELL DOCUMENT 12513-FR3-I**

# RESEARCH ON COMPUTATIONAL AND DISPLAY REQUIREMENTS FOR HUMAN CONTROL OF SPACE VEHICLE BOOSTERS

## Part I: THEORY AND RESULTS

**August 1967**

**GPO PRICE $**

**CFSTI PRICE(S) $**

**Hard copy (HC)** 3.00

**Microfiche (MF)** .65

ff 653 July 65

N67-40256 (ACCESSION NUMBER)

(THRU)

10 135 RS 22-25 (PAGES)

1 (CODE)

CR#89606 (NASA CR OR TMX OR AD NUMBER)

05 (CATEGORY)

FACILITY FORM 602

**HONEYWELL SYSTEMS & RESEARCH DIVISION**

12513-FR3-I August 1967

# PHASE III FINAL REPORT

# RESEARCH ON COMPUTATIONAL AND DISPLAY REQUIREMENTS FOR HUMAN CONTROL OF SPACE VEHICLE BOOSTERS

## PART I: THEORY AND RESULTS

Advanced Studies Office
Astrionics Laboratory
George C. Marshall Space Flight Center
National Aeronautics and Space Administration

Contract ~~No.~~ NAS 8-20023

Approved by: JD Gilchrist
J. D. Gilchrist
Project Engineer

Approved by: J.R. Post
J. R. Post
Systems Technology
Manager

Honeywell Inc.
Systems and Research Center:
Minneapolis, Minnesota

# FOREWORD

This is the final report on the third phase of a study on man-computer boost guidance techniques. The research wag sponsored by the Advanced Systems Office, Astrionics Laboratory, Marshall Space Flight Center, under Contract No. NAS **8-20023.** The research was performed by the Systems and Research Division of Honeywell Inc. at facilities in Minneapolis, Minnesota. Mr. J, F. Pavlick of MSFC was the contract monitor for the study. Project personnel were Dr. J. D. Gilchrist, principal investigator, P. A. Anderson, and W. J. Eckart. The report covers work extending from 1 March 1967 to 31 August 1967.

The report is in two parts. Part I, prepared by J. D. Gilchrist and P. A. Anderson, includes the theory, results of computer experiments, and conclusions. Part II provides descriptions, listings, and flow diagrams of computer programs developed during the study and was prepared by W. J. Eckart.

## CONTENTS

Page

SECTION 1 INTRODUCTION 1

1.1 Statement of the Problem 1
1.2 Background 2
1.3 Objectives 3

SECTION 2 SUMMARY, CONCLUSIONS, AND RECOMMENDATIONS 7

2.1 Phase I 7
2.2 Phase II 15
2.3 Phase III 20

SECTION 3 ACCOMPLISHMENTS AND RESULTS 27

3.1 General 27
3.2 ROT Guidance Techniques and Displays 28
  3.2.1 First-Stage Guidance -- Nominal Trajectory 28
  3.2.2 Second-Stage Guidance -- Predictive Model Guidance Scheme 29
3.3 Mathematical Model 33
  3.3.1 Target Orbit 34
  3.3.2 Lateral Guidance and Guidance Plane Geometry 35
  3.3.3 Fast-Time Model 37
3.4 Operator Work-Load Measurement and Display Evaluation 41
  3.4.1 Description of Operator Work-Load Measurement 41
  3.4.2 Operator Work Load - Subsidiary Task 44
  3.4.3 Operator Work Load - Loading Task 56
  3.4.4 Conclusions 61
3.5 Computer Requirements 62
  3.5.1 ROT Guidance and Navigation Computations 63
  3.5.2 Models for the PMGS 66
  3.5.3 Computer Mechanization of Equations 72

CONTENTS (Continued)

| | | Page |
|---|---|---|
| | 3.5.4 Results and Conclusions | 73 |
| | 3.6 Display Requirements | 79 |
| | 3.6.1 Display Format and Size | 80 |
| | 3.6.2 Computation Requirements | 81 |
| | 3.6.3 CRT and Electroluminescent (EL) Displays | 82 |
| SECTION 4 | MANUAL OPTIMAL GUIDANCE SCHEME - SUMMARY | 88 |
| | 4.1 Description | 88 |
| | 4.2 Computation Requirements | 91 |
| | 4.3 Display Requirements | 93 |
| | 4.4 Navigation Requirements | 93 |
| SECTION 5 | RECOMMENDATIONS FOR FUTURE WORK | 95 |
| | 5.1 Future Studies | 95 |
| | 5.2 Future Hardware Development | 96' |
| REFERENCES | | 97 |
| APPENDIX A | ROT REAL-TIME MATHEMATICAL MODEL AND DATA SUMMARY | |
| APPENDIX B | TAP-LIGHT BOX DESCRIPTION | |
| APPENDIX C | BIT BOX DESCRIPTION | |

# ILLUSTRATIONS

| Figure | | Page |
|---|---|---|
| 1-1 | Man-Computer Display Simulation System | 6 |
| 2-1 | Block Diagram of Indirect Method, Manual Iteration | 10 |
| 2-2 | Block Diagram of Simplified Direct Method, Manual Iteration | 11 |
| 2-3 | Elements of Optimal Atmospheric Path | 13 |
| 2-4 | Rating Summary of Manual and Automatic Guidance Schemes | 25 |
| 3-1 | Altitude-versus-Velocity Display Format | 30 |
| 3-2 | Altitude-versus-Flight-Path-Angle Display Format | 30 |
| 3-3 | Altitude-versus-Altitude-Rate Display Format | 30 |
| 3-4 | Guidance Plane Geometry | 32 |
| 3-5 | Fast-Time Coordinate System | 38 |
| 3-6 | Methods for Measuring Informational Work Load | 41 |
| 3-7 | Tap-Light Display | 45 |
| 3-8 | Operator Work Load versus Time -- Automatic Lateral Guidance | 47 |
| 3-9 | Operator Work Load versus Time -- Manual Lateral Guidance | 47 |
| 3-10 | Lateral Control versus Time | 48 |
| 3-11 | Pitch Attitude versus Time | 48 |
| 3-12 | Subsidiary Task Work Load versus Time -h-versus-V Display | 51 |
| 3-13 | Subsidiary Task Work Load versus Time -h-versus-h Display | 51 |
| 3-14 | Subsidiary Task Work Load versus Time -h-versus-y Display | 52 |
| 3-15 | Operator Response Bias | 57 |
| 3-16 | Subsidiary Task Work Load versus Time - h-versus-V Display, Accurate Model | 57 |
| 3-17 | Operator Work Load, Loading Task - h-versus-V Display | 59 |
| 3-18 | Operator Work Load, Loading Task - h-versus-h Display | 59 |
| 3-19 | Operator Work Load, Loading Task - h-versus-y Display | 60 |

3-20 Second-Stage Navigation and Guidance Block Diagram 67

3-21 Predicted Terminal Flight-Path Angle Error versus Number of Integration Steps 74

3-22 Predicted Terminal Altitude Error versus Number of Integration Steps 75

3-23 Basic CRT Block Diagram 86

3-24 EL Flight Model Block Diagram 87

4-1 Nominal Guidance Scheme Block Diagram 89

4-2 Predictive Model Guidance Scheme Block Diagram 90

## TABLES

| Table | | Page |
|---|---|---|
| 2-1 | Comparison of Methods for Predicting Trajectories | 8 |
| 2-2 | Comparison of the Nominal and Predictive Model Guidance Schemes | 19 |
| 2-3 | Comparison of Manual and Automatic Guidance Schemes | 24 |
| 3-1 | Comparison of Work Load and Display | 53 |
| 3-2 | Performance Summary - Subsidiary Task Method | 55 |
| 3-3 | Summary of PMGS Computer Requirements (ALERT Characteristics) | 71 |
| 3-4 | Computer Requirements by Function | 77 |
| 3-5 | Total System Computer Requirements by Guidance Scheme | 77 |
| 3-6 | Projected Avionic Display Technology | 84 |
| 3-7 | Comparison of CRT and EL Displays | 85 |

# ABBREVIATIONS

| | |
|---|---|
| CRT | Cathode Ray Tube |
| EL | Electroluminescent |
| PI | Performance Index |
| PMGS | Predictive Model Guidance Scheme |
| ROT | Reusable Orbital Transport |
| NGS | Nominal Guidance Scheme |
| IGS | Iterative Guidance Scheme |
| ms | millisecond |

# SYMBOLS

| | |
|---|---|
| A, B | Optimization parameters |
| a | Speed of sound |
| $C_{1,2}$ | Exhaust velocities |
| $C_{D_o}$ | Drag Coefficient at $\alpha = 0$ |
| $C_L$ | Lift curve slope |
| D | Drag |
| g | Gravity acceleration |
| $g_o$ | Gravity acceleration at sea level |
| $g_{x,z}$ | Gravity components for predictive model |
| h | Altitude |
| $h_e$ | Predicted altitude error |
| $h_P$ | Predicted altitude |
| i | Orbital inclination |
| K | Induced drag coefficient ($K = 1 \text{ rad}^{-1}$) |
| $K_Y$<br>$K_{\dot{Y}}$ | Lateral guidance law gains |
| L | Lift |
| M | Mach number |
| m | Mass |

## SYMBOLS (Continued)

| | |
|---|---|
| $m_0$ | Initial first-stage mass |
| $m_2$ | Initial second-stage mass |
| $Q_1$ | Coordinate transformation - earth-fixed to local horizon |
| Q2 | Coordinate transformation - local horizon to wind axis |
| $r$ | Radial distance from earth's center = $r_o + h$ |
| $r_0$ | Mean radius of earth |
| S | Vehicle reference area |
| T | Thrust |
| t | Time |
| V | Velocity |
| | Inertial velocity |
| $V_P$ | Predicted inertial velocity |
| $V_X, V_Z$ | Predictive model velocity components |
| $X_I', Y_I', Z_I'$ | Inertial positions |
| $X_I Y_I Z_I$ | Inertial positions defining the guidance plane |
| x, z | Predictive model position components |
| $\alpha$ | Angle of attack |
| $\delta_Y$ | Yaw steering engine gimbal angle |
| $\gamma$ | Flight-path angle (between V and local horizon) |
| $\gamma_{e,P}$ | Predicted inertial flight-path angle |

## SYMBOLS (Continued)

| | |
|---|---|
| $\gamma_I$ | Inertial flight path (between $V_I$ and local horizon) |
| $\theta_L$ | Pitch attitude |
| $e$ | Longitude |
| $\phi$ | Latitude |
| $\sigma$ | Bank angle |
| $\rho$ | Air density |
| $\rho_o$ | Air density at sea level |
| $\Psi$ | Heading angle or azimuth (between North and horizontal component of V) |
| $\Psi_I$ | Inertial heading angle or azimuth (between North and horizontal component of $V_I$) |
| $\omega_e$ | Earth's rotation rate (. 7291 x $10^{-4}$ rad/sec) |
| $\chi$ | Thrust attitude angle for fast-time model |
| P | In-plane range angle |
| $\beta_{1,2}$ | Mass flow rates |
| $\lambda$ | Scale height |
| v | Inertial longitude ($\theta_L + \omega_e t$) |
| $\tau$ | Prediction time to quickening symbol |
| At | Integration step size |
| $\mu$ | Gravitational constant ($g_o r_o^2$) |

# SECTION 1
# INTRODUCTION

This section includes a general statement of the problem, some background on the objectives and results of the two previous related phases of study (Refs. 8 and 3), and finally an outline of the objectives of the Phase III study.

Phase III is the final phase of a study effort whose goal is the development of minimum computation and display requirements which will allow full utilization of the capabilities of a human pilot to guide a launch vehicle during the ascent phase.

## 1.1 STATEMENT OF THE PROBLEM

[illegible]

The general problem considered in this study i~~s~~ the development of the minimum computational and display requirements which will allow the full utilization of a human pilot's capabilities to perform the boost guidance function in an efficient and near-optimal manner.

Previous investigations (e.g. , Refs. 9 and 10), have been conducted to define pilot ability to control vehicle attitude about a nominal trajectory. Steering the vehicle back to the nominal after large deviations, however, may not always be the most efficient or optimum way of guiding the vehicle to the desired target conditions.

Present implementations of automatic guidance schemes involve complex equations or complex iteration procedures to arrive at guidance commands which generate optimal trajectories. Generally, the result is that only the nominal trajectory is programmed in the vehicle computer. Deviations from the nominal trajectory can result from sensor or processing electronics failures, data noise, and mechanical failures. Redundant components, adaptive guidance schemes, and adaptive self-optimizing control systems are some of the measures used in automatic guidance and control systems to ensure fulfillment of mission objectives, but these have corresponding penalties in system weight, cost and complexity.

The possibility of manned launch vehicles with significant aerodynamic capabilities opens the question of the desirable division of navigation, guidance and control functions between the flight crew and automatic systems. A vital part of the answer depends on the information which defines the degree to which automatic equipment can be simplified by the inclusion of man in the guidance and control loop and still accomplish these functions in a near optimal manner. Information is required for manual optimal guidance schemes which determines the interrelationship of the computational and display requirements with pilot task loading.

## i.2 BACKGROUND

This third and final phase of the study to determine the minimum computational and display requirements for near-optimal guidance of an aerodynamic launch vehicle by a human pilot is based on results of the two previous phases (Refs. 8 and 3). The study vehicle used in all three phases of study is the Reusable Orbital Transport (ROT), a two-stage vehicle which uses a horizontal takeoff and develops considerable aerodynamic lift in the first stage. See section **3.** 3 for a complete description of the study vehicle.

The first phase (Ref. 8) was concerned with the determination of the boost-phase fuel-optimal guidance function. In that phase, various trajectory optimization methods were studied, with particular emphasis placed on the simplification of these methods by the use of man in the iterative computation loop. The results of that phase indicated that the optimization method based on results from the calculus of variations could be used in a manual optimal guidance scheme. A preliminary system, the Predictive Model Guidance Scheme, was defined, stating propcsed displays, computing method, and man's role in the proposed system.

The Predictive Model Guidance Scheme (PMGS) was the subject of the second phase (Ref. 3). The objective of the second phase of study was to provide analyses and simulation to further define the applicability and capability of manual determination of an optimal flight path for a launch vehicle. In the second phase, the pilot's role and the displays required for efficient implementation of the PMGS were determined. A manual Nominal Guidance Scheme (NGS) was also developed to be used as a basis for comparing the PMGS. The final outcome of the second phase was the definition of a manual guidance scheme for both stages of the boost phase which gave good injection accuracy, low pilot work load, minimum fuel requirements, mission flexibility, and minimum computational and display requirements.

## 1.3 OBJECTIVES

The main objective of Phase III of the study was to provide analyses which further determined the applicability and capability of manual determination and control of an optimal flight path for the study vehicle (ROT). In detail, the objectives were to:

(1) Extend the previously developed vehicle two-dimensional simulation model of the point-mass motion to the three-dimensional case. The two earlier phases used a two-dimensional simulation model.

(2) Incorporate the selected nominal and predictive guidance schemes in this three-dimensional simulation. The second phase recommended using the nominal guidance scheme during first stage and the predictive model scheme during second stage. These two schemes, developed for the planar case, were to be extended to the three-dimensional case.

(3) Define the required displays for each guidance scheme. The final display formats were to be chosen on the basis of:

  (a) Minimizing operator task loading

  (b) Optimizing total guidance system performance in terms of minimizing fuel requirements and orbit injection errors

  (c) Minimizing system hardware complexity

(4) Measure operator workload using two types of concomitant tasks, loading and subsidiary. The loading task is force paced and is primary to the guidance task. The subsidiary task is self-paced and is secondary to the guidance task. These two measurements must be made with a man-in-the-loop simulation. The results are to be used to evaluate display formats as well as to establish the reserve capacity of the operator while performing the guidance function.

(5) Evaluate different mathematical models for the predictive guidance scheme and choose one model on the basis of minimizing the computer requirements and operator work load.

(6) Analyze the tradeoff factors for each guidance scheme. Emphasis was placed on minimizing the computer requirements and operator task loading. From the results of Phase II, the predictive model scheme is more accurate and yields a lower operator work load than the nominal guidance scheme. The computation requirements, however, are higher than for the nominal scheme,

(7) Select and recommend a single manual optimal guidance scheme incorporating a minimum of computation and display requirements. Specify the guidance scheme in terms of:

   (a) Computational requirements

   (b) Display requirements

   (c) Navigational requirements

**(8)** Recommend new hardware development programs, if any, required for efficient implementation of the recommended manual guidance scheme.

(9) Recommend further studies needed on the basis of the results of the present study,

A real-time man-computer-display simulation of the guidance schemes was required in this study to fulfill the study objectives. A hybrid computing facility was used; the simulation of the point-mass vehicle dynamics was performed on the digital computer due to the nonlinearity of the equations and the large range of the variables. Manual control of the vehicle simulation was achieved with the analog computer. Figure 1-1 shows the. simulation facility.

To facilitate future statistical analysis of the results obtained in this study, the data from 120 runs were recorded on magnetic tape. This represents a total of approximately 12 hours of man-in-the-loop hybrid simulation.

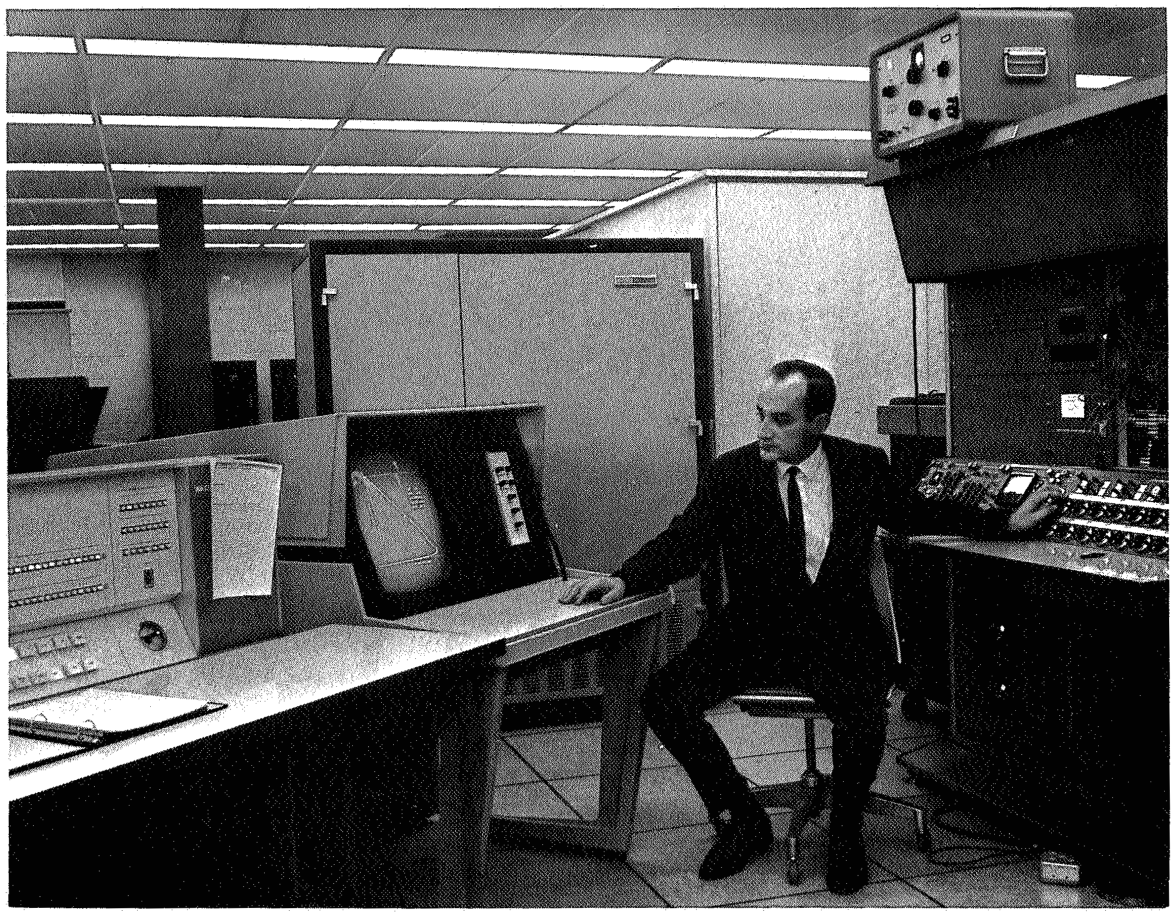

Figure 1-1. Man-Computer Display Simulation System

# SECTION 2
# SUMMARY, CONCLUSIONS, AND RECOMMENDATIONS

To provide sufficient background on the total study, this section includes a summary, conclusions and recommendations of the two previous phases as well as of Phase III. Thus, the objectives and results of the over-all study are presented here.

## 2.1 PHASE I

The approach followed in the first phase (Ref. 8) was to take existing trajectory optimization methods, define displays which would permit man to participate effectively in the computation loop, and evaluate the relative performance of each method by numerical experiment. The existing optimization techniques studied were: (1) the indirect method and (2) the direct method. The use of these terms is by no means universal; however, the distinguishing characteristics of each, as well as other approaches studied, are presented in Table **2-1.**

The indirect method consists of using theory from the calculus of variations to convert the original problem of finding a fuel-optimal steering angle to the two-point boundary value problem. The two-point boundary value problem consists of finding initial conditions (optimization parameters) on the adjoint or auxiliary variables so that the desired terminal conditions on the trajectory are satisfied., The direct method attacks the problem of finding the optimal steering angle directly. An initial guess is made for the steering-angle time history, and this initial guess is then modified in an iterative fashion until the optimal steering-angle time history is determined.

# Table 2-1. Comparison of Methods for Predicting Trajectories

Guidelines for Study:

- Guidance scheme capable of handling large parameter variations and large disturbances
- Attempt a fuel-optimal scheme
- Use man's capabilities

Imply a man-computer-display system preferably not using perturbation type guidance schemes

| Properties | Method | | | |
|---|---|---|---|---|
| | Indirect | Direct | Simplified Direct | Simplified Indirect |
| Iteration required to obtain solution | Yes | Yes | Yes | No |
| Relative complexity of computations | Low | Medium | LOW | LOW |
| Characteristic Feature | TPBV problem | Steepest descent | Can specify control function using various types of parameters | Combination of two simpler problems |
| Quantity to choose | Initial conditions on auxiliary variables | Control function | Parameters describing control function | Choose attitude as su gested by solution to two simplf problems |
| Relative storage requirement | Low | High | None | Low |
| Man's task in iteration | Choose I.C. on auxiliary variables | Choose step size | Choose parameters for control function | Non-iterative |
| Undesirable features | jectory to small perturbations in auxiliary variable initial conditions | at the minimum | Does not generate an optimal trajectory | Based on knowledge of nominal trajectory |
| Desirable features | Relative simplicity | Judgment and prior knowledge can be used to best advantage | e Judgment and prior knowledge can be used to best advantage<br>■ Man's task becomes easier as flight time increases | Relative simplicity |
| Optimum trajectory | Yes | Yes | NO | Near optimal for optimal and small disturbances |
| Does method lend itself to a closed-loop predictive guidance scheme" | Yes | No (too complicated) | Yes | Closed-loop non-predictive |
| Studied during research program? | Yes | Yes | Yes | Yes |
| Information requirements | Vehicle state variables, V, h, $\gamma$ | Target errors | Angle of attack, state variables V. h,$\gamma$ | Vehicle state variables V,h,$\gamma$ |
| Can method handle acceleration constraints? | Yes | Yes | Yes | Yes |

To implement the indirect method for manual iteration, it was found that a two-dimensional display of altitude versus velocity for the trial solution was adequate, although the addition of flight-path angle was helpful when the solution approached orbit injection conditions. This is because flight-path angle must be zero at injection. This was based on results obtained for a planar model. Figure 2-1 shows the manual iteration procedure for the indirect method. The most difficult task is finding an initial guess for the two optimization parameters which results in a physically realistic trajectory. Once this occurs, however, manual iteration presents no difficulties. In this process, it appears that man uses the characteristic shape of the optimal trajectory to aid in his guesses, rather than just the error at the cutoff condition.

Therefore, a display of the entire predicted trajectory conveys more information than does the terminal error alone. Further investigation involving man in a real-time simulation was needed,

Implementation of the direct method required no displays since the steepest-descent technique is essentially automatic, Man's task consists of varying the size of the step in the descent procedure to avoid oscillations of the solution about the minimum. This task was found to be difficult near the minimum point (the guidance function which minimizes the cost function) because of a mathematical singularity at the minimum, For this reason, the direct method using steepest descent was eliminated from consideration for an onboard manual guidance scheme.

Because of the problems with the steepest-descent direct method, a simplified direct method was devised. It was assumed that the control function could be presented in time by a succession of straight lines. For example, if vehicle attitude is the control variable, the linear segments represent flight at different constant-attitude rates. The "corners" of these control functions can be adjusted by man to hit the target (see Figure 2-2). Although this method

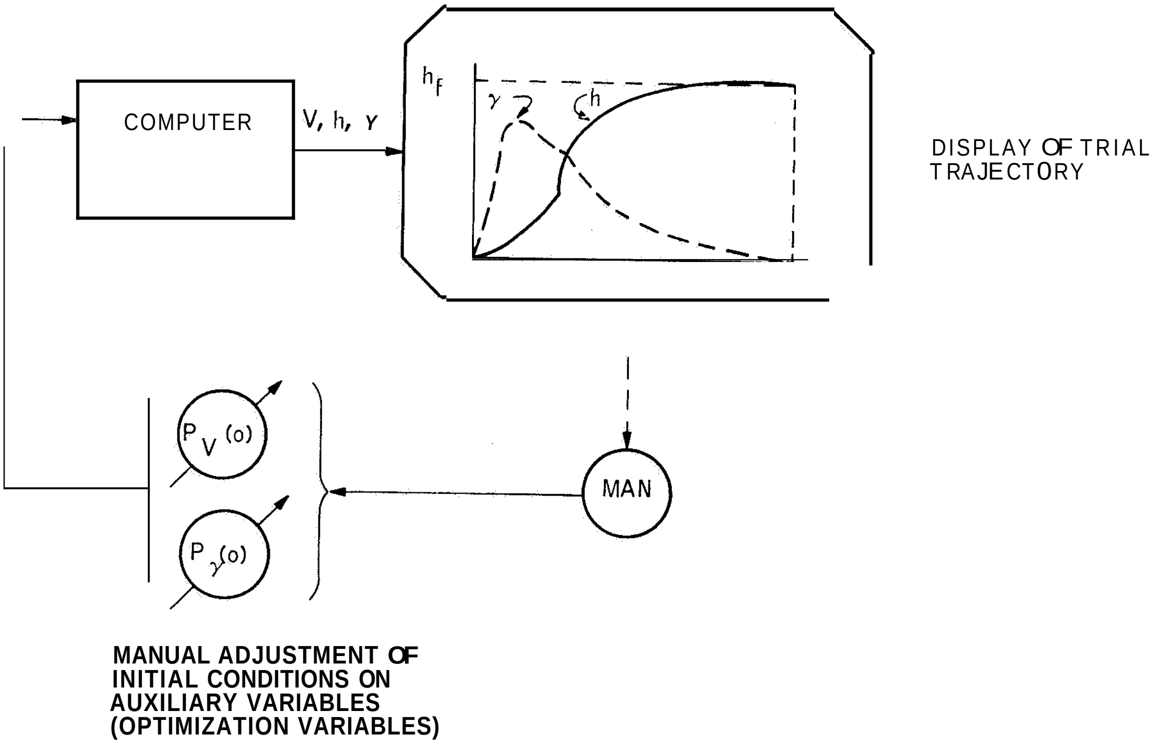
COMPUTER
V, h, γ
$h_f$
γ
h
DISPLAY OF TRIAL TRAJECTORY
$P_V(o)$
$P_\gamma(o)$
MAN
MANUAL ADJUSTMENT OF INITIAL CONDITIONS ON AUXILIARY VARIABLES (OPTIMIZATION VARIABLES)

Figure 2-1. Block Diagram of Indirect Method, Manual Iteration

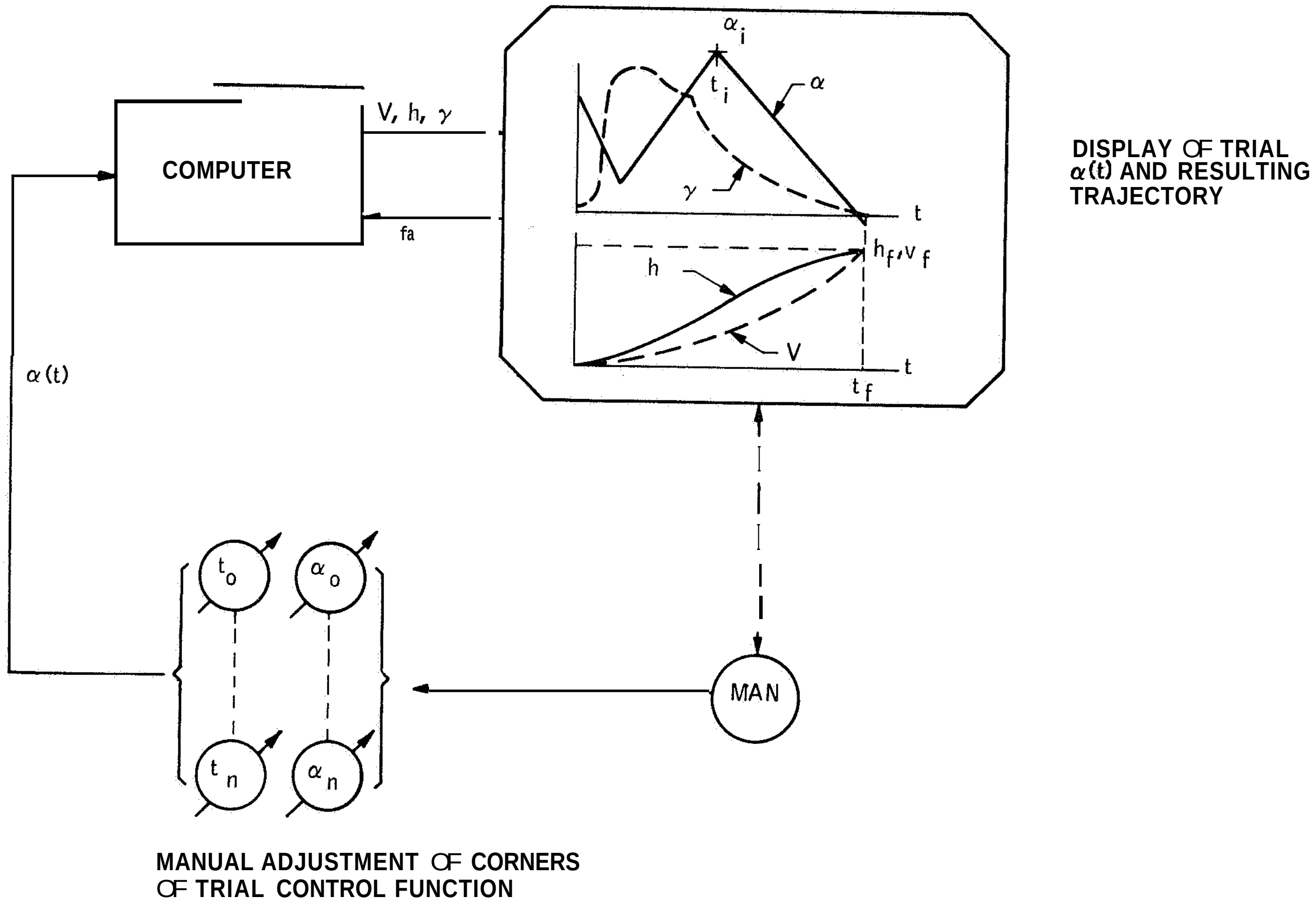
COMPUTER
V, h, γ
fa
α(t)
$\alpha_i$
$t_i$
α
γ
t
$h_f, V_f$
h
V
t
$t_f$
DISPLAY OF TRIAL
α(t) AND RESULTING
TRAJECTORY
MAN
$t_o$
$\alpha_o$
$t_n$
$\alpha_n$
MANUAL ADJUSTMENT OF CORNERS
OF TRIAL CONTROL FUNCTION

Figure 2-2. Block Diagram of Simplified Direct Method, Manual Iteration

is not strictly optimal, by proper choice of the number of corners, near-optimum performance can be achieved. For example, in an experiment using an angle-of-attack steering program consisting of three straight-line segments, the resulting penalty in vehicle weight at second-stage cutoff was 1.5 percent.

The approximation to the continuous optimal control, and hence the performance, improves with the number of corners, but man's ability to make corrections degrades as the number of variables to adjust increases. Thus, there is a tradeoff between performance and the complexity of the manual task. This appears to be a feasible approach for manual guidance, but further investigation was required.

Analytical investigations of the atmospheric portion of the optimal solution resulted in these conclusions:

- The major portion of the optimal path in the atmosphere consists of a "basic" path, uniquely defined in the altitude-velocity plane, with thrust as a parameter, This path is independent of initial conditions, the remaining portion of the trajectory being a transition path to put the vehicle on this path after takeoff (see Figure **2-3).**

- The transition path of "climbout" should be as low as possible, consistent with a smooth transition to the basic h-versus-V path, to achieve maximum vehicle performance.

- The basic atmospheric path, in addition to being a minimum-time trajectory also maximizes the power excess (available power minus power required to offset drag) for constant value of the energy height.

$$h_e = h + \frac{V^2}{2g}$$

- The control required to keep the vehicle on the basic path can easily be calculated. The control required to perform the transition needed further study.

- The attitude of the vehicle for the basic path is very nearly constant.

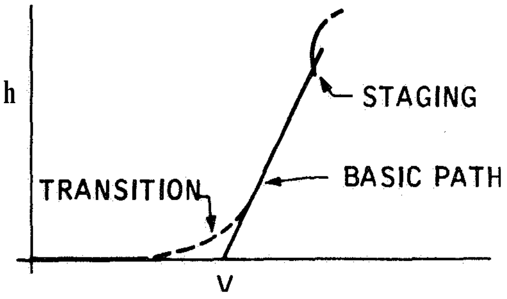

Figure 2-3. Elements of Optimal Atmospheric Path

A perturbation model was defined for the ROT vehicle, and sensitivity of the optimal-control and trajectory to the perturbations was determined to aid in eventually defining computer and display requirements. The results of the sensitivity study show that the deviation from the nominal due to perturbations is minor, particularly in the first stage. Consequently, it was recommended that some consideration be given to manual guidance about a nominal in the first stage. Other studies have investigated such a scheme only for non-atmospheric flight and with only moderate success (Refs 9 and 10). Based on the results of those studies, as well as this one, the primary consideration in the second stage should be accuracy, with little performance loss occurring for suboptimal schemes, whereas payload appears more critically affected by the first-stage guidance.

From the results of the first phase of this study, the following conclusions were made regarding onboard manual guidance concepts:

- Between the direct steepest-descent and indirect optimization methods, the indirect method is the most promising as the basis of a closed-loop scheme since the steepest-descent method requires a larger computer than the indirect method and does not converge well in the vicinity of the optimum trajectory. In the closed-loop scheme, two parameters are continually updated from a display of a faster-than-real-time prediction of the trajectory,,
- For man to be effective in this closed-loop scheme, the time interval between predictions must be fairly small, on the order of 1 second, This can be achieved with a simpler model, but performance will then be somewhat degraded; thus, a computation complexity/vehicle performance tradeoff is involved.
- The feasibility of this approach was established by simulation of a simple example of a second-order system. By slowly varying the initial state to simulate disturbances, the ability of a man to track the optimal solution was demonstrated,,
- Other simplified closed-loop schemes have been defined for both first and second stages. These schemes are suboptimal but have considerably less computation and display requirements than the optimal prediction method described above. Further investigation will establish which combination of simplified methods are best for the ROT boost phase.

## 2.2 PHASE II

Based on the conclusions and recommendations of Phase I, two manual optimal schemes, the Predictive Model Guidance Scheme (PMGS) and the Nominal Guidance Scheme (NGS) were defined for the ROT vehicle and were successfully simulated on a real-time basis with a pilot actively engaged in the guidance function (Ref. 3). After analysis and careful evaluation of the results from Phase I, the PMGS was simulated for second-stage guidance only, This decision was based on the following reasons:

- The sensitivity of the desired terminal conditions to the optimization parameters increases as the required flight time increases; thus, if the PMGS is used for both stages, five significant figures are required on the optimization parameters during the first stage. Only three-figure accuracy is required during the second stage.

- The fast-time model required in the first stage to account for the aerodynamic effects is more complex than for the vacuum phase. The effectiveness of the predictive model scheme decreases as the fast-time solution rate decreases. Also, this solution rate must necessarily 'decrease as the fast-time predictive model complexity increases.

- In the first phase of study (Ref, 8), it was determined that the fuel-optimal path in the atmosphere consists of a "basic" path, uniquely defined in the altitude-velocity plane, with thrust as a parameter. This path is independent of initial conditions, the remaining portion of the trajectory being a transition path to put the vehicle on this path after takeoff or after some disturbance, In view of this, an optimal nominal trajectory is close to an optimal trajectory for other conditions since all optimal trajectories have a portion of this "basic" path in common.

In summary, sensitivity and predictive model complexity are degrading characteristics of the predictive model scheme during the first stage. A nominal guidance scheme, however, is particularly well suited to the atmospheric phase due to the "basic" path features and the reduced computation requirements.

As the result of a successful simulation of the Predictive Model Guidance Scheme for second-stage guidance, the following conclusions were reached:

- A human operator is effective in the manual scheme with a fast-time solution rate of one per second.
- A meter-type display of the predicted terminal errors in altitude and flight-path angle during the terminal phase of boost is a definite requirement to obtain the desired accuracy in the terminal conditions unless scale changes are incorporated in the CRT display.
- A two-dimensional display of the predicted trajectory in the altitude-velocity plane is useful to the pilot for the iterative task of "shaping" or synthesizing the predicted trajectory. After the trajectory has the proper shape, the meter display is required to yield the desired accuracy in the terminal conditions.
- Only two optimization parameters are required by the pilot to steer the planar vehicle model to the desired terminal conditions.
- From the experience gained in experimenting with the scheme, it is concluded that the work load is a function of the mission time, The work load is moderate initially, then decreases to zero, and finally, towards cutoff conditions, increases again. This area needed further investigation.

- The amount of operator training required for efficient operation of the manual guidance scheme is low.,

Study of the NGS was undertaken for purposes of comparison with the PMGS. On the basis of simulation, the following conclusions were reached:

- The NGS was used for guidance of both stages. The altitude-versus altitude-rate display format was recommended on the basis of minimizing the operator work load and minimizing terminal errors. This display evaluation needed further work if the NGS is used only for the first stage, Typical errors at staging are 4100 feet for altitude, 0.2 degree for flight-path angle, and 21 ft/sec for velocity,

- A display of the predicted state, based on derivative information of the present state, was used in the study. Experience indicates that the predicted-state display is not required if the present state remains on the nominal trajectory. If the present-state, display is off the nominal, the predicted-state display is useful to the pilot in steering back to the nominal. It was concluded that the predicted-state display is not absolutely essential for the nominal guidance scheme,

- In addition to a display of the nominal trajectory along with the vehicle's present state, a meter-type presentation of the present state is a definite requirement for the terminal phase of the mission, The use of the meter presentation of the present state results in an improvement in the terminal error by almost an order of magnitude,, The meter presentation of body attitude is useful throughout the flight, whereas the remaining information of the present state is useful towards the end of the flight.

- The display requirements have been determined during this study. The actual implementation of these displays required further study. Possibilities include a continuous cathode-ray-tube (CRT) presentation of the nominal along with the present state and a CRT presentation of the present state and a plastic overlay display of the nominal trajectory.

- The effects of random disturbances due to winds are negligible on the pilot's ability to manually steer the vehicle along a nominal trajectory, The effects would not be negligible with the inclusion of rotational dynamics to the model.

The NGS and PMGS were compared on the basis of:

- Accuracy
- Pilot work load
- Mission flexibility
- Fuel requirements
- Display requirements
- Computational requirements
- Training requirements
- Pilot's role

Table 2-2 summarizes the comparison of the NGS with the PMGS. The PMGS is accurate, flexible, fuel-optimal, and the pilot work load is low. The computer and display requirements are moderate. On the other hand, the NGS is simple, has basically no computer requirements, and the display requirements are low. These low computation and display requirements assume there are no requirements for display of the nominal trajectory. The NGS,

Table 2-2. Comparison of the Nominal and Predictive Model Guidance Schemes

| Vehicle Stage | Guidance Scheme | Pilot Workload | Fuel Requirement | Complexity | | Mission Flexibility | Terminal Error |
|---|---|---|---|---|---|---|---|
| | | | | Computer | Display (CRT) | | |
| Stage 1 | NGS | Low | Near-optimum (function of off-nominal I. C., external disturbances and parameter variations) | Low-if nominal is not stored in computer<br>Moderate-if nominal is stored on computer | Moderate-if CRT is used to display nominal<br>Low-otherwise | No | Typical Errors:<br>Altitude = 4100 ft<br>Flight-path angle = 0.2°<br>Velocity = 21 fps |
| | PMGS | Moderate | Near-optimum (function of approximations in fast-time model) | Moderate | Moderate | Yes | |
| Stage 2 | NGS | High | Non-optimum | Low | Moderate-if CRT is used to display nominal<br>Low-otherwise | No | Typical Errors:<br>Altitude = 2200 ft<br>Flight path angle = 0.17° |
| | PMGS | Low | Optimum | Moderate | Moderate | Yes | Typical Errors:<br>Altitude = 1700 ft<br>Flight path angle = 0.007° |

however, is less accurate than the PMGS; it is not flexible; it is not fuel-optimal if large disturbances are present; and the pilot work load is higher than that of the PMGS. Thus, the basic tradeoff between the two schemes is between an accurate, fuel-optimal, flexible low-work load scheme and a manual guidance scheme which is simple and which has low computer and display requirements.

Typical terminal errors with the PMGS were 1700 feet in altitude and 0.007 degree in flight-path angle. The corresponding errors with the NGS were 2200 feet and 0.17 degree.

This phase of study recommended that the NGS be used for first-stage guidance and the PMGS for second-stage guidance. To further evaluate these schemes, it was recommended that the simulation model be extended to the three-dimensional case. Further work was required on evaluating display formats for each stage on the basis of minimizing operator task loading, terminal errors, and system hardware complexity.

## 2.3 PHASE III

A three-dimensional, spherical earth model for the ROT vehicle was simulated as part of Phase III of this contract. As recommended in Phase II, the Nominal Guidance Scheme (NGS) was used as first-stage guidance, with second-stage guidance being the Predictive Model Guidance Scheme (PMGS).

Operator task loading (work load) was evaluated by two methods; the first used guidance as the primary task (subsidiary task method), and the second used guidance as the secondary task (loading task method).

Major objectives of the Phase III study were to choose an optimal display for each stage and to analyze the tradeoffs between computational requirements and pilot work load. (Previous evaluation of the displays and guidance schemes was conducted under the assumption of a two-dimensional, non-rotating earth). As a result of a successful simulation and demonstration of the feasibility of the proposed manual guidance schemes, the following conclusions and recommendations are presented.

- The feasibility of the two guidance schemes developed under a planar, non-rotating earth model was successfully demonstrated using a more realistic spherical earth, rotating earth model. Automatic lateral guidance was employed to hold the vehicle in the launch plane;

- The optimal display format was found to be altitude versus velocity (h versus V) for both stages. When compared with displays of altitude versus altitude rate and altitude versus flight-path angle, this display minimized the operator task loading, using the subsidiary task method in which guidance is the primary task for evaluation of work load. This display of h versus V also gave the best performance in terms of altitude and flight-path-angle errors at orbital injection. Work-load measurement using the method of Task Loading in which guidance is the secondary task for evaluating the displays gave inconclusive results due to an insufficient amount of data. With sufficient data, the displays could possibly be differentiated on the basis of unused information handling capacity of the operator. The display yielding the maximum unused capacity would be the best display format.

- The subsidiary task method (guidance task is primary) of work-load evaluation provided a quantitative measurement of the critical times (high pilot involvement) during the flight. This measurement resulted in a time history of pilot work load (see Figure 3-12). The loading method of measurement indicated the operator has at least 4. 75 bits per second of unused information-handling capacity while adequately performing the guidance function.

- Evaluation of the fast-time portion of PMGS was conducted using three mathematical models (see Table 3-3. ) These models varied in accuracy depending on the numerical integration scheme used and the approximation to the real vehicle. Model II (i. e., trapezoidal integration and spherical earth gravity calculation) is the obvious choice because it retains its accuracy down to a very low number of steps required for integration to form the predicted trajectory. This model also significantly reduces pilot work load as seen in Figure 3-16, (The display formats were evaluated with Model I.)

- Evaluation of both the PMGS and the NGS was conducted using actual data for computer/display requirements and work load (see Tables 3-4 and 3-5). The conclusions from Phase II of this contract were validated (i. e,, use of NGS for the first stage and PMGS for the second stage). Required hardware is:

  (1) Computer -- memory - 1045 24-bit words
  solution time 834 ms - PMGS
  535 ms - NGS

  (2) Display -- standard analog-driven CRT

  (3) Navigation and Control -- same as Saturn V

- No new hardware is required over the current Saturn V state-of-the art to implement the NGS for the first stage and the PMGS for the second stage. However, due to the advantages of an integrated, multi-format display concept for future spacecraft, it is recommended that a new program be initiated to continue development of a computer-driven solid-state display device such as EL.

- No major further studies are required to demonstrate the feasibility of the proposed manual guidance schemes. Certain human factors studies are recommended, however, to maximize the effectiveness of man's role in the guidance and control of future spacecraft. Some specific recommended studies are included in section 5.1.

- In light of the excellent results from Honeywell's fixed-base simulation of manual guidance, it is recommended that the proposed NGS and PMGS be evaluated under more realistic conditions, such as moving-base simulation using trained astronauts or possibly a test flight on a Saturn launch vehicle. The manual guidance schemes are completely compatible with Saturn hardware, with only the addition of a display and reprogramming of the onboard digital computer required to implement the manual system.

Because of the current interest in the comparison between manual and automatic guidance and control, the characteristics of an automatic guidance scheme--i. e., , Iterative Guidance Scheme (IGS) of Saturn V-- are included when comparing the manual schemes. Table **2-3** summarizes the characteristics of the IGS, PMGS, and NGS. A rating summary is also included in Figure 2-4, based only on the characteristics investigated during the three phases of this contract,

## Table 2-3. Comparison of Manual and Automatic Guidance Schemes

| Guidance Scheme | Complexity | | Terminal Error | Pilot Workload | bility |
|---|---|---|---|---|---|
| | Computer | Display | | | |
| Iterative Guidance Scheme (IGS)<br>(Automatic - Saturn V) | HIGH<br>Memory = 1530 words*<br>Solution time = 1000 ms | NONE | LOW<br>$\lvert h_e \rvert$ = 65 ft[†]<br>$\lvert \gamma_e \rvert$ = 0.001°[††]<br>PI = 0.012 | ZERO<br>(Automatic scheme) | MEDIUM |
| Predictive Model Guidance Scheme (PMGS)<br>(Manual) | MEDIUM<br>Memory = 845 words<br>Solution time = 834 ms | MODERATE<br>(CRT required) | MEDIUM<br>$\lvert h_e \rvert$ = 529 ft<br>$\lvert \gamma_e \rvert$ = 0.007°<br>PI = 0.083 | MEDIUM<br>(Average 23.1% workload) | HIGH |
| Nominal Guidance Scheme (NGS)<br>(Manual) | LOW<br>Memory = 525 words<br>Solution time = 535 ms | MODERATE<br>(CRT required) | HIGH<br>$\lvert h_e \rvert$ = 2200 ft<br>$\lvert \gamma_e \rvert$ = 0.170°<br>PI = 1.15 | HIGH<br>(Average 50%** workload) | LOW |

* The actual Saturn V computer memory is much larger than 1530 words due to calculations required for flight out of orbit.

** Estimated from Phase II

[†] $h_e$ = terminal altitude error

[††] $\gamma_e$ = terminal flight-path angle error

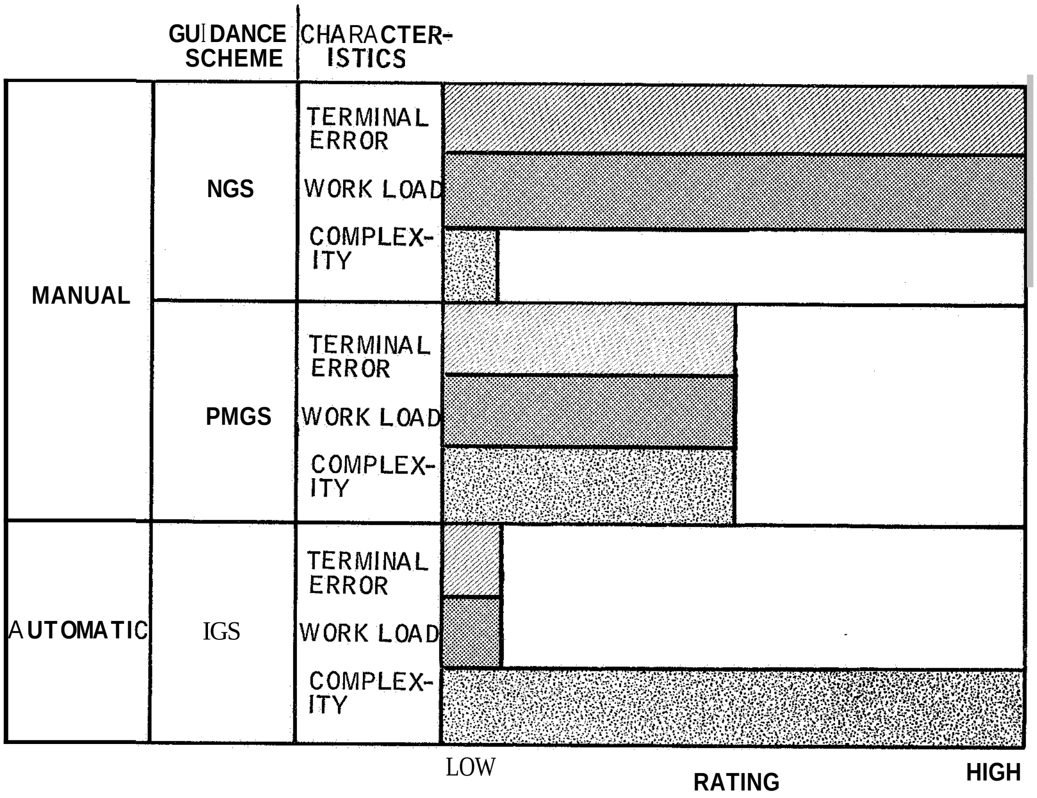

Figure 2-4. Rating Summary of Manual Automatic Guidance Schemes

As expected, Figure 2-4 shows the inverse relationship between hardware complexity (computer requirements) and both terminal error and pilot work load. That is, there is a major tradeoff involed when choosing between guidance schemes--hardware complexity versus system performance and human involvement in the guidance loop. The automatic IGS and manual NGS lie on opposite ends of this tradeoff scale, with the manual PMGS falling in the middle as a comparison.

This comparison does not include such important features as reliability and flexibility, and the final choice of guidance scheme must depend on the particular mission under consideration.

# SECTION 3
# ACCOMPLISHMENTS AND RESULTS

## .1 GENERAL

This section represents the main body of this report and presents the details of all the work accomplished in the third and final phase of the study. The manual guidance techniques and displays are discussed in section 3.2. The nominal guidance scheme (NGS) is used for first-stage guidance and the predictive model guidance scheme for second stage. The model used for the real-time simulation of the ROT vehicle is discussed in section 3.3. The equations of motion, which are written in a wind-axis (flight-path) coordinate system assuming a spherical rotating earth, are presented in Appendix A. Also included is a discussion of the target orbit, guidance plane geometry and the equations of motion for the fast-time model required in the PMGS. Section 3.4 contains the results of the operator work-load measurement and display format evaluation.

The computational and display requirements are presented in sections 3.5 and 3.6 respectively.

## 3.2 ROT GUIDANCE TECHNIQUES AND DISPLAYS

The proposed guidance techniques and displays for a ROT three-dimensional ascent to orbit are summarized in this subsection. The first stage is manually guided about an optimal nominal trajectory. Second-stage guidance is based on either the PMGS or a nominal guidance scheme (NGS) as studied in an earlier phase of the contract (Ref. 3, pp. 43-72). The choice of second-stage guidance is a tradeoff between the relatively high computer requirements, adaptability, and low pilot work load for the PMGS versus the low computer requirements, inflexibility, and high pilot work load for the NGS.

The function of lateral or yaw-axis guidance is to keep the vehicle in the launch plane. Only an automatic scheme was considered for this study.

### 3. 2. 1 First-Stage Guidance -- Nominal Trajectory

Manual guidance about an optimized nominal trajectory was chosen as the first-stage guidance scheme because of its basic simplicity. The nominal trajectory was generated in an earlier phase of the contract under a two-dimensional, non-rotating earth assumption. However, it is felt that these restrictions would not have a detectable influence on the more complete three-dimensional, rotating earth model, considering the relatively short flight time for the first stage (137 sec) and the small out-of-plane motion.

Another reason for the selection of the nominal trajectory is that there is no need for any great flexibility in selection of the first-stage trajectory. Earlier studies demonstrated that optimal trajectories for off-nominal initial conditions varied little. It appears, then, that there is little merit in selecting a predictive- or adaptive-type guidance scheme for the first stage with its accompanying complexity and greater computer requirements.

The pilot's task in following the nominal is simplified by the addition of a simple predictive symbol on the display. The symbol is driven by a first-order expansion about the present state:

$$x(t + \tau) = x(t) + \tau \dot{x}(t)$$

where $\tau$ is the length of time in seconds that the pilot desires to predict ahead. In addition to the prediction, the current-state conditions are displayed in digital form.

Three displays were evaluated:

- Altitude versus velocity
- Altitude versus flight-path angle
- Altitude versus altitude rate

Figures 3-1, 3-2, and 3-3 show the three display formats with the PMGS used as second-stage guidance.

### 3.2.2 Second-Stage Guidance - Predictive Model Guidance Scheme

The proposed second-stage guidance scheme is actually a hybrid having characteristics of both open-loop and closed-loop schemes. It takes advantage of the inherent accuracy of a closed-loop scheme and the simplicity of an optimal open-loop scheme (see Ref. 3, pp 18-32 for a more complete description).

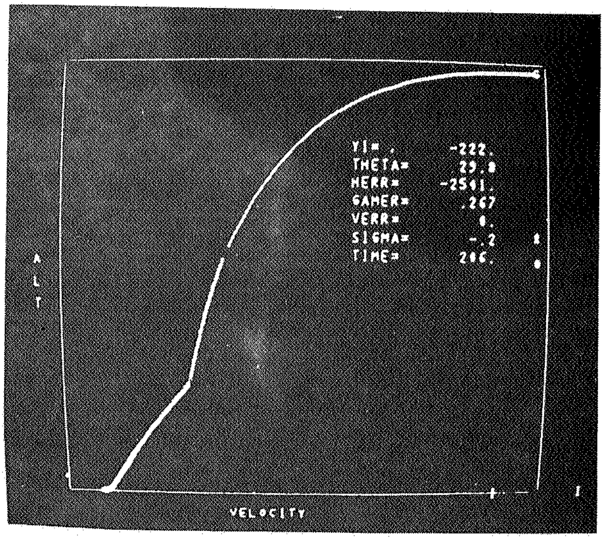
YI= . -222.
THETA= 29.8
HERR= -2541.
GAMER= .267
VERR= 0.
SIGMA= -.2
TIME= 206.
ALT
VELOCITY

Figure 3-1
Altitude-versus-Velocity
Display Format

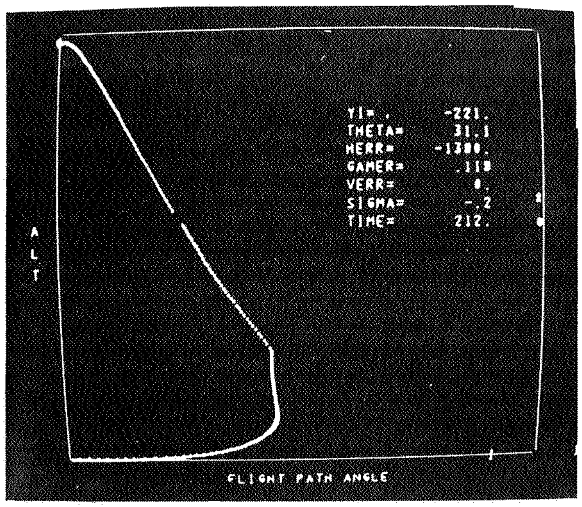
YI= . -221.
THETA= 31.1
HERR= -1300.
GAMER= .118
VERR= 0.
SIGMA= -.2
TIME= 212.
ALT
FLIGHT PATH ANGLE

Figure 3-2
Altitude-versus-Flight-Path-Angle
Display Format

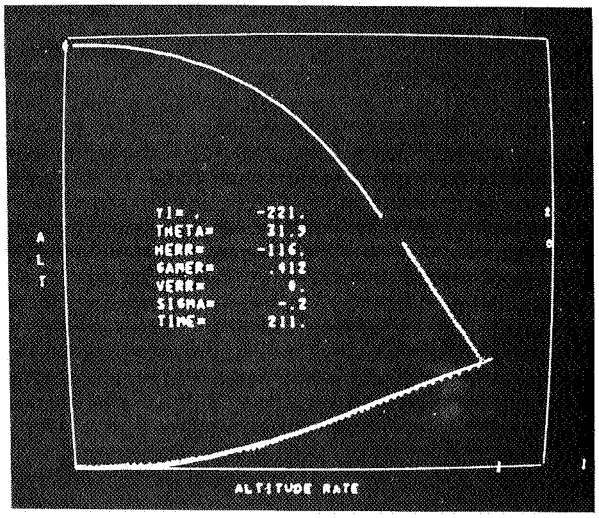
YI= . -221.
THETA= 31.9
HERR= -116.
GAMER= .412
VERR= 0.
SIGMA= -.2
TIME= 211.
ALT
ALTITUDE RATE

Figure 3-3
Altitude-versus-Altitude-Rate
Display Format

Based on a two-dimensional, flat-earth approximation to the real situation, a time-optimal solution for the time history of the vehicle attitude angle ($\chi$) is obtained in closed form (see section 3. 5. 1):

$$\text{Tan } \chi = A + Bt$$

By knowing the constants A and B, a predicted open-loop trajectory can then be repetitively computed in fast-time and displayed to the pilot. If this trajectory does not hit the specified target orbit conditions, the pilot adjusts A and B, thus closing the guidance loop.

### 3. 2. 3 Lateral Guidance and Display

To stay in the launch plane, the inertial position $Y_I$ must be zero (see Figure 3-4). An obvious form of a lateral guidance law, then, is to make the bank angle ($\sigma$) or gimbal angle ($\delta_Y$) proportional to $Y_I$ plus a rate term for damping:

$$\sigma, \delta_Y = K_Y Y_I + K_{\dot{Y}} Y_I$$

The gains $K_Y$ and $K_{\dot{Y}}$ can be constant or varied by the pilot as he monitors a display of lateral error. The display consists of a symbol moving up the $Y$ axis of the display simultaneously with altitude, while the X axis is proportional to the lateral error. The pilot can also adjust the scale factor to allow for large plane changes and greater sensitivity. Lateral manual guidance is also possible with the pilot monitoring the display and controlling the bank angle or yaw-axis gimbal angle.

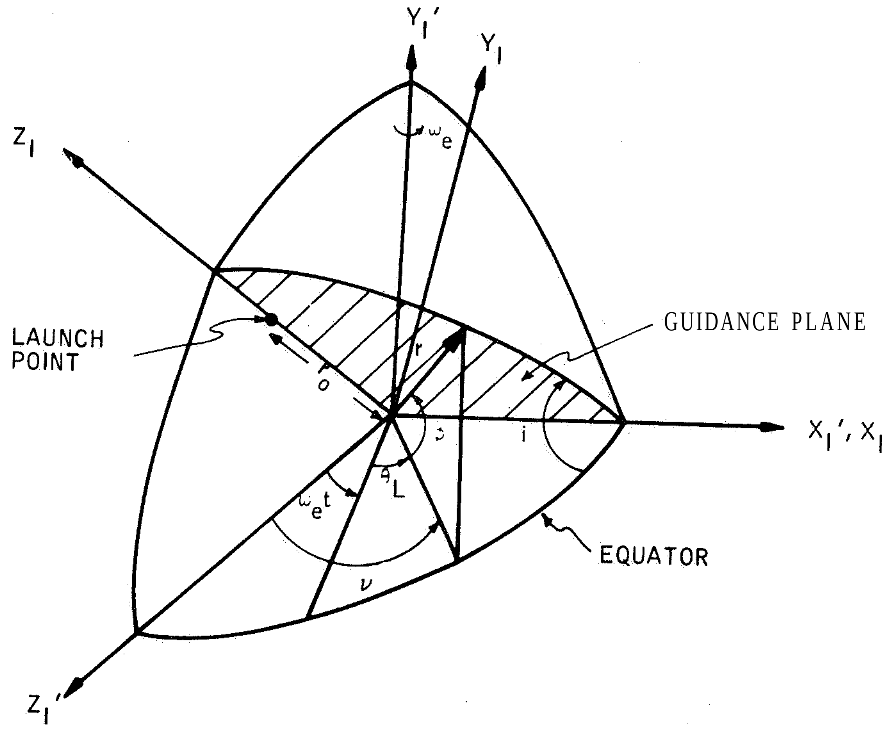
$Y_I'$
$Y_I$
$Z_I$
$\omega_e$
LAUNCH POINT
$r_o$
$r$
GUIDANCE PLANE
$X_I', X_I$
$\omega$
$i$
$\theta_L$
$\omega_e t$
$\nu$
EQUATOR
$Z_I'$

Figure 3-4. Guidance Plane Geometry

For this study, only automatic lateral guidance with constant gains in the lateral guidance law was considered. With

$K_Y = 0.001$ deg/ft and

$\dot{K}_Y = 0.1$ deg/fps.

the typical out-of-plane error at orbital injection is 400 feet with an orbit inclination error of 0.0013 degree,

## 3.3 MATHEMATICAL MODEL

This subsection presents a general description of the mathematical models used for the simulation of the ROT and the manual guidance schemes. The three-dimensional, point-mass equations of motion for the real-time simulation are written in a flight-path (wind-axis) coordinate system, assuming a spherical, rotating earth, This axis system was chosen over two other commonly used systems (i. e., inertial and local horizon) because of compatibility with earlier phases of this study in which a two-dimensional, non-rotating earth wind-axis model was used. Rotational and control system dynamics are neglected. The details of the simulation are presented in Appendix A.

The first stage of the proposed ROT system is a horizontally launched, reusable winged booster with approximately 1,800,000 pounds of thrust. Delivery of the second stage to its staging point is the primary mission of the first-stage. Sled-assisted horizontal takeoff provides a velocity initial condition of 650 fps with staging occuring at the following conditions:

| | |
|---|---|
| Inertial velocity ($V_I$) | 7041.1 fps |
| Altitude (h) | 168,323 ft |
| Inertial flight-path angle ($\gamma_I$) | 21.88 deg |

After separation, the first stage coasts to an altitude of 288,000 feet before re-entering the earth's atmosphere.

The second stage of the ROT system is a lifting-body vehicle. However, for this study it is assumed that staging occurs outside the sensible atmosphere, and therefore aerodynamic effects are neglected. Second-stage thrust is approximately 300,000 pounds. Both stages are restricted to a 3-g acceleration limit. Reference 1 contains a complete description of the ROT system.

### 3. 3. 1 Target Orbit

The equations for the real-time simulation are written in terms of quantities relative to the earth, and, since the target orbit is relative to inertial space, there must be a transformation from a relative to an inertial reference frame. In this study, the down range is unconstrained since a simple solution for the optimum thrust direction is obtained using the range free transversality conditions.

The circular target orbit of 100 nautical miles is defined by four parameters:

- Altitude (h) - 608, 020 ft
- Orbital inclination (i) - 30 deg
- Inertial velocity ($V_I$) - 25, 570. 5 fps
- Inertial flight-path angle ($\gamma_I$) - 0 deg

These parameters in terms of earth-referenced quantities are:

$$\dot{h} = \dot{r} = V \sin \gamma$$

$$\cos i = \cos \phi \sin \Psi_I$$

$$V_I = \left[ V^2 + 2 V \cos \gamma \sin \Psi \, \omega_e r \cos \phi + (\omega_e r \cos \phi)^2 \right]^{1/2}$$

$$\sin \gamma_I = \frac{V \sin \gamma}{V_I}$$

$$\sin \Psi_I = \frac{V \cos \gamma \sin \Psi + \omega_e r \cos \phi}{V_I \cos \gamma_I}$$

### 3.3.2 Lateral Guidance and Guidance Plane Geometry

One of the envisioned benefits of the ROT class of vehicles is the possibility of "offset" launch capabilities in which the launch vehicle performs a significant lateral displacement. However, the first-stage nominal trajectory and the second-stage fast-time model were generated in earlier phases of the study assuming planar motion, and it was out of the scope of this contract to generate new nominal trajectories and a fast-time model. Therefore, for this study, it is assumed that launch occurs in the plane of the target orbit and that the function of lateral guidance is to hold the vehicle in that plane. The bank angle during first-stage flight and the engine yaw gimbal angle during second-stage flight are the control variables.

The plane of the target orbit is defined by

$$\cos i = \cos \phi \sin \Psi_I \tag{3-1}$$

Since the target orbit has an inclination, $i = 30°$, and a due east launch is assumed to take full advantage of the earth's rotation, the launch latitude becomes

$$\phi_o = 30''$$

from Equation (3-1).

From Figure 3-4, the guidance plane is defined by the $X_I$, $Z_I$ coordinates with the $Y_I$ being the out-of-plane position. These coordinates must be computed in terms of latitude and longitude for the simulation. Referring again to Figure 3-4, the inertial positions $X_I'$, $Y_I'$, $Z_I'$ are easily written in terms of the spherical coordinates $r$, $\phi$, $\nu$ as:

$$X_I' = r \cos \phi \sin \nu$$

$$Y_I' = r \sin \phi$$

$$Z_I' = r \cos \phi \cos \nu$$

where: $r$ = distance to vehicle from earth's center

$\phi$ = latitude

$\nu$ = inertial longitude = $\theta_L + \omega_e t$

$\theta_L$ = longitude ($\theta_L = 0$ at launch)

$\omega_e$ = earth's rotation rate

The $X_I'$, $Y_I'$, $Z_I'$ system is transformed into $X_I$, $Y_I$, $Z_I$ by rotating about $X_I'$ through the angle $i$:

$$\begin{bmatrix} X_I \\ Y_I \\ Z_I \end{bmatrix} = \begin{bmatrix} 1 & 0 & 0 \\ 0 & \cos i & -\sin i \\ 0 & \sin i & \cos i \end{bmatrix} \begin{bmatrix} X_I' \\ Y_I' \\ Z_I' \end{bmatrix}$$

Then:

$$X_I = r \cos \phi \sin v$$

$$Y_I = r \sin \phi \cos I - r \cos \phi \cos v \sin i$$

$$Z_I = r \sin \phi \sin i + r \cos \phi \cos v \cos i$$

The in-plane range angle $\beta$ is required for transformation to the fast-time model and is given by:

$$\tan \beta = \frac{X_I}{Z_I}$$

### 3. 3. 3 Fast-Time Model

The equations of motion for the fast-time predictive model are written in a two-dimensional inertial coordinate system. The relationship between this simplified coordinate system and the real-world simulation is shown in Figure 3-5.

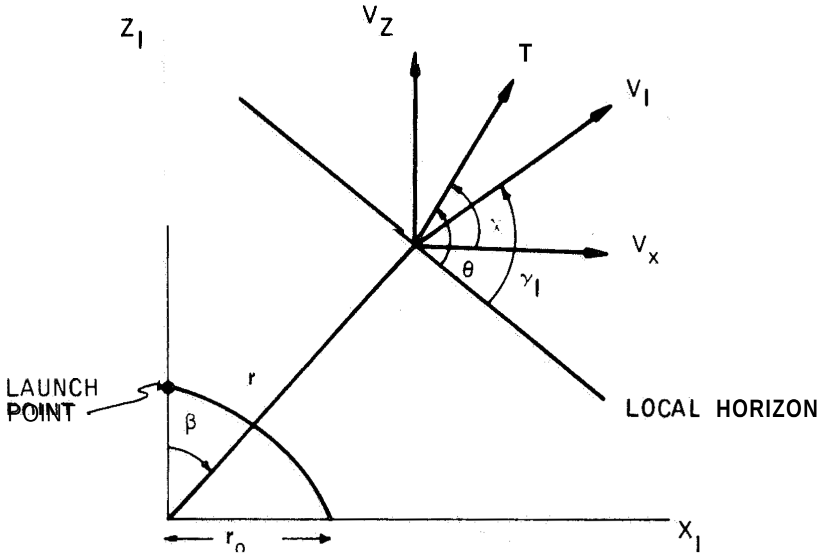
$Z_I$
$V_Z$
T
$V_I$
$V_X$
χ
θ
$\gamma_I$
LOCAL HORIZON
LAUNCH POINT
r
β
$r_0$
$X_I$

Figure 3-5. Fast-Time Coordinate System

The equations of motion, assuming no aerodynamics, are:

$$
\begin{aligned}
x &= V_x \\
z &= V_z \\
V_x &= \frac{T}{M} \cos x - g_x \qquad (3\text{-}2) \\
V_z &= \frac{T}{M} \sin \chi - g_z \\
M &= -\beta_2 \\
\tan \chi &= A + Bt \quad \text{:(optimal linear tangent law)}
\end{aligned}
$$

where

$g_x$ and $g_z$ are the components of gravity along the x and z directions, depending on the assumption of a flat earth or spherical earth when calculating the gravity (see section 3. 5. 2). The constant A in Equations **(3-2)** is updated automatically every iteration (1 second) so that the pilot need not be concerned about the variation of A as the flight time increases if he has chosen the correct current value to satisfy the end conditions:

$$A_{NEW} = A_{OLD} + B_{OLD} \cdot A\ t.$$

The control variable ($\theta$), the pitch attitude, for the real vehicle is calculated every iteration from:

$$\theta = \tan^{-1}(A) + \beta.$$

The initial conditions for the fast-time model are:

$$x(0) = X_I$$

$$z(0) = Z_I$$

$$V_x(0) = V_I \cos (\gamma_I - \beta)$$

$$V_z(0) = V_I \sin (\gamma_I - \beta)$$

For the display of the fast-time predicted trajectory the following transformations are required:

$$V_p = \sqrt{V_x^2 + V_z^2} \quad \text{- velocity}$$

$$h_P = \sqrt{x^2 + z^2} - r_o \quad \text{- altitude}$$

$$\gamma_p = \mathrm{Tan}^{-1} \sqrt{\frac{xV_x + zV_z}{zV_x - xV_z}} \quad \text{- flight-path angle}$$

The predicted terminal errors are also displayed to the pilot and are given by:

$$h_e = h_P(T) - 608020.$$

$$\gamma_e = \gamma_p(T) - 0° = \gamma_p(T)$$

where $h_P(T)$ and $\gamma_P(T)$ are the predicted altitude and flight-path angle at velocity cutoff.

## 3.4 OPERATOR WORK-LOAD MEASUREMENT AND DISPLAY EVALUATION

This subsection describes the two simulation techniques used to evaluate the operator work load while performing the manual guidance functions. These measures may be used to establish the reserve capacity of an operator. This reserve will be required if the operator is to perform the vehicle attitude control function in addition to the guidance function. Evaluation of display formats is also performed by measuring the operator work load. The display yielding the lowest value of work load is considered the best.

Section 3. 4. 1 describes the two methods, the data obtained are presented in sections 3. 4. 2 and 3. 4. 3, and the conclusions are given in section 3. 4. 4.

### 3.4.1 Description of Operator Work-Load Measurement

Figure 3-6 provides a classification of the various measures which can be used for establishing the reserve capacity of an operator. Review articles by Brown (Ref. 11) and Knowles (Ref. 12) summarize the more important studies relating to these measures. Of the two general classifications, "information sampling" and "concomitant tasks", only the latter is examined in this study.

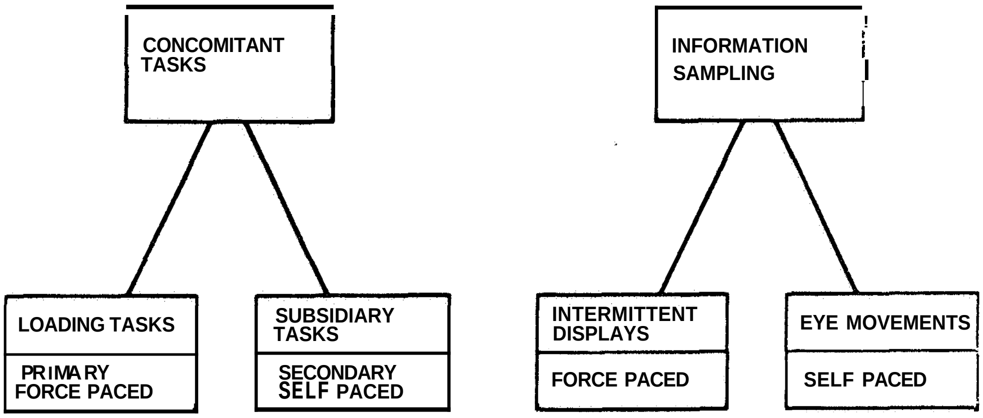
CONCOMITANT TASKS
LOADING TASKS
PRIMARY FORCE PACED
SUBSIDIARY TASKS
SECONDARY SELF PACED
INFORMATION SAMPLING
INTERMITTENT DISPLAYS
FORCE PACED
EYE MOVEMENTS
SELF PACED

Figure 3-6. Methods for Measuring Informational Work Load

Concomitant tasks can be of two types, loading tasks or subsidiary tasks. Loading tasks are characterized by two features: First, the subject is instructed to perform the loading task at the expense of his performance on the primary task. Second, the loading task is force-paced so that the subject does not control the rate at which he must respond. In this study, the loading task is considered the subject's primary task, and the guidance function is the secondary task. In the case of the subsidiary task, however, the operator is instructed to perform this task only when he feels he can respond with no decrement in his performance on the primary tasks, i. e., the guidance task. Thus the subsidiary task is self-paced.

The rationale for the use of subsidiary tasks is that, as the information processing load of the primary task is increased, the operator's information rates on subsidiary tasks are decreased. If it is assumed that these rates are inversely proportional, then one can obtain a direct measure of primary task work load. Ekstrom (Ref. 13) used this method in evaluating various control systems for an aircraft using a self-paced, choice-reaction subsidiary task. If, when also performing the primary task, the subsidiary task response rate was reduced to 50 percent of the level obtained when performing the subsidiary task alone, she concluded that the operator needed only 50 percent of his attention to perform the primary control task. She found that, although measured system performance for two different control systems was the same, one control system required much less operator attention. In the present study, a subsidiary task is used to evaluate a number of possible display formats. The display format yielding the lowest primary task work load is considered the best. Section 3. 4. 2 covers the description and results of these experiments in more detail.

Perhaps the most serious problem with the subsidiary task measure involves the response bias of the operator. If any subsidiary task will cause some decrement in the primary task, the question is: how much decrement in the primary task is tolerable? This question must be resolved by the subject.

Typically, the subject is instructed to maintain high performance on the primary task, and to perform the subsidiary task when possible. Results are presented in section 3.4. 2 which indicate the decrement in the guidance task with the addition of the subsidiary task.

The rationale for the use of loading tasks is that, as the information processing demands of the loading task is increased, performance on the primary task will deteriorate. To determine the reserve capacity of an operator at some specified minimum performance level on the primary task, the attentional demand of the loading task is increased until the primary task is reduced to the selected level of performance. The information rate on the loading task then represents the operator's reserve capacity since he is performing at this level while maintaining the selected performance level on the primary task. In other words, the capacity used on the loading task could be applied to another ("second primary") task by substituting the "second primary" task for the loading task. In effect, the loading task represents information processing requirements of other primary tasks. Since the loading task is force-paced, the problem of operator response bias can be avoided.

A problem in using loading tasks is that, since they are force-paced, they may require the operator's attention during critical periods of the primary task. The subsidiary task does not have this disadvantage since the operator selects when to perform the subsidiary task, This objection is not serious since, in operational man/machine systems, other primary tasks (represented here by the loading task) often require attention at critical times. In this applied sense, the forced-pace nature of loading tasks may be realistic.

### 3.4.2 Operator Work Load - Subsidiary Task

3.4.2.1 Description of the Technique -- The subsidiary task used to evaluate the operator work load consisted of the operator responding to one lighted button out of a 4 x 4 array by pressing it to turn it off. The 16 buttons are lighted (one at a time) at random through a 64-position stepper switch. A photograph of the tap-lights is shown in Figure 3-7. The device with 16 lights in a display panel was mounted near the CRT display within the peripheral vision of the subject *so* that an eye movement to and from the control panel was required to extinguish any energized light. The device was set *so* that only one tap-light energized at a time. (Appendix B describes the circuits). The readout relays remained energized until the tap-light switch was depressed by the operator. Light activity was recorded on a strip-chart recorder from an output connection on the selector box.

Using this method, a time history of work load (throughout the entire flight) can be recorded. Critical times (high work load) during the flight are then easily seen. A quantitative measure of work load is made from the formula:

$$WL = \left(1 - \frac{R_1}{R_2}\right) \times 100\%$$

where $R_1$ = rate of handling lights during a simulated flight

$R_2$ = maximum rate of handling lights.

In other words, this formula gives a number signifying the percentage of time required to guide the vehicle. If $WL = 100\%$, i.e., $R_1 = 0$, the pilot is devoting all his time to monitoring the display and/or manipulating the guidance controls. If $WL = 0$, i.e., $R_1 = R_2$, the pilot is devoting no time to the guidance task and is able to devote 100 percent of his time to the secondary task.

A measure of the total operator work load in each run can be obtained by integrating the time history of work load.

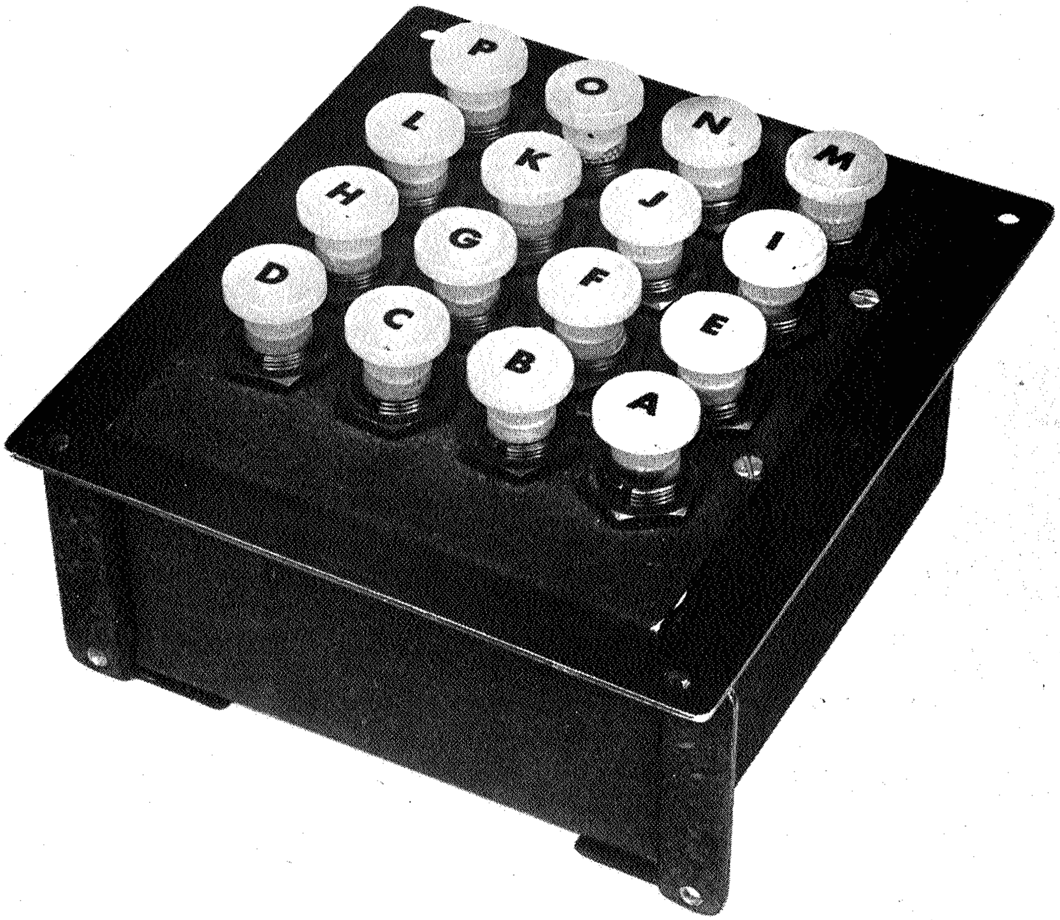
P
O
N
M
L
K
J
I
H
G
F
E
D
C
B
A

Figure 3-7. Tap-Light Display

3.4.2.2 Experimental Results -- The subsidiary task work-load measurement technique was used to evaluate display formats as well as to determine the critical times (high work load) during the flight. The guidance task is primary and the subsidiary task is secondary, Figure 3-8, and 3-9 are examples of the type of unsmoothed data recorded. Figure 3-8 shows raw work-load data for an altitude-versus-velocity display in first and second stages with automatic lateral guidance. Figure 3-9 shows operator work load using the same display but using manual lateral guidance. Figure 3-10 shows the corresponding control variable time histories for manual and automatic lateral steering. Although these three figures represent raw data from only two runs, there are certain points which should be made.

- In Figure 3-8, the work load is initially fairly high but, at about 50 seconds, it remains constant at 15 percent until staging at 140 seconds, The low level (15 percent) represents a monitoring task where the operator is not applying any control signals but is merely monitoring the display. The nominal guidance scheme is used in the first stage and the pitch attitude is a constant after 50 seconds (see Figure 3-11). Thus, the period of monitoring is from 50 to 140 seconds,

  The predictive. model guidance scheme is used in the second stage which begins at about 140 seconds. The work load is high from 140 to 170 seconds due to the operator making adjustments to the guidance parameters A and B. This is followed by a long, basically monitoring, period from 170 to 350 seconds. Notice that there are two midcourse corrections made during this period. From 350 seconds until cutoff, the workload is high due to the operator making vernier adjustments to parameters A and B.

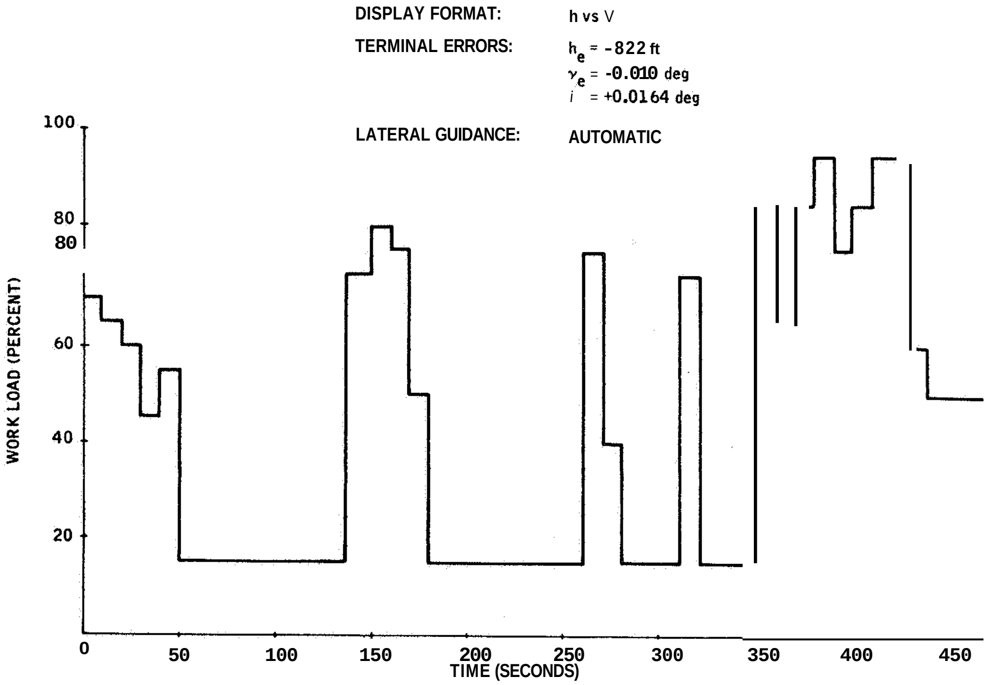

Figure 3-8. Operator Work Load versus Time - Automatic Lateral Guidance

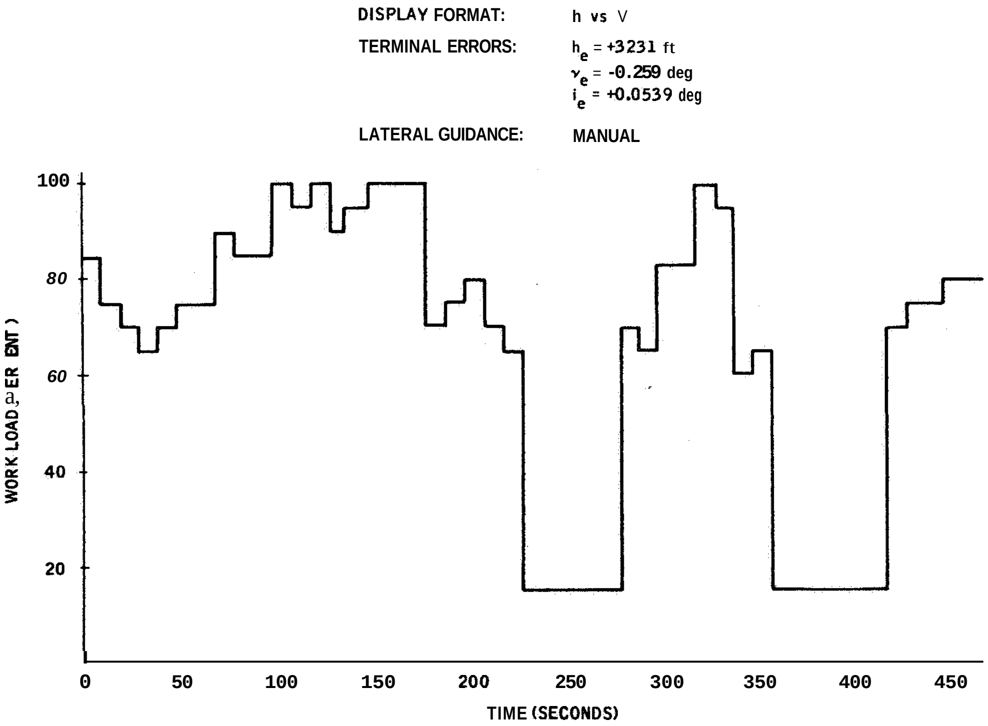

Figure 3-9. Operator Work Load versus Time - Manual Lateral Guidance

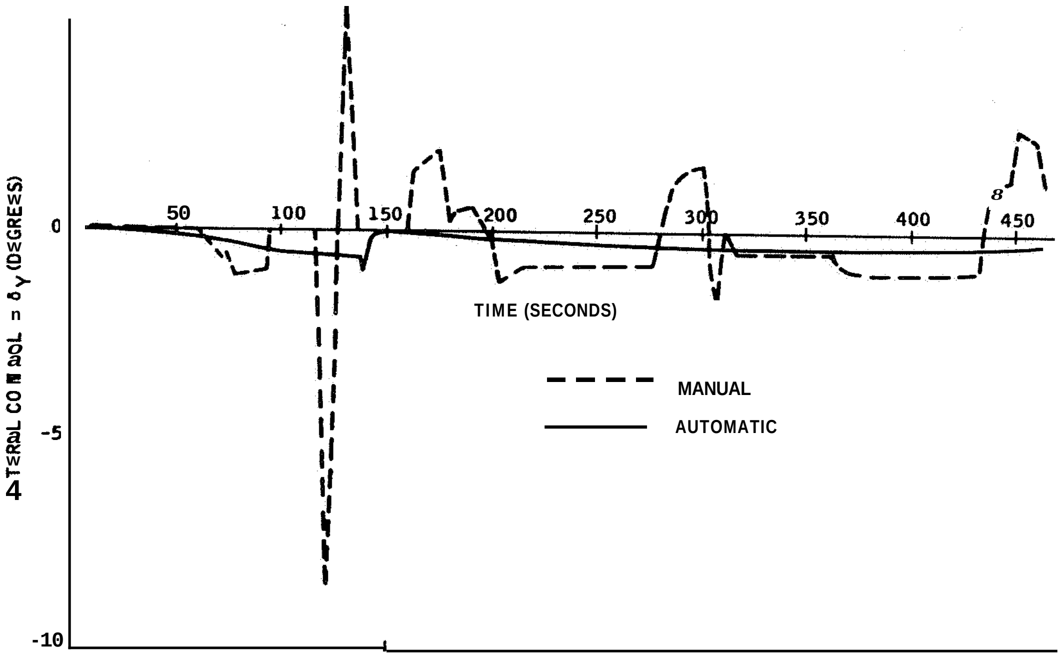

Figure 3-10. Lateral Control versus Time

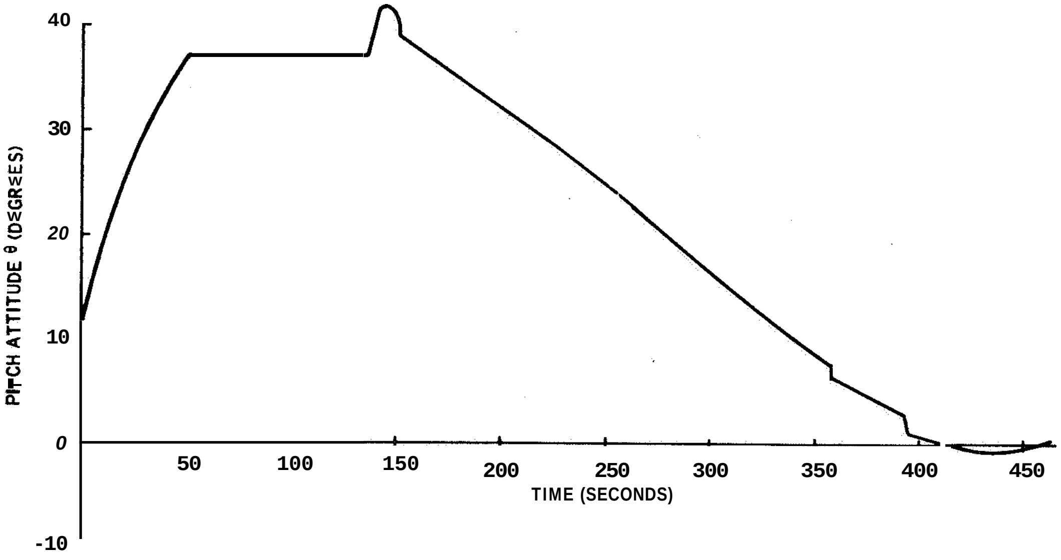

Figure 3-11. Pitch Attitude versus Time

- Comparison of Figure **3-9** with **3-8** indicates the additional work load imposed by the manual lateral guidance. The work load is generally higher with fewer monitoring periods. The terminal errors are also larger when the operator performs the lateral guidance.

- During the course of the study, it was decided to use automatic lateral guidance due to the relatively simple automatic scheme used and the relatively large increase in operator work load with the addition of the manual lateral guidance task. All data presented in the remaining portion of this report was obtained using an automatic lateral guidance system.

- Figure 3-10 illustrates the large deviations in lateral control variable (bank angle $\sigma$ in the first stage, engine yaw gimbal angle $\delta_Y$ in the second stage) when manual lateral guidance is used, With sufficient training, however, this lateral control variable time history would be smoother,

To properly evaluate the different display formats, a number of simulation runs were made. The rate of handling lights during the flight ($R_1$) is counted in 10-second intervals. The operator work load was recorded for each run, and these curves were then averaged. The resulting averaged curve of operator work load versus time was then smoothed in time, using a 40-second moving average. Three two-dimensional display formats were considered:

- Altitude versus velocity (h versus V) -- see Figure **3-1**
- Altitude versus altitude rate (h versus $\dot{h}$) -- see Figure **3-3**
- Altitude versus flight-path angle (h versus $\gamma$) -- see Figure **3-2**

All runs were made with two experienced operators; the runs being equally divided between the two.

Figure 3-12, 3-13 and 3-14 show the averaged and time-smoothed work load-versus-time curves for each display format,, All data was obtained using Model I for the fast-time model (see 3.5). On the basis of these data, the following conclusions are made:

- In the first stage, where the nominal guidance scheme was used, the work load is initially high and then decreases after about 50 seconds. This is generally true with the three displays, This general shape is due to the nature of the proper pitch attitude time history (see Figure 3-11) which rises linearly to about 37 degrees at 40 seconds and then remains constant until staging.

- The h-versus-V format yields the lowest work-load-versus-time curve in the first stage. Notice that the work load definitely decreases to a monitoring level after about 50 seconds.

- The next best display format for first-stage guidance is h versus $\dot{h}$ which is followed by the h-versus-y display format. Both these formats show a low level of work load after 50 seconds, but the level is larger than for monitoring, This indicates the operator is making small corrections to the pitch attitude which is nominally constant from 50 seconds to staging, The h-versus-h and h-versus y display formats are more sensitive than the h-versus-V display. This sensitivity enables the operator to see his error from the naminal more readily and thus make more corrections. This sensitivity explains the higher-than-monitoring level for the h-versus-y and h-versus-$\dot{h}$ display formats.

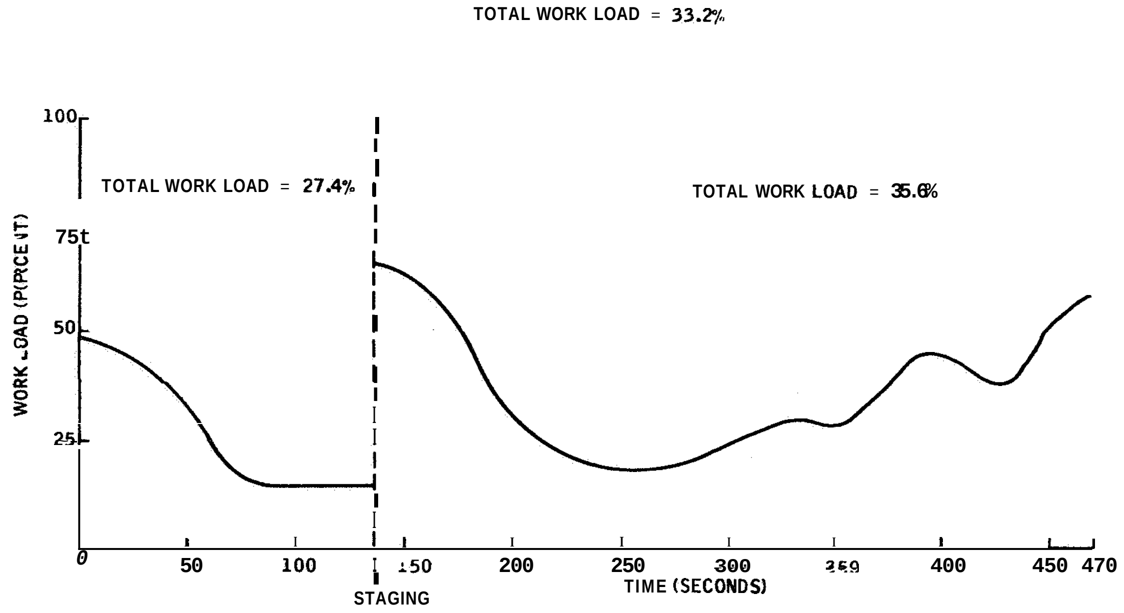

Figure 3-12. Subsidiary Task Work Load versus Time - h-versus-V Display

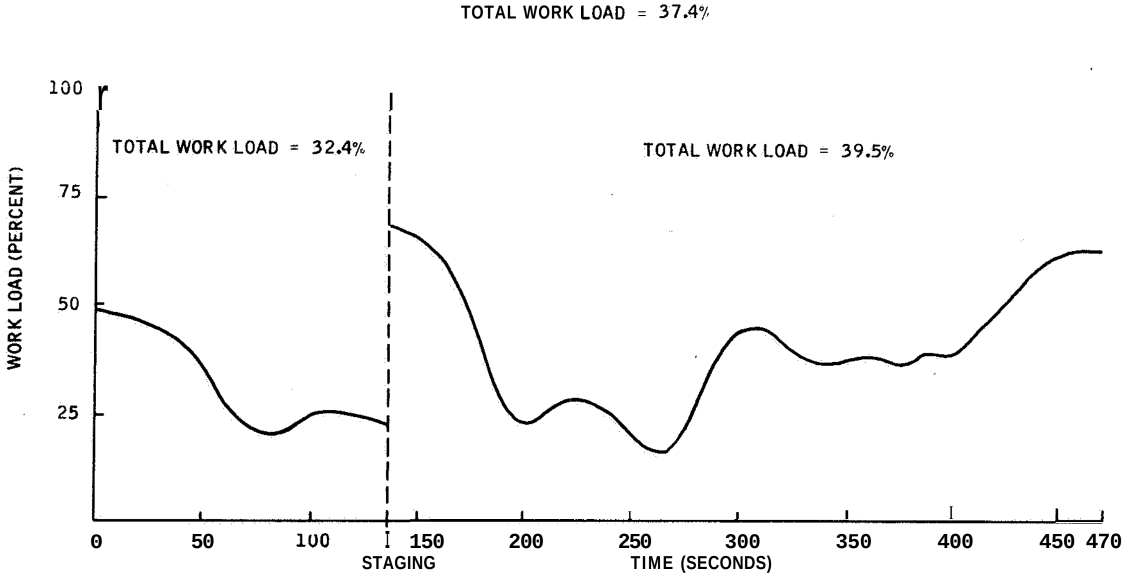

Figure 3-13. Subsidiary Task Work Load versus Time - h-versus-h Display

TOTAL WORK LOAD = 35.5%

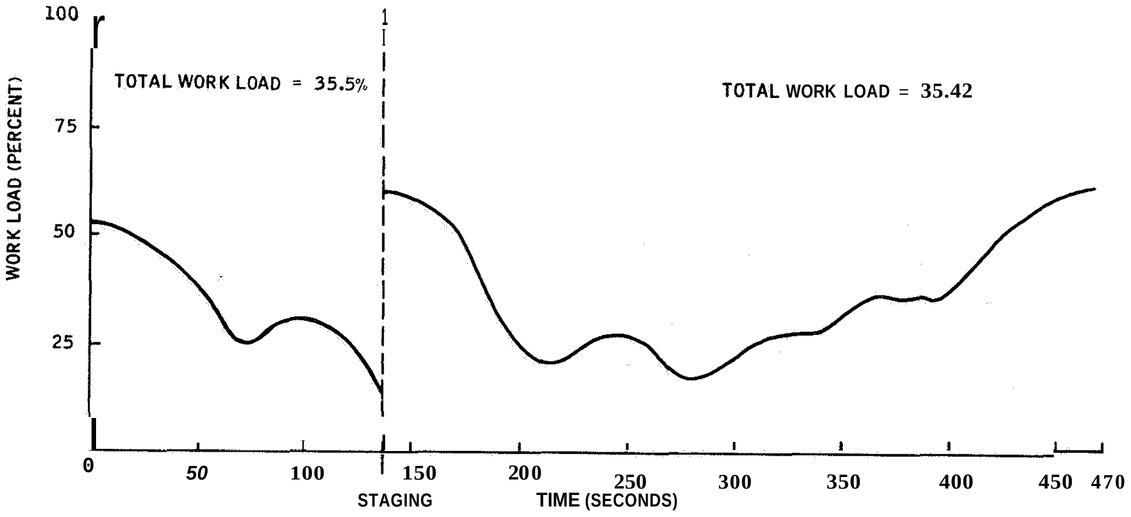

Figure **3-14.** Subsidiary Task Work Load versus Time - h-versus-$\gamma$ Display

- Table 3-1 summarizes total work load (area under the curve) versus display format for the first stage. On the basis of minimum total work load for first-stage manual guidance, the h-versus-V display format is best.

- In the second stage, where the predictive model guidance scheme was used, the work load is initially high, then decreases towards a monitoring level, and then increases again as the cutoff time is approached. This is generally true with the three displays, The initial high level is due to the operator making gross corrections to the guidance parameters A and B. These corrections are required due to the off-nominal second-stage initial conditions. The operator then monitors the display until about 300 seconds when he starts making corrections to null out the predicted terminal errors. The corrections are required partially as a result of the fast-time model inaccuracies and partially as a vernier adjustment to the initial corrections.

- Table **3-1** summarizes total work load (area under the curve) versus display format for second-stage guidance. On the basis of minimum total work load, per second-stage manual guidance, the h-versus V display format is best.

| Display | Work Load | |
|---|---|---|
| | First Stage | Second Stage |
| h vs V | **27.4** | **32.2** |
| h vs $\dot{h}$ | **32.4** | **39.5** |
| h vs $y$ | **35.5** | **35.4** |

Evaluation of display formats was performed on the basis of operator work load and guidance system performance. The results of the evaluation on the basis of work load have been presented. Guidance system performance is interpreted as the accuracy in achieving the target orbit conditions which are specified by target altitude, flight-path angle, velocity, and orbital inclination. Since automatic lateral guidance and automatic velocity cutoff were assumed in the study, the operator had no control over inclination or terminal velocity. As a result, only altitude and flight-path angle are considered in the manual guidance system performance. To have one measure of terminal error instead of two terminal errors (altitude and flight-path angle errors) a performance index is defined by

$$PI = \frac{1}{\sqrt{2}} \sqrt{\left( \frac{h_e}{h_{e_{max}}} \right)^2 + \left( \frac{\gamma_e}{\gamma_{e_{max}}} \right)^2} \qquad (3\text{-}3)$$

This performance index is simply a weighted root-mean-square measure of the terminal errors. The weight factors are $h_{e_{max}}$ and $\gamma_{e_{max}}$

Table 3-2 summarizes the system performance data obtained using the subsidiary task method of measuring pilot work load with Model I for the fast-time model (see 3. 5). The data are presented as absolute-value averages of six runs for each of seven display combinations investigated. The system performance index (PI) is calculated from Equation (3-3) with

$$h_{e_{max}} = 4643 \text{ ft}$$

$$\gamma_{e_{max}} = 0.109 \text{ deg}$$

These weighting factors represent the maximum terminal errors obtained in all the simulation runs made with the subsidiary task work load measurement technique.

The last three columns of Table 3-2 are measures of total work load and are calculated from the areas under the curves in Figures 3-12, 3-13, and 3-14.

The subsidiary task method for work-load measurement was used to evaluate the display formats under consideration on the basis of performance index and total work load. The conclusions are:

- On the basis of performance index, the optimum display formats are h versus $\dot{h}$ in stage 1 and h versus V in stage 2. However, h versus V in both stages resulted in a performance index value only slightly larger than the h-versus-$\dot{h}$ and h-versus-V displays.

- On the basis of total work load, h versus V in both stages shows a definite improvement over the other displays. Therefore, on the basis of operator work load and guidance system performance, the best display format is h versus V in both stages.

Table 3-2. Performance Summary - Subsidiary Task Method

| First-Stage Display | Second-Stage Display | $\mid h_e \mid$ | $\mid \gamma_e \mid$ | Time (sec) | PI | Percent Total Work Load | | |
|---|---|---|---|---|---|---|---|---|
| | | | | | | Total | First | Second |
| h vs V | h vs V | 400 | 0 008 | 49.17 | 0.0803 | 30.8 | 28.6 | 31.7 |
| h vs V | h vs $\gamma$ | 1530 | 0 005 | 49.06 | 0.2388 | 31.2 | 24.7 | 33.9 |
| h vs $\gamma$ | h vs V | 1022 | 0 017 | 48.96 | 0.1938 | 32.9 | 37.9 | 30.8 |
| h vs $\dot{h}$ | h vs V | 460 | 0 005 | 49.07 | 0.0737 | 34.0 | 33.9 | 34.1 |
| h vs V | h vs $\dot{h}$ | 1739 | 0 002 | 49.20 | 0.2645 | 34.2 | 26.6 | 37.4 |
| h vs $\gamma$ | h vs $\gamma$ | 1158 | 0 003 | 49.36 | 0.2800 | 36.9 | 35.7 | 37.4 |
| h vs $\dot{h}$ | h vs $\dot{h}$ | 1928 | 0 007 | 49.21 | 0.2940 | 37.0 | 31.7 | 39.3 |

Figure 3-15 shows the response bias of the operator. As discussed in 3.4.1, the addition of a subsidiary task sometimes causes a decrement in the primary task, even though the operator has been instructed to maintain high performance on the primary task. Figure 3-15 shows no decrement in performance of the primary task for the h-versus-V and h-versus-h display formats. For the h-versus-? format, however, the performance index increased by 43 percent with the addition of the subsidiary task. This data shows that for the h-versus-y format, the operators did not follow instructions.

In section 3.5, various fast-time models for the predictive model guidance scheme are discussed, and one is chosen (Model II) on the basis of minimizing computer requirements and operator work load. The resulting work-load-versus-time curve is shown in Figure 3-16. This work-load curve, obtained using an h-versus-V display format for second-stage manual guidance, is the average of five runs made by two experienced operators. It represents the operator work load as a function of mission time for the best fast time model and best display format, Note that there is a large period of monitoring, 200-370 seconds. The total work load is 23 percent which is a definite reduction from 33 percent (Figure 3-12) obtained using Model I. This Model I was used in evaluating the three display formats.

### 3.4.3 Operator Work Load - Loading Task

3.4.3.1 Description of the Technique -- The loading task used to evaluate operator work load consisted of the operator responding vocally to a visual stimulus. Nine random letters (A-I) generated by the computer are displayed randomly (uniform distribution) in the top center of the CRT. In all three displays, the position of the letters is within 4 inches of the position of the digital readout of the terminal errors. These letters are displayed at a specified rate which is an input to the computer at the beginning of each simulation run. Work

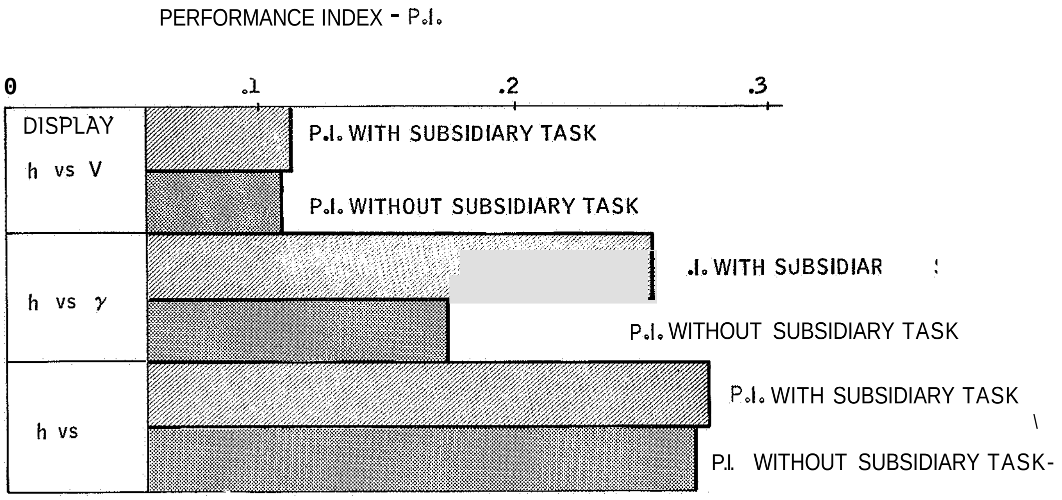

Figure 3-15. Operator Response Bias

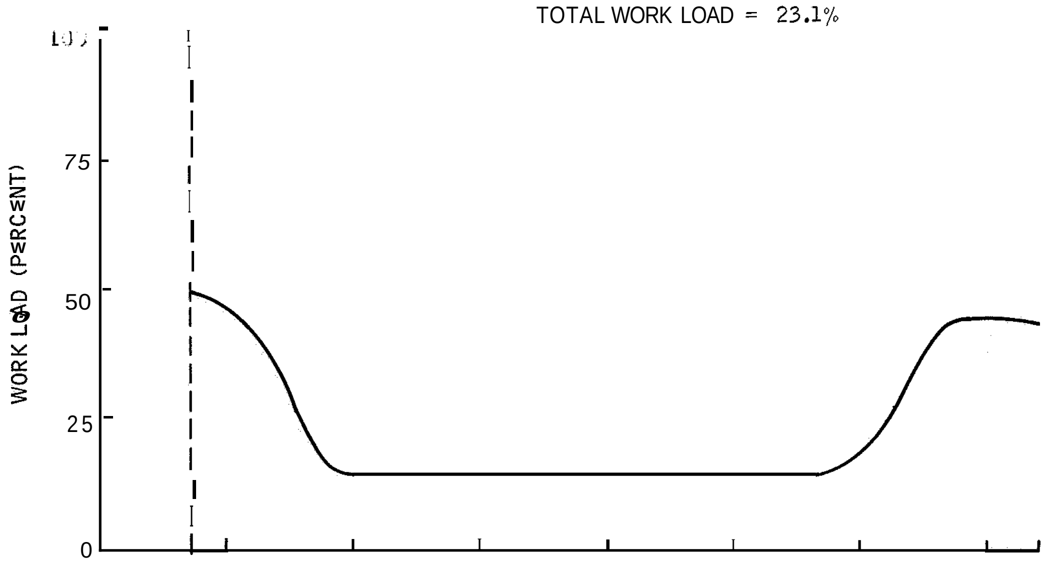

load is expressed as the number of random letters per second that the operator must respond to. The operator was instructed to maintain high performance on the loading task and to perform the guidance task when possible.

Appendix C describes a "bit box" which can be used to give a visual presentation of random numbers to an operator. Such a device can be used as a measurement device of operator work load if the simulation system does not have a computer-driven CRT display facility.

3.4.3.2 Experimental Results -- To determine the operator's reserve capacity while performing the manual guidance task, a series of runs was made by two experienced operators. For a specified display format and a specified random letter rate, five runs were made. These data are presented in Figures 3-17, 3-18, and 3-19. The system performance index from Equation (3-3) is plotted against the random-letter rate or equivalent information rate.

The information content of the letter source is given by:

$$H = \sum_{i=1}^{N} p_i \log_2 \frac{1}{p_i}$$

where

$p_i$ = probability of occurrence of $i^{th}$ letter

$N$ = total number of letters

For a uniform distribution of nine letters the information content is:

$$H = \log_2 9$$

$$= 3.17 \text{ bits}$$

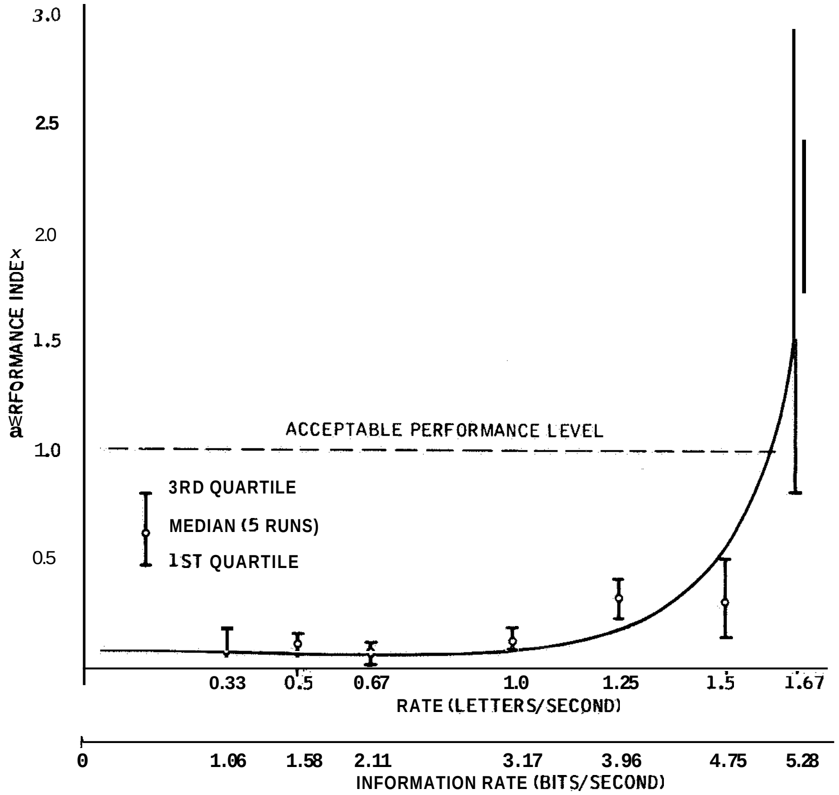

Figure 3-17. Operator Work Load, Loading Task - h-versus-V Display

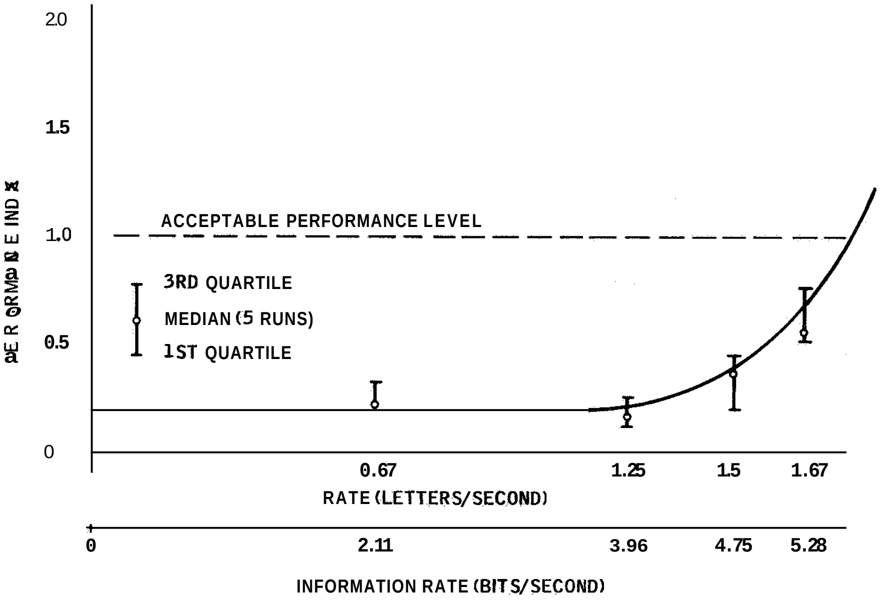

Figure 3-18. Operator Work Load, Loading Task - h-versus-$\dot{h}$ Display

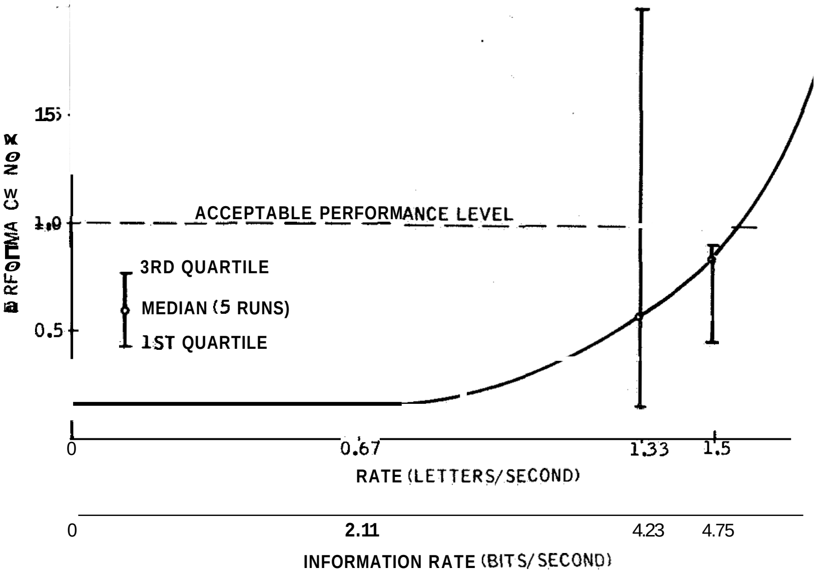

Figure 3-19. Operator Work Load, Loading Task - h-versus-$\gamma$ Display

At a rate of, say, 1-1/2 letters per second, the information rate is 3.17 x 1.5 = 4.75 bits/sec.

In presenting the data, the median and first and third quartiles are plotted.

The level of acceptable performance was chosen assuming ICBM quality in the booster guidance system (Ref. 14). Tolerable errors on altitude and flight-path angle were chosen as:

Ah = ± 1 mile

$\Delta\gamma$ = 0.1 deg

These yield a value for performance index of 1.0, assuming

$h_{e_{max}}$ = 4600 ft

$\gamma_{e_{max}}$ = 0.11 deg

From Figures 3-17, 3-18, and 3-19, the operator has a reserve capacity of at least 4.75 bits/sec to perform additional tasks to the guidance task. Although the reserve capacity varies somewhat between display formats, there was not enough data taken to make any firm conclusion about the best format on the basis of maximizing the reserve capacity of the operator.

In performing this loading task without the addition of the guidance task, the operator was able to handle 2.25 letters/sec or, equivalently, 10.7 bits/sec.

### 3.4.4 Conclusions

(1) Based on the subsidiary task method of measuring operator task loading, the best display on the basis of minimum work load and minimum performance index is the h-versus-V format in both stages.

(2) The operator uses about 33 percent of his total available work capacity on the guidance task. The remainder is available for other control tasks.

(3) The operator work load is a function of mission time (Figure 3-12). It is high for the first 50 seconds, then decreases to a monitoring level (15 percent) until staging. At staging the work load increases to about 65 percent then decreases to a monitoring level at 250 seconds and then gradually increases to 60 percent at cutoff.

(4) The average performance index for the h-versus-V display is 0.11 (see Figure 3-15). This is equivalent to errors in altitude and flight-path angle of:

$$|\Delta h| = 600 \text{ ft}$$

$$|\Delta \gamma| = 0.01 \text{ deg}$$

(5) In measuring the work load by the subsidiary task method with an h-versus-V display, there was no operator bias (see Figure 3-15).

(6) Based on the loading task method of measuring operator task loading, the operator has an unused information handling capacity of at least 4.75 bits/sec. This assumes a level of adequate performance equivalent to an altitude error of

$$Ah = \pm 1 \text{ mile}$$

and flight-path angle error of

$$\Delta\gamma = 0.1 \text{ deg}$$

(7) There was not sufficient data taken with the loading task method to differentiate between the three display formats on the basis of unused information handling capacity.

(8) The Information handling capability of an operator performing only the loading task is 2.25 letters/sec or 10.7 bits/sec.

## 3.5 COMPUTER REQUIREMENTS

The computer requirements for the PMGS are presented in this subsection. They are then compared with the automatic Iterative Guidance Scheme (IGS) used for Saturn V and the Nominal Guidance Scheme (NGS) studied in Phase II of this contract in terms of memory requirements and solution time.

### 3.5.1 ROT Guidance and Navigation Computations

For this study, it is assumed that guidance, navigation and control system hardware is patterned after the Saturn V system (Ref. **4).** The navigation equations provide the PMGS with position, velocity and acceleration initial conditions in the appropriate coordinate system (i. e. , $X_I$, $Y_I$, $Z_I$ system in Figure 3-4).

The PMGS consists of a simplified mathematical model of the real vehicle, The model differential equations are then integrated in fast-time with a velocity cutoff.

The predicted terminal altitude and terminal flight-path angle errors are displayed to the pilot along with the predicted trajectory. These errors and predicted trajectory are updated once per second. The guidance function is then performed manually by the pilot by adjusting the constants A and B in the linear tangent law for an optimum thrust angle ($\chi$):

$$\text{Tan}\,\chi = A + Bt, \text{ where } t = \text{time.}$$

This equation is derived using calculus of variations to convert the minimum-time (fuel) problem into a two-point boundary value problem assuming a flat earth and constant gravity. Saturn V boost guidance into orbit is also accomplished basically by this method, although totally automatic, and is described in Reference 4.

Referring to the equations for the fast-time model (section 3. 3. 3), the linear tangent law is easily formed from a definition of the Hamiltonian:

$$H = p_X V_X + p_Z V_Z + p_{V_X} (T/m \cos \chi) + p_{VZ} (T/m \sin \chi - g) - 1$$

The control variable is $\chi$ and for a minimum-time solution, the necessary condition is:

$$\frac{\partial H}{\partial \chi} = 0 = p_{V_x} \; T/m \sin \chi + p_{V_z} \; T/m \cos \chi \quad \text{or,}$$

$$\text{Tan } \chi = \frac{p_{V_z}}{p_{V_x}}$$

The adjoint equations are:

$$\dot{p}_x = -\frac{\partial H}{\partial x} = 0$$

$$\dot{p}_z = -\frac{\partial H}{\partial z} = 0$$

$$\dot{p}_{V_x} = -\frac{\partial H}{\partial V_x} = -p_x$$

$$\dot{p}_{V_z} = -\frac{\partial H}{\partial V_z} = -p_z$$

Boundary conditions €or the adjoint variables are:

$p_x(t_f) = 0$ (due to unconstrained down range)

$p_z(t_f)$, $p_{V_x}(t_f)$, $p_{V_z}(t_f)$ unspecified

Hence, the solutions €or the adjoint variables are:

$$p_x = 0$$

$$p_z = p_{zo}$$

$$p_{v_x} = p_{v_{zo}}$$

$$p_{v_z} - p_{v_{zo}} - p_{zo}t \quad \text{and}$$

the optimal thrust angle becomes:

$$\text{Tan}\,\chi = \frac{p_{v_z}}{p_{v_x}} - \frac{p_{v_{zo}} - p_{zo}t}{p_{v_{xo}}} = A + Bt$$

The primary purpose of the computer system is to issue control commands to the vehicle during flight. These control commands are evaluated in a major and minor computation cycle. During the major cycle, which occurs once per second, the navigation equations are solved, and the predicted trajectory is generated. Vehicle attitude corrections are performed during the minor computation loop. Attitude correction outputs to the control computer are dependent on the platform gimbal angles and the results of the guidance equations calculated in the major loop. The minor loop calculations require 18 ms for solutions on the Saturn V computer and are made 25 times per second (Ref. 2, p. 58).

Approximately 45 ms are required to solve the navigation equations. This is an estimate made from the equations given in Reference 4, p. 894, for the Saturn V computer. The velocity readings from the platform integrating accelerometers are combined with the gravitational acceleration to yield the inertial velocity components, $X_I$, $Y_I$, $\dot{Z}_I$. By integration of the velocity components, the vehicle position $X_I$, $Y_I$, $Z_I$ is obtained.

To obtain the thrust acceleration T/m required for the PMGS, the velocity readings are digitally differentiated. From the resulting acceleration components, the term T/m is computed by taking the square root of the sum of the squares.

The solution time of 480 ms for the IGS was estimated from information provided by Reference 2:

$$(\text{Solution Time})_{\text{IGS}} = \text{Total Solution Time} - \text{Navigation} - \text{Attitude Correction} - \text{Executive System}$$

$$(\text{Solution Time})_{\text{IGS}} = 1000 - 45 - 18 \times 25 - 25 = 480 \text{ ms.}$$

The rate of solution for the major computation loop is the total solution time (1 iteration/sec). An executive system or general program housekeeping such as interrupt processing is estimated to require 25 ms out of one iteration. Figure 3-20 is a block diagram of the total system.

A. 24-bit word length for the memory is sufficient for accuracy requirements. This corresponds to about 7 decimal digits. The greatest accuracy requirement is for the distance from the earth's center to the vehicle (r) which is approximately $21 \times 10^6$ feet. The altitude (h) can then be calculated to approximately ±10 feet since $h = r - r_o$. Double precision arithmetic could also be used when greater accuracy is required.

### 3. 5. 2 Models for the PMGS

Three models for the PMGS were considered in this study on the basis of computer requirements and accuracy. The differences between models are the accuracy of the equations describing the model and the numerical integration scheme, The integration schemes were:

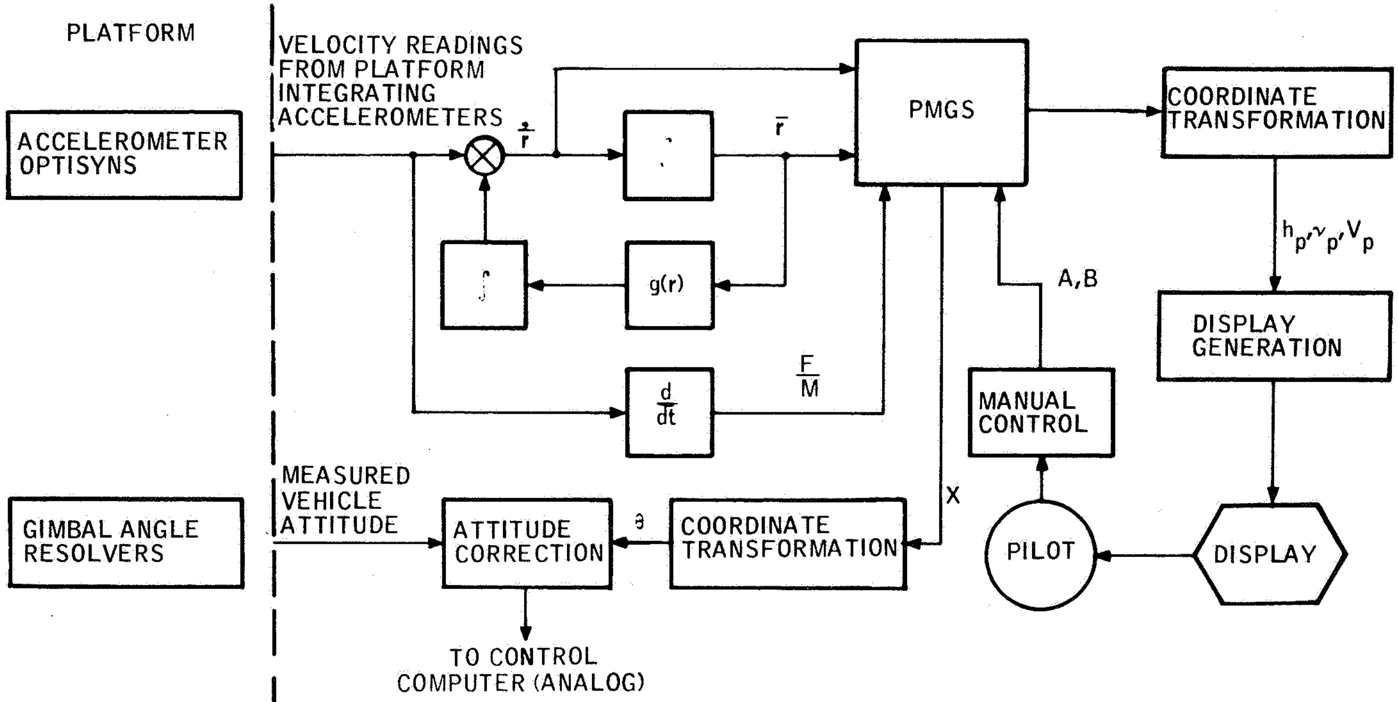
PLATFORM
ACCELEROMETER OPTISYNS
GIMBAL ANGLE RESOLVERS
VELOCITY READINGS FROM PLATFORM INTEGRATING ACCELEROMETERS
$\dot{\bar{r}}$
$\bar{r}$
g(r)
$\frac{d}{dt}$
$\frac{F}{M}$
PMGS
A,B
X
COORDINATE TRANSFORMATION
$h_p, \gamma_p, V_p$
DISPLAY GENERATION
DISPLAY
PILOT
MANUAL CONTROL
MEASURED VEHICLE ATTITUDE
ATTITUDE CORRECTION
$\theta$
COORDINATE TRANSFORMATION
TO CONTROL COMPUTER (ANALOG)

Figure 3-20. Second-Stage Navigation and Guidance Block Diagram

- Rectangular or first-order Taylor series
- Second-order Taylor series
- Trapezoidal

Accuracy of the model equations depends on (1) flat earth (constant gravity) or spherical earth calculation of gravity and (2) calculation of the acceleration provided by the engines (the real vehicle is thrust limited to 3 g's, and therefore vehicle mass is no longer linear with time).

The models considered are:

I.
- Rectangular or first-order Taylor series integration
- Constant gravity
- No thrust limiting

II.
- Trapezoidal integration
- Spherical earth gravity
- Thrust limiting

III.
- Second-order Taylor series integration
- Spherical earth gravity
- Thrust limiting

The fast-time model vehicle equations of motion are repeated below for convenience.

$$\dot{V}_x = \frac{T}{m} \cos \chi - g_x$$ x acceleration

$$V_z = \frac{T}{m} \sin \chi - g_z$$ z acceleration

$$x = V_x$$ x velocity

$$\dot{z} = V_z$$ z velocity (3-4)

$$T = C_2 \beta_2$$ thrust

$$m = m_o - \beta_2 t$$ mass

$$\mathrm{Tan}\, \chi = A + Bt$$ thrust attitude angle

Equations **(3-4)** are integrated and yield predicted values for the position and velocity of the vehicle. A velocity cutoff is used to terminate the integration. In addition, coordinate transformations are required for the display to the pilot and for the attitude control system. For the display:

$$hP = \sqrt{x^2 + z^2} - ro$$ predicted altitude

$$V_P = \sqrt{\dot{x}^2 \ddagger \dot{z}^2}$$ predicted velocity (3-5)

$$\gamma_p = \tan^{-1} \left( \frac{xV_x + zV_z}{zV_x - xV_z} \right)$$ predicted flight-path angle

Command vehicle pitch angle ($\theta$) is required for the attitude control system:

$$\theta = \chi + \tan^{-1} \left| \frac{X_I}{Z_I} \right) = + \beta \qquad (3\text{-}6)$$

where $X_I$ and $Z_I$ are the current planar coordinates of the real vehicle.

The integration schemes considered are represented by:

- $x_{N+1} = x_N + At\,x$ Rectangular or first-order Taylor series
- $x_{N+1} = x_N + \frac{At}{2}(\dot{x}_{N+1} + \dot{x}_N)$ Trapezoidal
- $x_{N+1} = x_N + At\,x_N + \frac{At^2}{2}\ddot{x}_N$ Second-order Taylor series

Equations (3-4) through (3-6) together with an integration scheme then represents the computations requirements for the PMGS. Table 3-3, summarizes the requirements for the various models, "Thrust Limit" refers to the limiting of (T/m) to 3 g's. "Constant Gravity" means a flat earth approximation and, therefore, in Equations (3-4):

$$g_x = 0$$

$$g_z = -31 \text{ ft/sec}^2$$

"Spherical Earth Gravity" implies in Equations (3-4):

$$g_x = -\mu x/r^3$$

$$g_z = -\mu z/r^3$$

where

$\mu$ = gravitational constant

r = distance to vehicle from earth's center

Table 3-3. Summary of PMGS Computer Requirements (ALERT Characteristics)

| Second-Stage PMGS | Storage (24-bit words) | Solution Time (ms) |
|---|---|---|
| Model I<br>o Rectangular Integration<br>o Constant Gravity<br>o No Thrust Limit | 460 | Loop time - 1.05<br>Misc - 1.22<br>Total - 11.7<br>(10 steps/iteration) |
| Model II<br>o Trapezoidal Integration<br>o Spherical Earth Gravity<br>o Thrust Limit | 510 | Looptime - 1.24<br>Misc - 1.29<br>Total - 13.7<br>(10 steps/iteration) |
| Model III<br>● Second-Order Taylor Series Integration<br>o Spherical Earth Gravity<br>● Thrust Limit | 520 | Looptime - 1.30<br>Misc - 1.43<br>Total - 14.3<br>(10 steps/iteration) |
| First Stage - Nominal Trajectory | 200 | 0.34 |

### 3.5.3 Computer Mechanization of Equations

For practical implementation on the computer, Equations (3-4) are modified slightly. The sin $\chi$ and cos $\chi$ are calculated from

$$\sin \chi = \tan \chi / \sqrt{1 + \tan^2 \chi}$$

$$\cos \chi = 1 / \sqrt{1 + \tan^2 \chi}$$

The calculation of (T/m) is impractical because there is no measurement available for mass flow rate ($\beta_2$) and initial mass ($m_o$) at the beginning of each iteration. However, $T/m_o$ is available as an initial condition. Therefore,

$$\frac{T}{m(t)} = \frac{T}{m_o} \Big/ \left(1 - \frac{T}{m_o} \frac{t}{C_2}\right)$$

where $C_2$ = exhaust velocity and is a known constant.

The following assumptions were used in estimating the computer requirements for the PMGS:

- Initial conditions are provided by navigation systems.
- Lateral guidance is automatic and not considered in the estimation.
- A/D and D/A conversions are not considered.
- Display generation calculation and storage is not considered.
- Altitude versus velocity is displayed to pilot.

Honeywell's general-purpose airborne computer, the ALERT, is used to estimate the computer requirements.

The version of the ALERT considered here has the following characteristics (Ref. 5):

- DRO miniaturized core memory (2-μ sec cycle time)
- 24-bit word
- 4-μ sec ADD time
- 14-μ sec MULTIPLY time
- 4-μ sec READ time
- 6-μ sec WRITE time

Estimates were made by determining the time required for solution of the PMGS model in the actual simulation on the SDS 9300 and comparing speeds of the 9300 and ALERT. It was found that the ALERT is about 20 percent slower for equivalent fixed-point SDS 9300 calculations.

### 3.5.4 Results and Conclusions

Table 3-3 summarizes the computer requirements for the three models. The requirements of the square-root and arc-tan subroutines are included. Requirements for the first-stage nominal trajectory and associated calculations are also shown; however, it is seen that they are minor when compared with the PMGS. To evaluate the effect of the number of integration steps on the terminal errors in each of the three models, the associated differential equations were integrated in fast-time from 140 seconds to velocity cutoff conditions for a representative number of integration steps. The results are shown in Figures 3-21 and 3-22. In Figure 3-21, the predicted terminal errors in flight-path angle at velocity cutoff are plotted against the number of integration steps. In Figure 3-22, the predicted terminal altitude errors are plotted versus the number of integration steps.

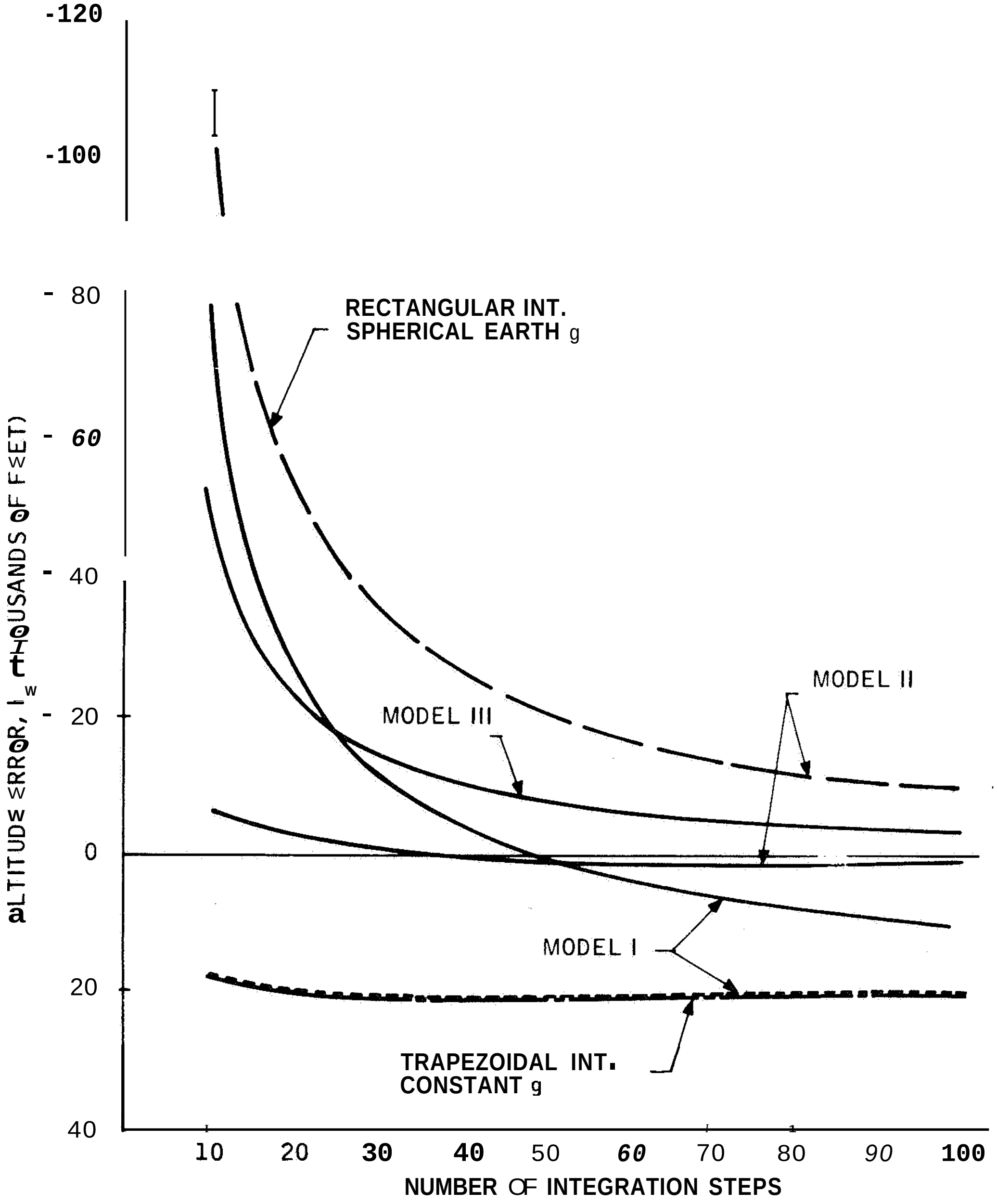

Figure 3-21. Predicted Terminal Flight-Path Angle Error versus Number of Integration Steps

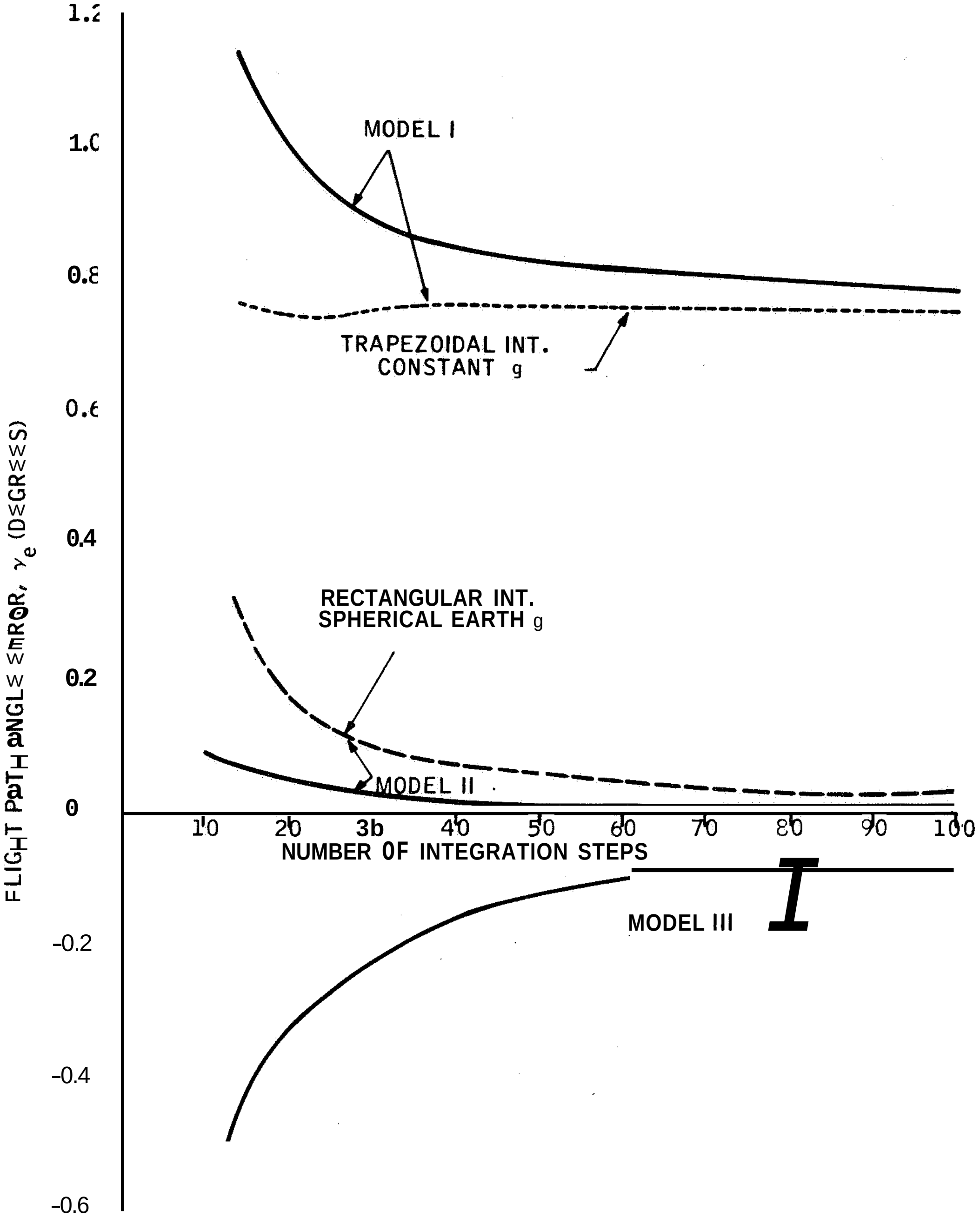

Figure 3–22. Predicted Terminal Altitude Error versus Number of Integration Steps

Two combinations of models I and II are also included to help isolate the important characteristics of each model. Constant values of A and B in Equation (3-4) were used:

$$A = 0.7453$$

$$B = -0.003226 \text{ sec}^{-1}$$

These constants resulted in final errors of -26.0 feet in altitude and -0.026 degree in flight-path angle.

From Figure 3-21 it is seen that the flight-path-angle error is very sensitive to the calculation of gravity; the spherical-earth gravity calculation is an order of magnitude better than the flat-earth constant gravity calculation and is relatively independent of the integration scheme. However, altitude error (Figure 3-22) is strongly dependent on both the integration scheme and the gravity calculations.

The errors in predicted altitude and flight-path angle are due primarily to:

- Inaccurate integration
- Model approximation to the real world (no earth's rotation, etc.)

The inaccurate integration is generally dominant when a small number of steps are used, For many steps, the solutions tend to converge, and errors are the result of the approximations made for the model.

Table 3-4 summarizes computer requirements by function for all parts of the total guidance, navigation and control system. Solution times for both the Saturn V computer and the ALERT are included. By comparing the instruction times of the two computers, it is estimated that the ALERT is approximately 22 times faster than the Saturn V computer. The memory requirements include

Table 3-4. Computer Requirements by Function

| Function | Memory (24-bit words) | Solution Time (ms) | | Solution Rate |
|---|---|---|---|---|
| | | Saturn V Computer | Honeywell ALERT | |
| Predictive Model Guidance Scheme (PMGS) | 510 | 305.0 | 14.3 | 1/sec |
| Iterative Guidance Scheme (IGS) Saturn V Automatic | 1250 | 480.0 | 23.0 | 1/sec |
| Nominal Guidance Scheme (NGS) | 200 | 12.5 | 0.34 | 1/sec |
| Attitude Correction | --- | 18.0 | 0.82 | 25/sec |
| Navigation Equations | 280 | 45.0 | 2.02 | 1/sec |
| Display (NGS) Generation | 45 | 2.2 | 0.1 | 1/sec |
| Display (PMGS) Generation | 55 | 8.8 | 0.4 | 1/sec |
| Executive Program (Interrupt Processing etc.) | --- | 25.0 | 1.14 | ----- |

| Guidance Scheme | Memory (24-bit words) | Solution Time per Second (ms) | |
|---|---|---|---|
| | | Saturn Computer | Honeywell ALERT |
| Predictive Model Guidance Scheme (PMGS) | 845 | 834 | 38.0 |
| Iterative Guidance Scheme (IGS) | 1530 | 1000 (1 sec) | 45.4 |
| Nominal Guidance Scheme (NGS) | 525 | 535 | 24.2 |

any necessary subroutines. Five milliseconds are added to the PMGS and NGS solution times to allow for data conversions between analog and digital portions of the system. When comparing the PMGS and IGS alone, the PMGS (Model II, 10 steps/iteration) requires approximately 40 percent of the IGS memory and 64 percent of the IGS solution time. The requirements for the NGS are minor.

Comparing the guidance schemes alone, however, does not give a true picture of the actual situation. Therefore, Table 3-5 was generated to give a more realistic comparison of the three guidance schemes. The individual functions of Table 3-4 are summed together as a total system consisting of navigation, guidance, control and display. The solution times are based on an iteration rate of one per second. Thus, when comparing the guidance schemes from a total system point of view, the PMGS does not offer a large saving over the IGS in solution time. (834 ms for the PMGS versus 1000 ms for the IGS.) However, the solution time for the PMGS can probably be lowered by more efficient programming of the computer.

Comparison of the PMGS and the NGS with the IGS shows a 45 percent decrease in memory requirements for the PMGS and a 66 percent decrease for the NGS. Solution rates are improved by 17 percent for the PMGS and 47 percent for the NGS.

Three general conclusions can be drawn from the study of computer requirements:

- For the PMGS to compete with the IGS in terms of solution rate, Model II with 10 steps/iteration must be chosen as the model for the PMGS. From Figures **3-21** and 3-22, it is seen that Model II is still quite accurate at 10 steps while the other models have been significantly reduced in performance. If a greater number of steps are used, the solution time of the PMGS approaches or exceeds that of the IGS, and there is no longer any advantage for the PMGS in terms of computer requirements.

- NGS offers a significant decrease in computer requirements over either the PMGS or the IGS.
- The choice between the IGS and PMGS is not clear from the computer requirements alone. Other considerations such as flexibility, reliability and type of mission must be considered,

## 3.6 DISPLAY REQUIREMENTS

In this subsection, the display requirements for the manual guidance task of the ROT are described. A standard analog-driven CRT will satisfy the minimum display requirements; sections 3.6.1 and 3.6.2 describe the system in more detail.

However, display systems for manned spacecraft have grown to the state where many separate devices are required in the cockpit. In the Apollo command module alone over a hundred various display devices are used, and prime panel space is at a premium. Recent advances in computer-driven, multiformat displays may offer an interesting solution to this undesirable trend for next-generation spacecraft. This display system can act as communication channel in the manual guidance loop as well as in a manual control loop, it can present navigational data to the pilot; it can monitor the status of crucial systems and instruct the pilot in emergency situations.

Although a standard CRT will satisfy the minimum display requirements, digital-computer-driven, multi-format CRT or Electroluminescent (EL) display should also be considered for the ROT; a comparison of the two is included in section 3.6.3.

### 3.6.1 Display Format and Size

As discussed in section 3.4, the display of altitude versus velocity (h versus V) is the best display in terms of performance and pilot task loading for both first and second stages. In the PMGS simulation, a general-purpose, digitally driven CRT was used. (see Figure 1-1). Predicted terminal errors were also displayed to the operator. These digital displays are necessary to achieve the reported performance and are assumed to be the outputs of digital voltmeters when determining minimum display requirements. With this assumption, a standard laboratory-type CRT may be used to display the nominal and predicted trajectories.

A 12-inch usable area (12 inches on a side) CRT was used in the simulation. This however, is obviously impractical for the cockpit of a spacecraft. The minimum ideal display size depends (aside from cockpit space constraints) on the resolution of the display, the resolution of the eye, and the normal viewing distance. Resolution is governed by the eye which in cockpit viewing distances (nominally 2 feet) is 75 lines/inch (Ref. 6, p. 338). The eye resolution is about one minute of arc and, under vibration, deteriorates by a factor of 2 to 5. Thus 75 lines/inch provides adequate resolution over a wide range of viewing distances. A practical size for a cockpit CRT is 6 to 8 usable inches. The display should then have a resolution of about 600 lines.

In the simulation, scale factors of about 50,000 ft/in. in altitude and 200 fps/in. in velocity were used. Some human factors work must be done to define the scale factors, since the actual display will be smaller than the laboratory model. Through a change in scale factors during a flight, the requirement for display of the terminal errors might also be eliminated.

In addition to the display of actual position on the first-stage nominal trajectory, a "quickened" symbol is displayed to the pilot. This display allows the pilot to see approximately what effect his current input has $\tau$ seconds in the future. The quickened symbol is driven by a simple first-order Taylor series expansion about the current position:

$$h(t+\tau) = h(t) + \tau \dot{h}(t)$$

$$v(t+\tau) = v(t) + \tau \dot{v}(t)$$

where $\tau = 20$ seconds in the simulation.

Although this quickening is not necessary to fly the vehicle, it is convenient and reduces work load, especially when a large off-nominal condition develops.

### 3.6.2 Computation Requirements

The computation required for display of the predicted and nominal trajectories can be broken down as follows:

(1) Storage of the points as they are computed (not required for nominal trajectory)

(2) Scaling of the points to be displayed

(3) Processing of interrupts for display refreshing

(4) Output (digital to analog) to CRT display

These computations are included in the summary of computer requirements in Table 3-4. Points (1) and (2) require an iteration rate of one per second (same as major computation loop) and are listed as "Display Generation" in the table. The Executive program is assumed to handle the interrupt processing and output to the scope. Interrupt frequency must be high enough to eliminate flicker and depends on the display hardware. The refresh rate for a fast-erase storage tube would be one per second, while a conventional CRT requires 20 to 50 per second.

### 3.6.3 CRT and Electroluminescent (EL) Displays

With increasing emphasis being given to man's role in spacecraft, the guidance of his activities is one of the most challenging areas in display technology. At the same time, however, the constraints put on such displays -- low weight, high reliability, and reluctance to use untried techniques -- are leading to a cautious approach to the procurement of flight hardware. As a result, the spacecraft display field is a field full of new ideas, but the hardware being developed is mostly conventional.

The use of computer-driven, multi-format CRT and/or EL displays appear to be the best solution to the ambitious goal of an integrated cockpit display panel. However, a direct comparison of CRT and EL displays is, at best, difficult because of differences in hardware and stages of development. The increasing level of support being given to EL research affords excellent prospects that the post-1970 cockpit will be equipped with computer-controlled EL, indicator panels, replacing the conventional dial and tape-driven indicators of today's aerospace vehicles. With respect to the dynamic display requirement such as manual guidance, typically provided by CRT's, more fundamental difficulties exist. The advances required over the current state of the art for EL's are discussed later in this subsection. Five or more years is estimated as the time required before EL displays can compete with the performance of present CRT's for dynamic displays. Table 3-6, taken from Reference 6, presents projected display technology for avionic systems. It appears, then, that the first generation integrated cockpits may be a combination -- EL's for indicator panels and CRT's for dynamic situation displays.

The advantages enjoyed by CRT's are largely in their high state of development and high resolution (100 lines/in., typically). A CRT for energy management is currently being used in the X-15. Main advantages of EL's are their flat, sturdy screens with high reliability and low power requirements. The greatest problems at present are low resolution and large computer memory requirement posed by the high scanning rates which must be developed to address the X-Y grid configuration. CRT's have the disadvantages of being complex and being incompatible with crowded cockpit weight and volume constraints. Table 3-7 is a generalized comparison of EL and CRT's when applied to a dynamic display situation.

For EL to compete with CRT displays, the following advances must be made over the state of the art:

- Higher resolution (75 to 100 lines/in.)
- Availability of a batch-fabricated device incorporating the necessary properties for addressing, drive and interframe memory
- Availability of a batch-fabricated data buffer to reduce input/output traffic between the central computer and the display

Figures 3-23 and 3-24 are typical block diagrams for CRT and EL display systems. The block diagram for a general-purpose computer-driven CRT display such as one used for the ROT simulation is shown in Figure 3-23. A laboratory flight model of an EL display system taken from Reference 7 is shown in Figure 3-24.

Table 3-6. Projected Avionic Display Technology

| Item | Operational Use Date | | | |
|---|---|---|---|---|
| | 1965 | 1966 | 1969-70 | 1973-78 |
| System Display Functions | Pilotage, navigation, weapons delivery | Same, with pilotage augmented by transition and hover requirements | Augmented by reconnaissance functions | Same |
| Heads-Up Display | Bright CRT and projection system; mechanical reticles | Same, with addition of electronic reticles and higher brightness tube | Same, with ±25-degree optics (spherical lens) | Same, with possibility of transparent EL |
| Instruments | Round dial | Tape | High-contrast EL panels | EL panels with improved contrast and brightness |
| Multisensor | Direct view storage | Multimode storage | High-resolution flat-tube CRT with scan conversion; adaptable to varying sensor data rates vs rapid-erase storage tubes | EL panels vs CRT and scan conversion vs rapid-erase storage tube |
| Horizontal Situation Display | Conventional mechanization indicators | CRT display; superimposed map; electronic symbol; generator; selectable and superimposed video | Same, plus improved display tubes | Rapid-erase storage tube; solored symbology |
| Navigation and Tactical Maps Display | Paper maps, hand-held | Integrated into horizontal situation display | Same | Same |
| Physical Characteristics | | Fully electronic display system | 20 percent weight reduction through scan conversion; lower power; higher display legibility | Additional volume savings through flat EL displays |
| Total System | | | | |
| Weight (lbs) | | 150 | 120 | 100 |
| Volume (cu. in.) | | 6400 | 5200 | 3700 - 5000 |
| Power (watts) | | 800 | 625 | 600 |
| MTBF (hrs) | | 1000 | 2000 | 3000 |

Table 3-7. Comparison of CRT and EL Displays

| Characteristic | Electroluminescent (EL) Display | Cathode Ray Tube (CRT) Display |
|---|---|---|
| Cockpit Display Weight and Volume | Low | High |
| Power Requirements | Low | High |
| Complexity | Low | High |
| Reliability | High, potentially | Medium |
| Development Risk | High | Low |
| Production Cost | Low, potentially | High |
| Failures | Gradual (one element at a time) | Catastrophic (tube burn-out) |
| Associated Computer Requirements | High | Medium |
| Resolution | Low (25-40 lines/in state of art) | High |
| Viewability | High (flat screen) | Medium (parallax) |
| Compatibility with Integrated Circuits | Good, potentially | Poor |

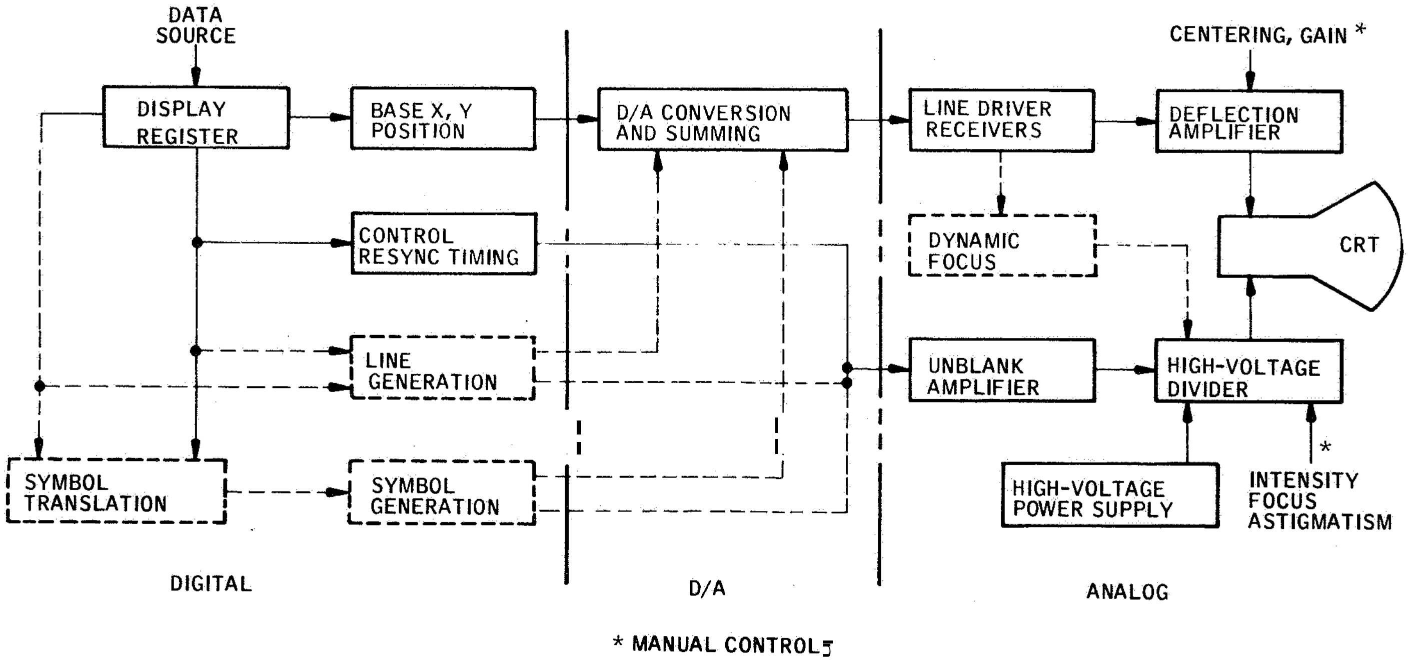
DATA SOURCE
DISPLAY REGISTER
BASE X, Y POSITION
D/A CONVERSION AND SUMMING
LINE DRIVER RECEIVERS
DEFLECTION AMPLIFIER
CENTERING, GAIN *
CONTROL RESYNC TIMING
DYNAMIC FOCUS
CRT
LINE GENERATION
UNBLANK AMPLIFIER
HIGH-VOLTAGE DIVIDER
SYMBOL TRANSLATION
SYMBOL GENERATION
HIGH-VOLTAGE POWER SUPPLY
*
INTENSITY
FOCUS
ASTIGMATISM
DIGITAL
D/A
ANALOG
* MANUAL CONTROLS

Figure 3-23. Basic CRT Block Diagram

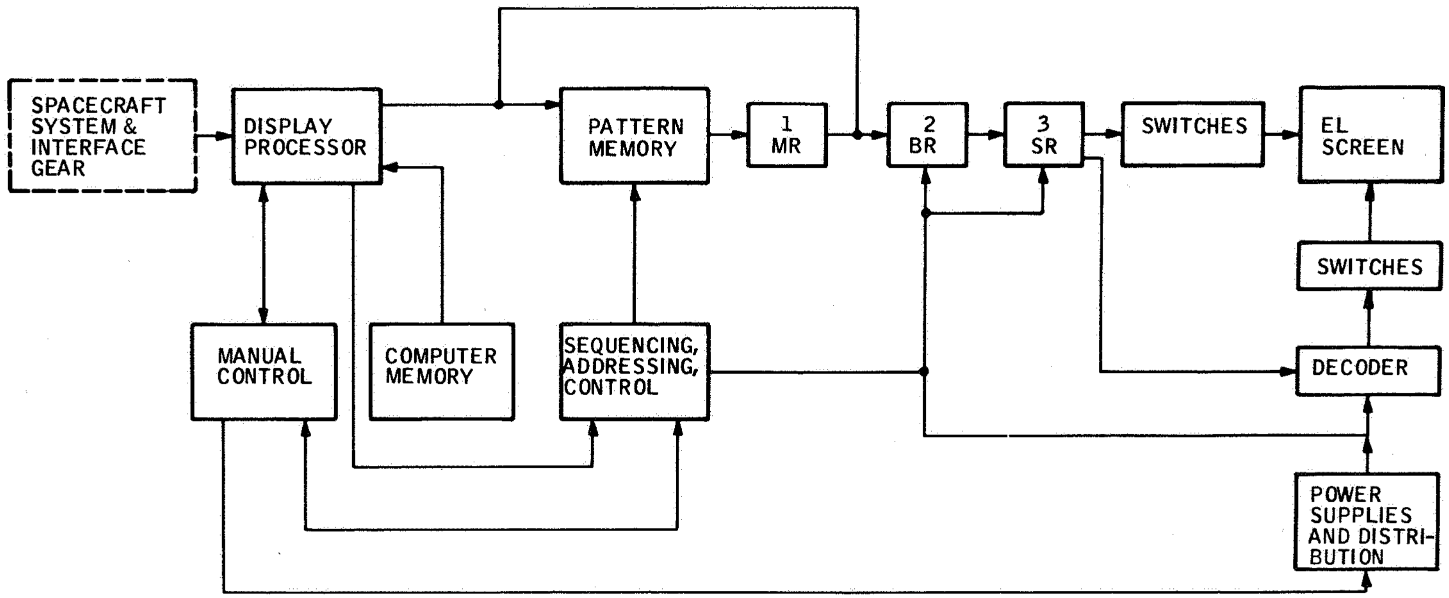
SPACECRAFT SYSTEM & INTERFACE GEAR
DISPLAY PROCESSOR
PATTERN MEMORY
1 MR
2 BR
3 SR
SWITCHES
EL SCREEN
SWITCHES
DECODER
POWER SUPPLIES AND DISTRI-BUTION
MANUAL CONTROL
COMPUTER MEMORY
SEQUENCING, ADDRESSING, CONTROL

EL SCREEN = 4 x 4 INCHES, 40 LINES/INCH
= 25,600 ELEMENTS
PATTERN MEMORY = 2048 - 24 BIT WORDS
COMPUTER MEMORY = 2048 - 24 BIT WORDS
DISPLAY PROCESSOR - PARALLEL ARITHEMTIC

1 MEMORY REGISTER
2 BUFFER REGISTER
3 SCREEN REGISTER

Figure 3-24. EL Flight Model Block Diagram

# SECTION 4
# MANUAL OPTIMAL GUIDANCE SCHEME - SUMMARY

This section summarizes the guidance scheme developed in this study in terms of a short description and a discussion of computation, display, and navigation requirements.

## 4.1 DESCRIPTION

The manual optimal guidance scheme for two-stage boost into a circular orbit consists of two schemes: a nominal guidance scheme during the first-stage aerodynamic phase and a predictive model scheme during the second-stage vacuum phase.

The nominal guidance scheme, (Figure 4-1) consists of a two-dimensional CRT display of the fuel-optimal trajectory from nominal initial conditions to staging conditions. This optimal trajectory is fuel-optimal for the total mission, i. e. , from liftoff to orbit injection. The nominal trajectory is stored in the onboard computer. The present vehicle state is displayed on the CRT so that the pilot is given information concerning his present status as well as where he should be (the nominal trajectory). A short-term (0-30 seconds) prediction of the vehicle state is also displayed on the CRT. This is helpful to the pilot in steering the vehicle along the nominal trajectory. This predicted state is obtained by measuring the derivative of the vehicle state and is approximated by:

$$X_p(t) = X\ (t + \tau) = X(t) + \tau\dot{X}\ (t)$$

where

$X(t)$ is the present state

$X_p(t)$, $X(t + \tau)$ is the predicted state or state at time $t + \tau$, t is present time.

A digital readout of present vehicle altitude and time are also available to the pilot.

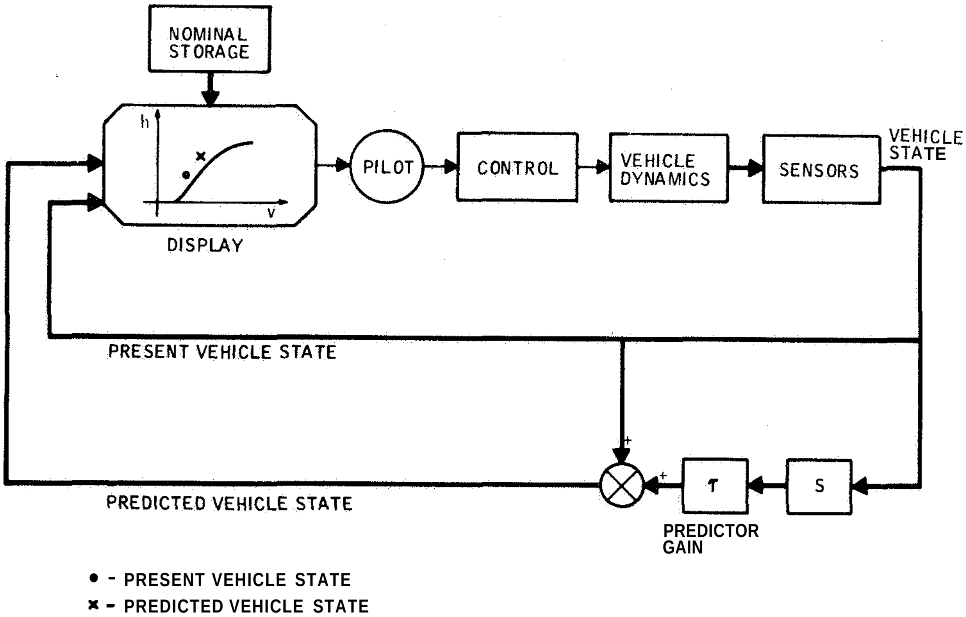
NOMINAL STORAGE
h
v
DISPLAY
PILOT
CONTROL
VEHICLE DYNAMICS
SENSORS
VEHICLE STATE
PRESENT VEHICLE STATE
+
+
τ
S
PREDICTOR GAIN
PREDICTED VEHICLE STATE
• - PRESENT VEHICLE STATE
× - PREDICTED VEHICLE STATE

Figure 4-1. Nominal Guidance Scheme Block Diagram

The pilot's task is to steer the vehicle (i. e. , control body attitude) so that the present vehicle state is on the nominal trajectory. The lateral guidance or out-of-plane motion is handled by an automatic system (see section 3. 3. 2).

The predictive model guidance scheme (Figure 4-2) consists of a simplified mathematical model of the vehicle dynamics which operates repetitively in faster than real time to give the pilot an accurate prediction of his flight path and predicted terminal errors. The pilot adjusts two optimization parameters (A and B in Figure 4-2). These parameters and the predicted

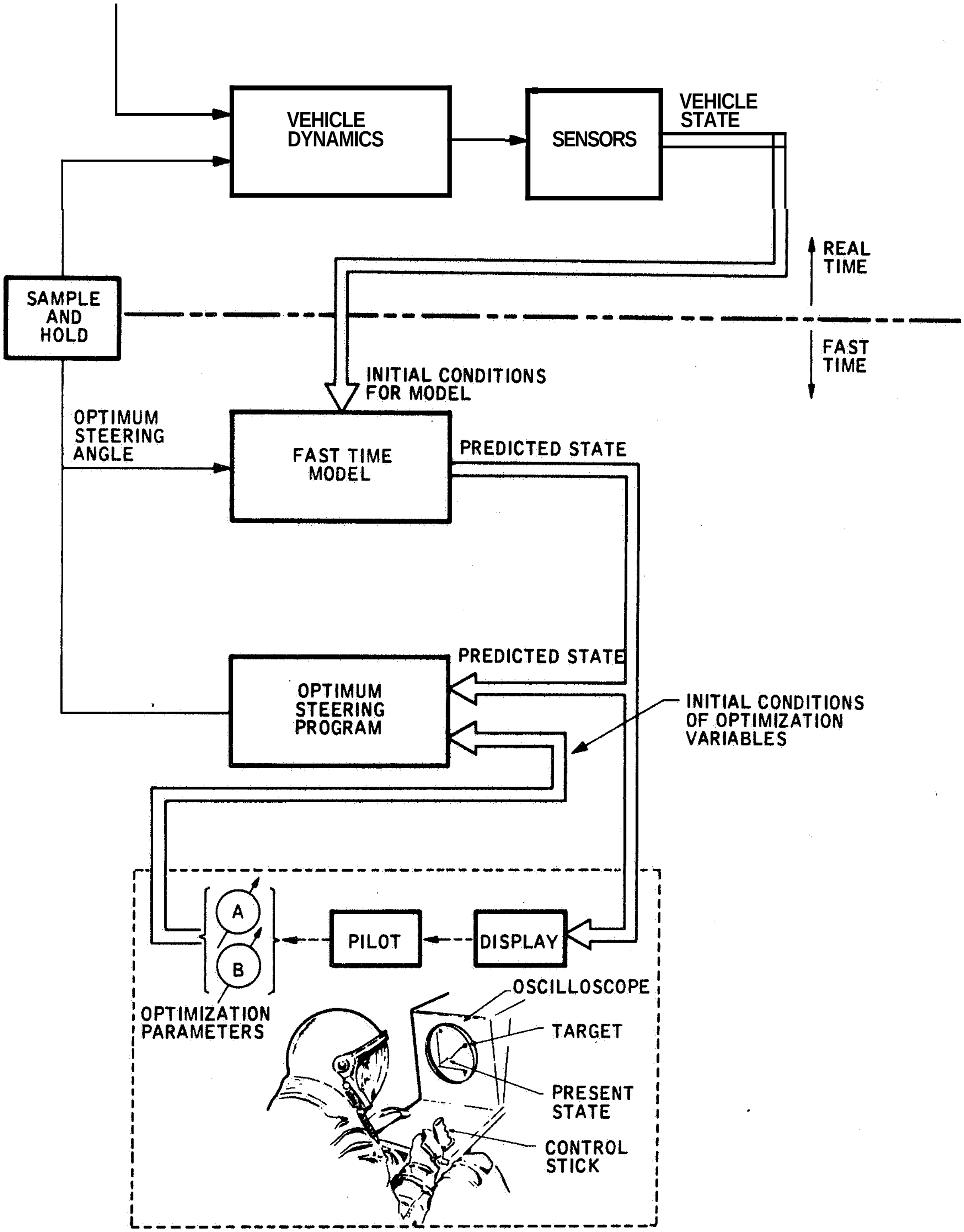
VEHICLE DYNAMICS
SENSORS
VEHICLE STATE
REAL TIME
SAMPLE AND HOLD
FAST TIME
INITIAL CONDITIONS FOR MODEL
OPTIMUM STEERING ANGLE
FAST TIME MODEL
PREDICTED STATE
PREDICTED STATE
OPTIMUM STEERING PROGRAM
INITIAL CONDITIONS OF OPTIMIZATION VARIABLES
A
B
PILOT
DISPLAY
OPTIMIZATION PARAMETERS
OSCILLOSCOPE
TARGET
PRESENT STATE
CONTROL STICK

Figure 4-2. Block Diagram of Predictive Model Guidance Scheme

vehicle state are inputs to the optimum steering program which generates the fuel-optimum steering angle time history for the fast-time model. The pilot adjusts A and B so that the predicted trajectory passes through the target conditions.

In addition to the two-dimensional display of the predicted trajectory, a digital read out of the predicted terminal errors is also displayed to the pilot.

The pilot's task in this guidance scheme is to continually adjust the optimization parameters A and B to minimize the predicted error in the altitude and flight-path angle. In detail, the operations are as follows:

(1) The pilot selects values for A and B.

(2) The computer then integrates the predictive model equations of motion and displays the resulting trajectory.

(3) On the basis of the resulting error in the predicted terminal conditions, the pilot makes an adjustment to the parameters A and B.

(4) This process is repeated at the rate of one fast-time solution per second until values for A and B are determined which yield zero error in the predicted terminal conditions.

## 4.2 COMPUTATION REQUIREMENTS

The digital computer requirements for the navigation, guidance, control and display computations for implementation of the manual guidance scheme developed during this study are presented in this section. These requirements are given for two state-of-the-art airborne digital computers, the Saturn V and Honeywell's ALERT.

- The requirements for first-stage guidance using the Nominal Guidance Scheme and assuming the data displayed is updated once per second are:

  (1) Memory - 525 24-bit words

  (2) Solution time, including attitude correction (25/sec), navigation computations, display generation, guidance computations, and executive program --

  | | |
  |---|---|
  | 535 ms/sec | (Saturn V) |
  | 24.2 ms/sec | (ALERT) |

- The requirements **for** second-stage guidance using the Predictive Model Guidance Scheme and assuming the data displayed is updated once per second are:

  (1) Memory - 845 24-bit words

  (2) Solution time, including attitude correction (25/sec), navigation computations, display generation, guidance computations and executive program --

  | | |
  |---|---|
  | 834 ms/sec , | (Saturn V) |
  | 38 ms/sec | (ALERT) |

Tables 3-4 and 3-5 summarized and compared the computer requirements for the manual and automatic (Saturn V - iterative guidance mode) guidance schemes.

## 4.3 DISPLAY REQUIREMENTS

The display requirements for implementation of the manual guidance scheme developed during this study are presented in this subsection.

- One standard analog-driven, single-gun, CRT for each stage with 6 to 8 inches of usable area is required.
- The display format for the first stage consists of an altitude-versus-velocity display of the nominal trajectory. The vehicle present state and predicted state are also displayed on the CRT. Although not essential to the manual guidance task, the pilot would also have the vehicle pitch attitude from the conventional attitude-ball and present time from the real-time clock.
- The display format for the second stage consists of an altitude-versus-velocity display of the predicted trajectory beginning with the present vehicle state and terminating with velocity cutoff conditions. This format is updated once per second.
- Two digital voltmeters are required for presentation of predicted terminal altitude and flight-path-angle errors. These meters are updated once per second. The pilot also has at his disposal vehicle attitude from the attitude ball and present time (nominal time-to-go) from the real-time clock.

Section 3.6 discusses the display requirements further and presents the details of the displays used in this simulation study.

## 4.4 NAVIGATION REQUIREMENTS

The navigational requirements for implementation of the manual guidance scheme developed during this study are identical with that of the Saturn-type launch vehicles (Ref. 2). In Reference 2, the ST124-M inertial platform system is described.

This system provides the integrated acceleration data, inertial reference coordinates, and vehicle attitude measurements for guidance and control of the Saturn space launch vehicle.

# SECTION 5
# RECOMMENDATIONS FOR FUTURE WORK

## 5.1 FUTURE STUDIES

The following items are recommended for future study.

(1) The application of the Predictive Model Guidance Scheme (PMGS) to other guidance phases; for example, re-entry, orbit-to-orbit, rendezvous, mid-course and boost for vehicles with an offset launch capability should be considered.

(2) Human factors studies are recommended on display formats for manual guidance and control relating to:

   (a) The choice of optimal scale factors.

   (b) The optimum position of the digital readout of predicted terminal errors with respect to the trajectory display in the Predictive Model Guidance Scheme.

   (c) The effect on the pilot and display formats of in-flight mission changes and equipment failures.

   (d) The effect on the pilot of inverting the axes of the display format, i.e., from altitude versus velocity to velocity versus altitude (is one format more desirable than the other?).

   (e) The effect on system performance of nulling the performance index rather than terminal altitude and flight-path-angle errors.

   (f) The effect on computer requirements and pilot performance of lowering the iteration rate, i.e., from 1/sec. to .5/sec.

(3) The minimum computer and display requirements for manual control of space booster vehicles must be determined. The present study was concerned with the manual guidance problem.

(4) A study is recommended to combine the present results on manual guidance with results from the study on manual control to form an integrated manual guidance and control system for booster vehicles.

(5) A study on the data processing requirements for multi-format cockpit hardware is timely and is strongly recommended.

## 5.2 FUTURE HARDWARE DEVELOPMENT

No hardware development program is needed to implement the optimal manual guidance scheme described in Section 4. However, due to the advantages of a multi-format display concept for future spacecraft, it is recommended that a new program be initiated to continue development of a computer-driven, completely solid-state display device such as EL.

# REFERENCES

1. Lockheed Technical Report IR 18387, "Reusable Orbital Transport - Baseline Vehicle, First-Stage Definition", December, 1964.
2. Haeusserman, W., "Guidance and Control of Saturn Launch Vehicles", AIAA Paper 65-304, July, 1965.
3. Gilchrist, J. D. , and Livingston, R., "Research on Computational and Display Requirements for Human Control of Space Vehicle Boosters", Honeywell Document 12513-FR2-I, November, 1966.
4. Martin, D. R., et al, "Saturn V Guidance, Navigation, and Targeting", Journal of Spacecraft, **4**, No. 7 (July, 1967), 891-898.
5. "General Description of the ALERT General Purpose Digital Computer", Honeywell Aerospace Division, St. Petersburg, Florida.
6. Pizzicara, D. J. , "Computers and Displays/Controls - State-of-the-Art Technology Studies", Litton Systems Inc., AD631663, February, 1966.
7. Acker, J. R., and Raymond, R. G., "Integrating the Operational Spacecraft Displays into Future Guidance and Control Systems", AIAA Paper 67-552, August, 1967.
8. Bates, J. C., Gilchrist, J. D., Harvester, V. G., and Soland, D. E., "Research on Computational and Display Requirements for Human Control of Space Vehicle Boosters", Honeywell Document 12513-FR1-I, July, 1966.
9. Hookway, R., et al, "Manual Guidance of Large Space Boosters", Conference Proceedings 1964 National Winter Convention on Military Electronics, IEEE PTGME, February. 1964.

10. Williams, D. F., et al, "Manned Booster Control - Man Capabilities", Boeing Document D5-11373, April 1964.

11. Brown, I. D., "The Measurement of Perceptual Load and Reserve Capacity", Applied Psychology Unit, Cambridge, Report No. APU 509, 1964.

12. Knowles, W. B., "Operator Loading Tasks", Human Factors, 1963, 5, 155-161.

13. Ekstrom, P. J., "Analysis of Pilot Work Loads in Flight Control Systems with Different Degrees of Automation". Paper presented at the International Congress of Human Factors in Electronics, Long Beach, California, 3-4 May, 1962.

14. Stearns, E. V. B., Navigation and Guidance in Space, Prentice-Hall, Inc., Englewood Cliffs, N. J., 1963.

# APPENDIX A
# ROT REAL-TIME MATHEMATICAL MODEL AND DATA SUMMARY

# APPENDIX A

# ROT REAL-TIME MATHEMATICAL MODEL AND DATA SUMMARY

A flight-path (wind-axis) coordinate system was used for the real-time simulation of the ROT. The equatians are derived assuming a spherical, rotating earth where the velocity (V), flight-path angle ($\gamma$), and heading angle ($\Psi$) define the system. This appendix contains an outline of the derivation of the equations as well as a summary of the equations and data used in the simulation.

The vector equation describing the point-mass motion is:

$$\overline{T} + \overline{A} + \overline{mg} = m \left( \frac{d}{dt} (\overline{V}) + 2 \overline{\omega}_e \times \overline{V} + \overline{\omega}_e \times (\overline{\omega}_e \times \overline{r}) \right) \tag{A1}$$

where $\overline{T}$ = thrust forces

$\overline{A}$ = aerodynamic forces

$\overline{g}$ = gravity forces

$\overline{V}$ = vehicle's velocity with respect to the earth

$\overline{\omega}_e$ = earth's rotation vector

$\overline{r}$ = radius vector to vehicle

Three coordinate systems are needed for the derivation:

(1) $\overline{i}_e, \overline{j}_e, \overline{k}_e$ - earth-fixed

(2) $\overline{i}_h, \overline{j}_h, \overline{k}_h$ - local horizon

(3) $\overline{i}_w, \overline{j}_w, \overline{k}_w$ - wind axis

($\overline{i}, \overline{j}, \overline{k}$ are unit vectors)

Figures A1 and A2 define these coordinate systems.

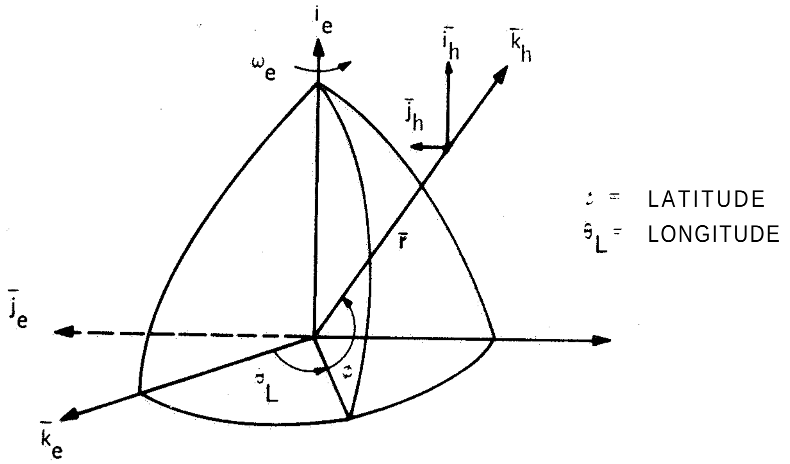
$\bar{i}_e$
$\omega_e$
$\bar{i}_h$
$\bar{k}_h$
$\bar{j}_h$
$\phi$ = LATITUDE
$\theta_L$ = LONGITUDE
$\bar{r}$
$\bar{j}_e$
$\theta_L$
$\phi$
$\bar{k}_e$

Figure A1. Local Horizon and Earth-Fixed Coordinate Systems

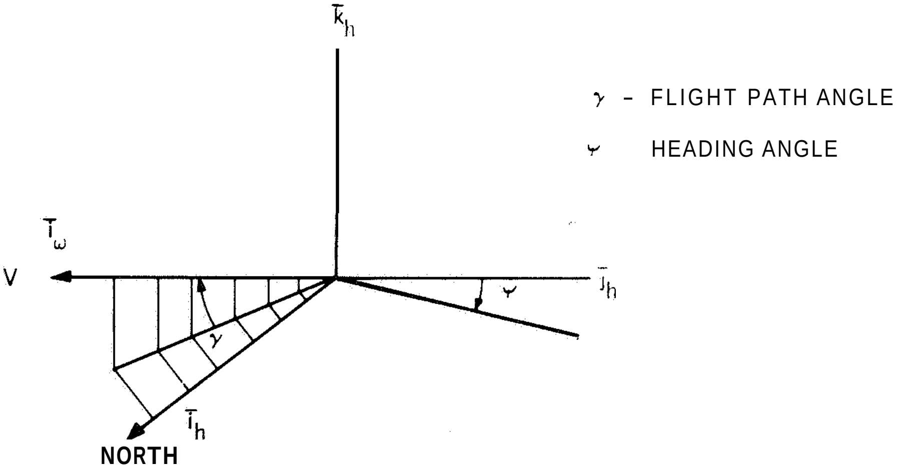
$\bar{k}_h$
$\gamma$ - FLIGHT PATH ANGLE
$\psi$ HEADING ANGLE
$\bar{i}_\omega$
V
$\bar{j}_h$
$\psi$
$\gamma$
$\bar{i}_h$
NORTH

Figure A2. Definition of Wind Axes

The following coordinate transformations are useful:

$$\begin{vmatrix} \bar{i}_h \\ \bar{j}_h \\ \bar{k}_h \end{vmatrix} = \begin{vmatrix} c\phi^{*} & s\phi s\theta_L & -s\phi c\theta_I \\ 0 & c\theta_L & s\theta_L \\ s\phi & -c\phi s\theta_L & c\phi c\theta_L \end{vmatrix} \begin{vmatrix} \bar{i}_e \\ \bar{j}_e \\ \bar{k}_e \end{vmatrix} = Q_1 \begin{vmatrix} \bar{i}_e \\ \bar{j}_e \\ \bar{k}_e \end{vmatrix} \qquad \text{(A2)}$$

(earth-fixed to local horizon)

$$\begin{vmatrix} \bar{i}_w \\ \bar{j}_w \\ \bar{k}_w \end{vmatrix} = \begin{vmatrix} c\gamma c\Psi & -c\gamma s\Psi & sy \\ s\Psi & CY & 0 \\ -s\gamma c\Psi & s\gamma s\Psi & cy \end{vmatrix} \begin{vmatrix} \bar{i}_h \\ \bar{j}_h \\ \bar{k}_h \end{vmatrix} = Q2 \begin{vmatrix} \bar{i}_h \\ \bar{j}_h \\ \bar{k}_h \end{vmatrix} \qquad \text{(A3)}$$

From Figure A1:

$$\bar{r} = r\,\bar{k}_h \qquad \text{(A4)}$$

$$\bar{\omega}_h = \theta_L\, c\,\phi\, \bar{i}_h + \phi\, \bar{j}_h + \theta_L\, s\,\phi\, \bar{k}_h \qquad \text{(A5)}$$

(Rotation of local horizon system with respect to earth - fixed system)

$$\bar{V} = V\,\bar{i}_w = V\,(c\gamma c\Psi \bar{i}_h - c\gamma s\Psi \bar{j}_h + s\gamma\, \bar{k}_h) \qquad \text{(A6)}$$

---

$^{*}c\phi = \cos(\phi)$

$s\phi = \sin(\phi)$

Also,

$$\overline{V} = \frac{d}{dt}(r) = \frac{d}{dt}\left(r\,\overline{k}_h\right) = \dot{r}\overline{k}_h + \omega_h \times r\,\overline{k}_h = \dot{r}\,\overline{k}_h - r\dot{\theta}_L c\phi\overline{j}_h + r\dot{\phi}\overline{i}_h \qquad \text{(A7)}$$

Now equating Equations (A6) and (A7) yields:

$$r = h = V \sin\gamma \qquad \text{(A8)}$$

$$\dot{\phi} = V \cos\gamma \cos\Psi / r \qquad \text{(A9)}$$

$$\dot{\theta}_L = V \cos\gamma \sin\Psi / r \cos\phi \qquad \text{(A10)}$$

The rotation of the wind axis with respect to the earth fixed system from Figure A2 is:

$$\overline{\omega}_w = p_w\,\overline{i}_w + q_w\,\overline{j}_w + r_w\overline{k}_w = \overline{\omega}_h - \dot{\gamma}\,\overline{j}_w - \Psi\overline{k}_h \qquad \text{(A11)}$$

or

$$\overline{\omega}_w = \begin{vmatrix} p_w \\ q_w \\ r_w \end{vmatrix} = \left| \begin{vmatrix} 0 & 0 & -sy \\ 0 & -1 & 0 \\ 0 & 0 & -cy \end{vmatrix} \begin{matrix} 0 \\ \gamma \\ \dot{\Psi} \end{matrix} \right| + Q_2\,\overline{\omega}_h \qquad \text{(A12)}$$

The projection of the earth's rotation rate on the wind axis is:

$$\overline{\omega}_e = \begin{vmatrix} p_{ew} \\ q_{ew} \\ r_{ew} \end{vmatrix} = Q2\,Q1 \begin{vmatrix} \omega_e \\ 0 \\ 0 \end{vmatrix} \qquad \text{(A13)}$$

From Figure A3, the thrust, aerodynamic and gravity forces in the wind axis system are:

$$\frac{\bar{T}}{m} = \frac{T}{m}\left( c\alpha\, \bar{i}_w - s\alpha\, s\sigma\, \bar{j}_w + s\alpha\, c\sigma\, \bar{k}_w \right) \tag{A14}$$

$$\frac{\bar{A}}{m} = -\frac{D}{m}\,\bar{i}_w - \frac{L}{m}\sin\sigma\,\bar{j}_w + \frac{L}{m}\cos\sigma\,\bar{k}_w \tag{A15}$$

$$\bar{g} = -g\,(s\gamma\,\bar{i}_w + c\gamma\,\bar{k}_w) \tag{A16}$$

where $\sigma$ = wind-axis bank angle.

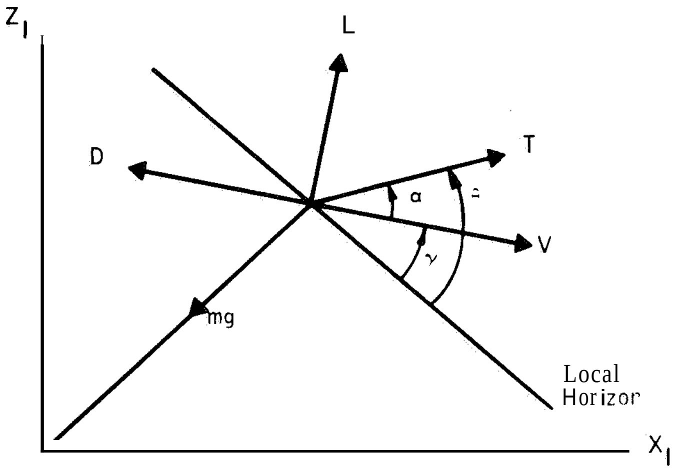

Figure A3. Force Diagram

Finally

$$\frac{d}{dt}(\bar{V}) = V\,\bar{i}_w + \bar{\omega}_w \times \bar{V} = V\,\bar{i}_w + V\,r_w\,\bar{j}_w - V\,q_w\,\bar{k}_w \tag{A17}$$

Equations for $\dot{V}$, $\dot{\gamma}$ , and $\dot{\Psi}$ can now be formulated by equating the components along the three axes from Equation (A1). The Coriolis and centrifugal acceleration terms are respectively in wind axes:

$$2\,\overline{\omega}_e \times \overline{V} = 2V\,(r_{ew}\,\overline{j}_w - q_{ew}\,\overline{k}_w) \tag{A18}$$

and

$$\overline{\omega}_e \times (\overline{\omega}_e \times \overline{r}) = \omega_e^{2}\, r\, Q_2 \begin{vmatrix} c\phi s\phi \\ o \\ -c^{2}\phi \end{vmatrix} \tag{A19}$$

Now substituting Equations (A14) - (A19) and equating terms yields:

$$\dot{V} = -\frac{D}{m} - g\sin\gamma + \frac{T}{m}\cos\alpha + \omega_e^{2} r\,[c2\phi\, s\gamma - c\gamma\, c\Psi\, c\phi\, s\phi] \tag{A20}$$

$$\dot{\gamma} = \left(\frac{L}{m} + \frac{T}{m}\sin\alpha\right)\frac{\cos\sigma}{V} - g\,\frac{\cos\gamma}{V} + \frac{V\cos\gamma}{r} + 2\,\omega_e\, c\phi s \Psi \tag{A21}$$

$$+\frac{\omega_e^{2} r}{V}\,(e\phi\, s\phi\, c\Psi\, s\gamma + c^{2}\phi\, c y)$$

$$\dot{\Psi} = \left(\frac{L}{m} + \frac{T}{m}\sin\alpha\right)\frac{\sin\sigma}{V\cos\gamma} + \frac{V}{r}\,\frac{c\gamma s\Psi\, s\phi}{c\phi} + 2\,\omega_e\,[s\phi - \frac{s\gamma\, c\Psi c\phi}{c\gamma} 3$$

$$+\frac{\omega_e^{2} r\, s\phi\, c\phi\, s\Psi}{V\cos\gamma} \tag{A22}$$

Equations (A20) - (A22) and (A8) - (A10) now define the vehicle's three dimensional position. Figure A4 is a summary of the real-time coordinate system.

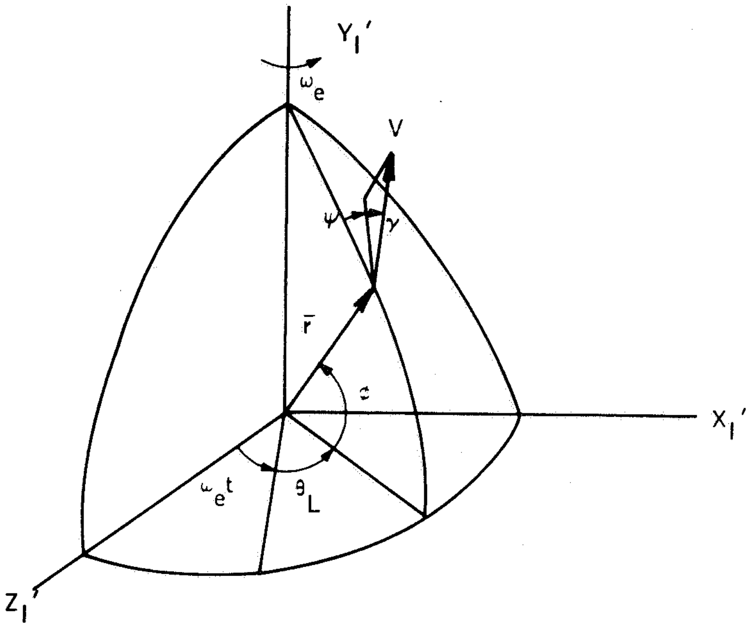
$Y_I'$
$\omega_e$
V
$\psi$
$\gamma$
$\bar{r}$
$\sigma$
$X_I'$
$\omega_e t$
$\theta_L$
$Z_I'$

Figure A4. Real-Time Coordinate System

For completeness, all data and equations describing the simulation are summarized below.

- First-Stage Model -

$$\dot{V} = \frac{T\cos\alpha}{m} - \frac{D}{m} - g\sin\gamma$$

$$+ \omega_e^2 r \left[\cos^2\phi \sin\gamma - \cos Y \cos\psi \cos\phi \sin\phi\right]$$

$$\dot{\gamma} = \left[\frac{T\sin\alpha}{mV} + \frac{L}{mV}\right]\cos\sigma - \left[\frac{g}{V} - \frac{V}{r}\right]\cos\gamma$$

$$+ 2\,\omega_e \cos\phi \sin\psi + \frac{\omega_e^2}{V}\left[\cos_\phi \sin\phi \cos\psi \sin\gamma + \cos^2\phi \cos\gamma\right]$$

$$\dot{\psi} = \left[\frac{T\sin\alpha}{mV} + \frac{L}{mV}\right]\frac{\sin\sigma}{\cos\gamma} + \frac{V}{r}\,\frac{\cos\gamma\,\sin\psi\,\sin\phi}{\cos\phi}$$

$$-\,2\,\omega_e\left[\frac{\sin\phi - \sin\gamma\,\cos\psi\,\cos\phi}{\cos\gamma}\right] + r\,\omega_e^{2}\,\frac{\sin\phi\,\cos\phi\,\sin\psi}{V\cos\gamma}$$

$$\dot{\phi} = \frac{V\cos\gamma\,\cos\psi}{r}$$

$$\dot{\theta}_L - \frac{V\cos\gamma\,\sin\psi}{r\cos\phi}$$

$$r = h = V\sin\gamma$$

$$L = \frac{1}{2}\,\rho V^2 S\, C_{L_{\alpha}}\,\alpha$$

$$D = \frac{1}{2}\,\rho\, V^2\, S\left[C_{D_o} + K\, C_{L_{\alpha}}\,\alpha^2\right]$$

$$\alpha = \theta - \gamma$$

$$\sigma = K_{\dot{Y}}\,Y_I + K_{\dot{Y}}\,\dot{Y}_I$$

$$\dot{m} = -\beta_1$$

$$T = C_1\beta_1$$

$$g = g_o\left(\frac{r_o}{r}\right)^2$$

$$\rho = \rho_o\, e^{-h/\lambda}$$

$$M = V/a$$

- Second-Stage Model - Some of the equations are modified somewhat for the second stage because aerodynamics are neglected. The modified equations are:

$$V = \frac{T}{m}\cos\delta_Y \cos a - g\sin\gamma$$

$$+\ \omega_e^2\ r\,[\cos2\phi\sin\gamma - \sin\phi\cos\phi\cos\psi\cos\gamma]$$

$$\dot{\gamma} = \frac{T}{mV}\sin\alpha\cos\delta_Y - \left[\frac{g}{V} - \frac{V}{r}\right]\cos\gamma + 2\,\omega_e\cos\phi\sin\psi$$

$$+\ \frac{\omega_e^2}{V}\,r\,[\cos\phi\sin\phi\cos\psi\sin\gamma + \cos^2\phi\cos YI$$

$$\dot{\psi} = \frac{T\sin\delta_Y}{mV\cos\gamma} + \frac{V\cos\gamma}{r\cos\phi}\sin\psi\sin\phi$$

$$-\ 2\,\omega_e\left[\frac{\sin\phi - \sin\gamma\cos\psi\cos\phi}{\cos y}\right] + \frac{\omega_e^2\,r}{V}\left[\frac{\cos\phi\sin\phi\sin\psi}{\cos\gamma}\right]$$

$$\delta_Y = KY\,Y_I + K_{\dot{Y}}\ Y_I$$

$$m = -\beta_2$$

$$T = C_2\beta_2$$

The following constants were used:

$C_1$ = 8417 ft/sec

$\beta_1$ = 216 slugs/sec

$C_2$ = 14490 ft/sec

$\beta_2$ = 21.95 slugs/sec

$m_o$ = 47124 slugs

$m_2$ = 9107.8 slugs

S = 5083 ft

$\rho_o$ = 0.002388 slugs/ft3

$\lambda$ = 23,600 ft

$g_o$ = 32.17 ft/sec

$r_o$ = 20.926 x 106 ft

$K_Y$ = 0.001 deg/ft

$K_{\dot{Y}}$ = 0.1 deg/fps

$\omega_e$ = 0.7291 x $10^{-4}$ rad/sec

K = 1.0 rad-’

The aerodynamic coefficients $C_L$ and $C_{D_O}$ are functions of the Mach number M and are given in Figure A5. Speed of sound and atmospheric density are presented in Figure A6.

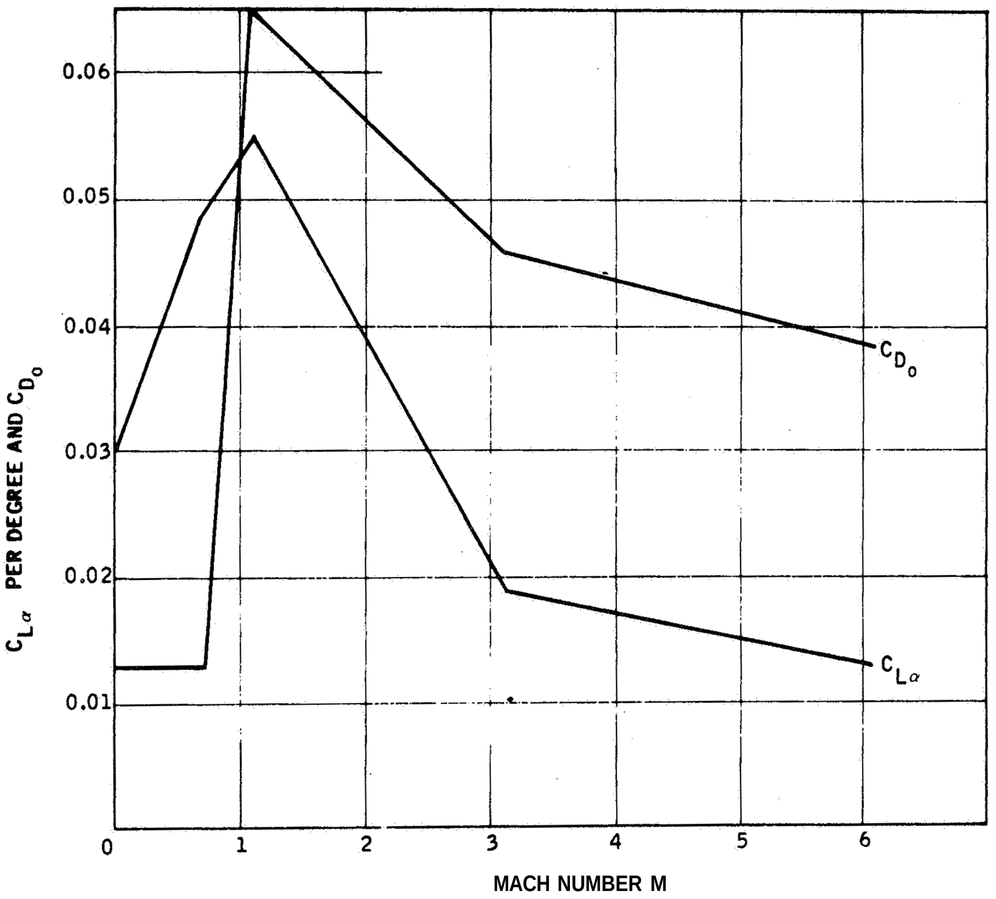

Figure A5. Aerodynamic Coefficients

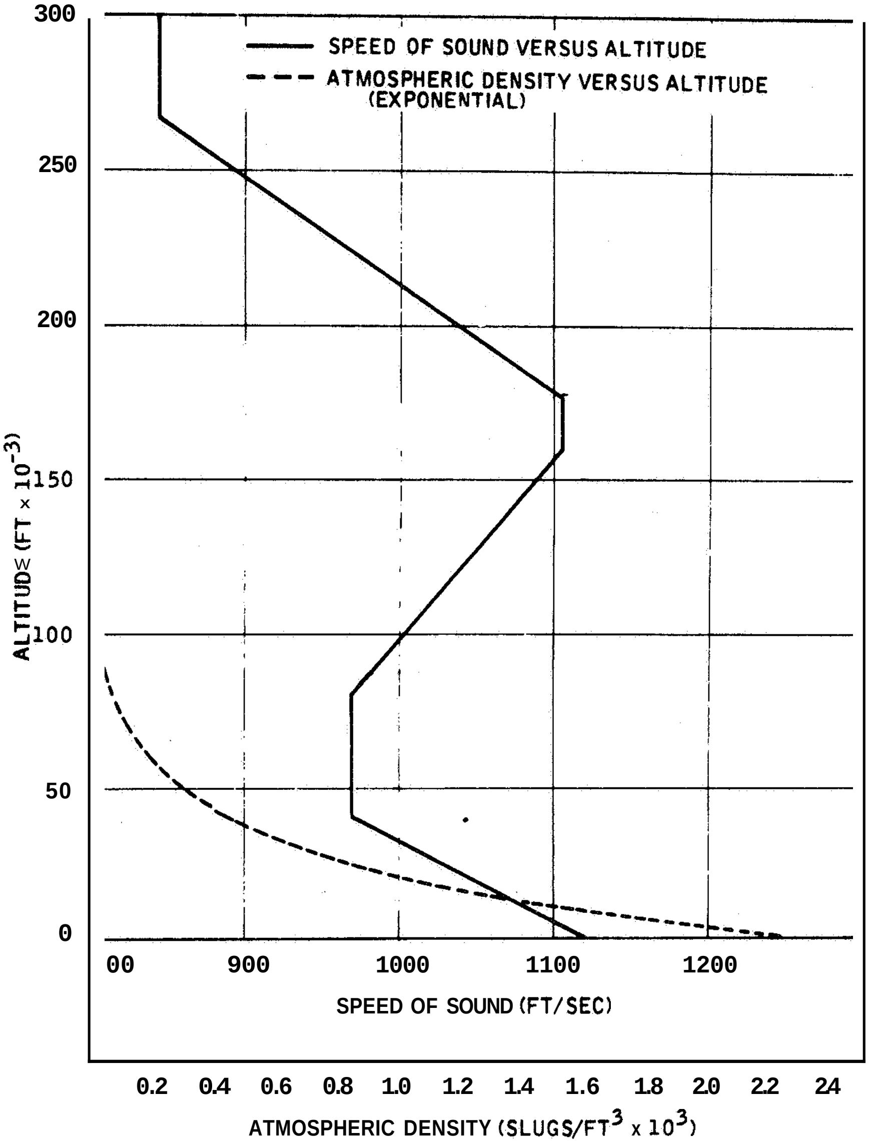

Figure A6. Speed of Sound and Atmospheric Density versus Altitude

# APPENDIX B
# TAP-LIGHT BOX DESCRIPTION

# APPENDIX B
# TAP-LIGHT BOX DESCRIPTION

A tap-light **box** is used to measure operator work load on some primary task such as guidance and control of a space vehicle. The device consists of a panel of 16 tap lights (see Figure **3-7)**. One of these lights is always lighted. The operator depresses the lighted button (microswitch) and releases. This action activates a stepper switch which turns a new light on. Figure B1 shows the circuit **for** this device. Lights were connected to the **26** positions of the stepper switch so that the sequence of lights repeated every **26** switchings.

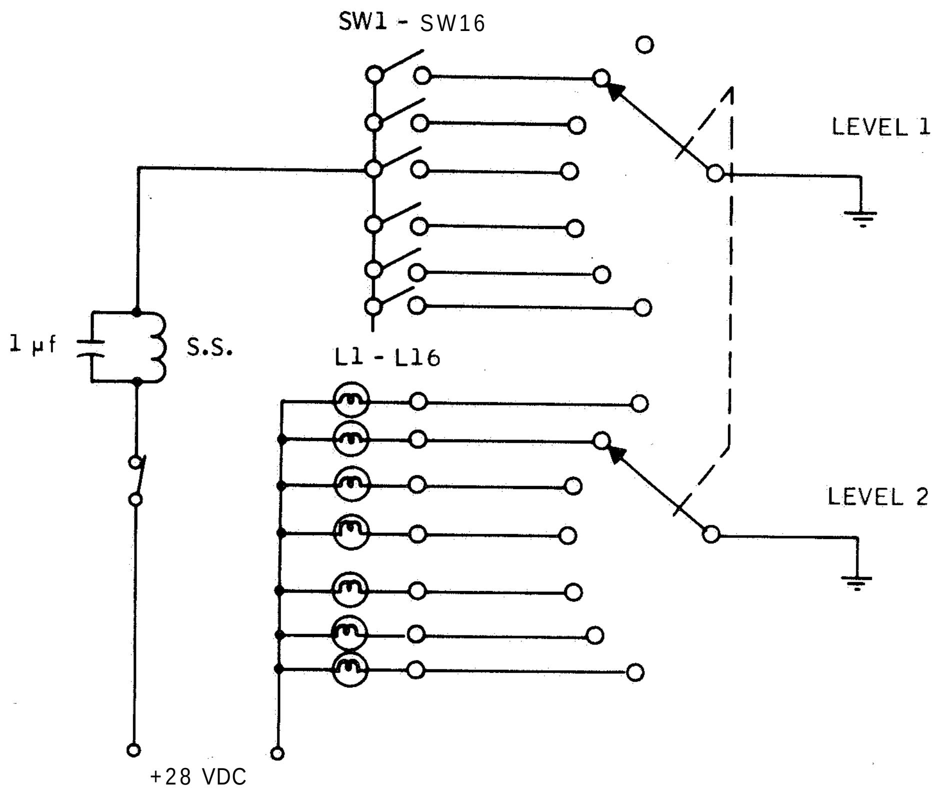
SW1 - SW16
LEVEL 1
1 μf
S.S.
L1 - L16
LEVEL 2
+28 VDC

| | |
|---|---|
| SS | STEPPER SWITCH, 26 POSITION 2 LEVEL |
| L1 - L16 | PUSH BUTTON LIGHTS |
| SW1 - SW16 | MICROSWITCH 52PB5 4T2 |

**Figure** B1. Work–Load Box Circuit

# APPENDIX C
# BIT BOX DESCRIPTION

# APPENDIX C
# BIT BOX DESCRIPTION

A "bit box" is used *to* measure operator work load on some primary task such as guidance or control of a space vehicle. Figure C1 is a block diagram showing the input-output relations of the bit box, the position of the subject, and the operator in the loop. The output from the box is a two-digit presentation of 64 different combinations of numerals 0 through 9 (excluding 7) displayed by two Nixie tubes. The subject calls out the displayed number, this vocal output activates the bit box, and a new number is displayed. With 64 numbers, each equally likely, the bit box has an information content of **6** bits. The operator has a separate display of the numbers, and his function is to monitor the subject's response.

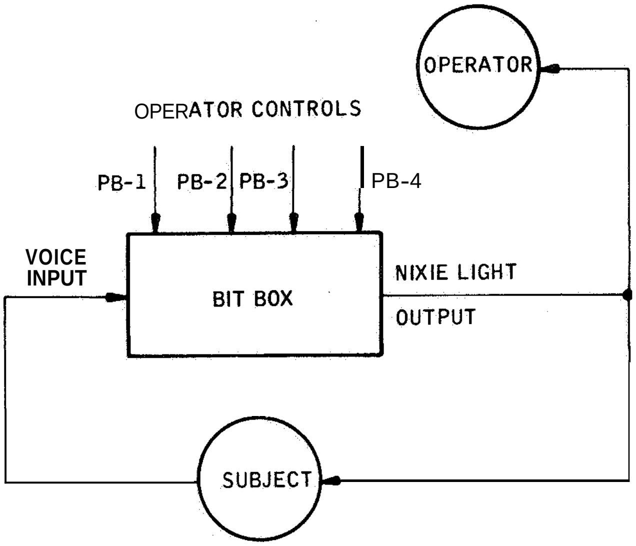
OPERATOR
OPERATOR CONTROLS
PB-1
PB-2
PB-3
PB-4
VOICE INPUT
BIT BOX
NIXIE LIGHT
OUTPUT
SUBJECT

Figure C1. Bit Box Block Diagram

The circuit diagrams for the bit box are shown in Figures C2, C3 and C4. A 26-position, 8-level stepper switch and two Nixie tubes are the main components of the box. If a separate displayis used for the operator and subject, four Nixie tubes are required. Figure C5 shows the wiring of the stepper switch. Note that the right-hand Nixie tube is controlled by levels 3, 4, and 5 of the stepper switch, and the left-hand Nixie tube is controlled by levels 6, 7, and 8 of the stepper switch. Each level has 26 positions, and the 26th position of level 1 is used *to* generate a pulse to activate a ring counter (see Figure **C3)** which transfers the stepper switch *to* a new level, The following are examples of the stepper switch wiring: levels 3 and 6 at position 1 represent digits 1, 9; levels 7 and 4 at position 18 represent digits 8, 8 and levels 8 and 5 at position 9 represent digits 2, 6.

Figure C2 shows the voice-activated delay circuit. A small time delay is required between the voice input and stepper switch output to prevent the subject from "answering" *too* quickly and in this way prevents the subject from upsetting the bit box. The 80-μf capacitor (top of Figure C2) controls the duration of this time delay, All relays are shown in the de-energized state.

In Figure C3 a number of operator and subject controls are shown. The function of these push buttons are as follows:

- Level Reset Push Button PB-1 -- Depressing PB-1 stops the sequence of 64 numbers and switches the stepper switch back to levels 6 and 3 while maintaining position.

- Homing Push Button PB-2 -- This controls only the stepper switch assembly. If held down, the stepper switch steps through all levels, stopping on levels 6 and 3 at position 1.

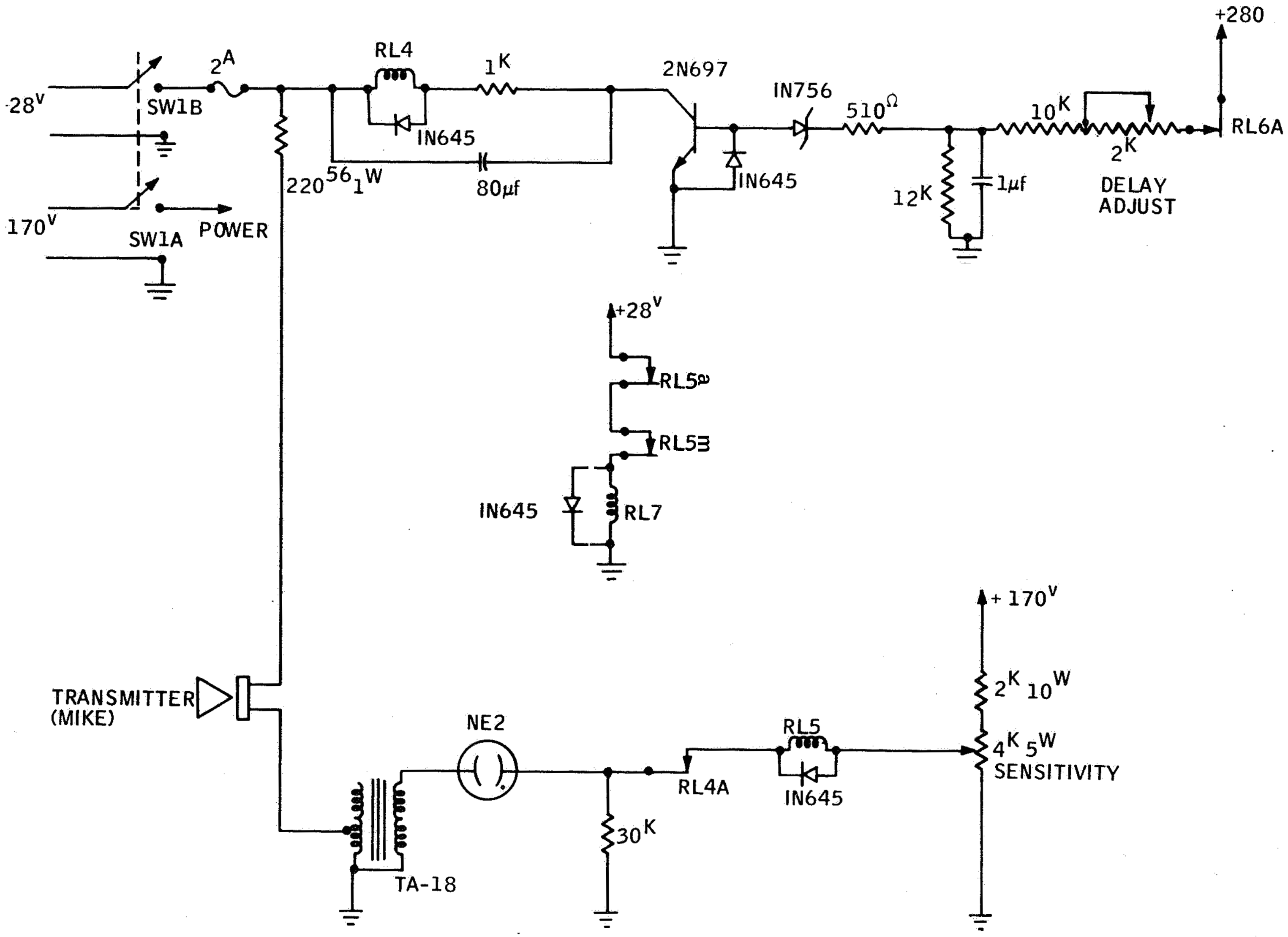
+280
-28V
SW1B
2A
RL4
IN645
1K
2N697
IN756
510Ω
10K
2K
RL6A
DELAY ADJUST
12K
1µf
IN645
220
56 1W
80µf
170V
SW1A
POWER
+28V
RL5a
RL5m
IN645
RL7
+170V
2K 10W
4K 5W
SENSITIVITY
TRANSMITTER (MIKE)
NE2
RL5
RL4A
IN645
30K
TA-18

Figure C2. Voice-Activated Delay Circuit

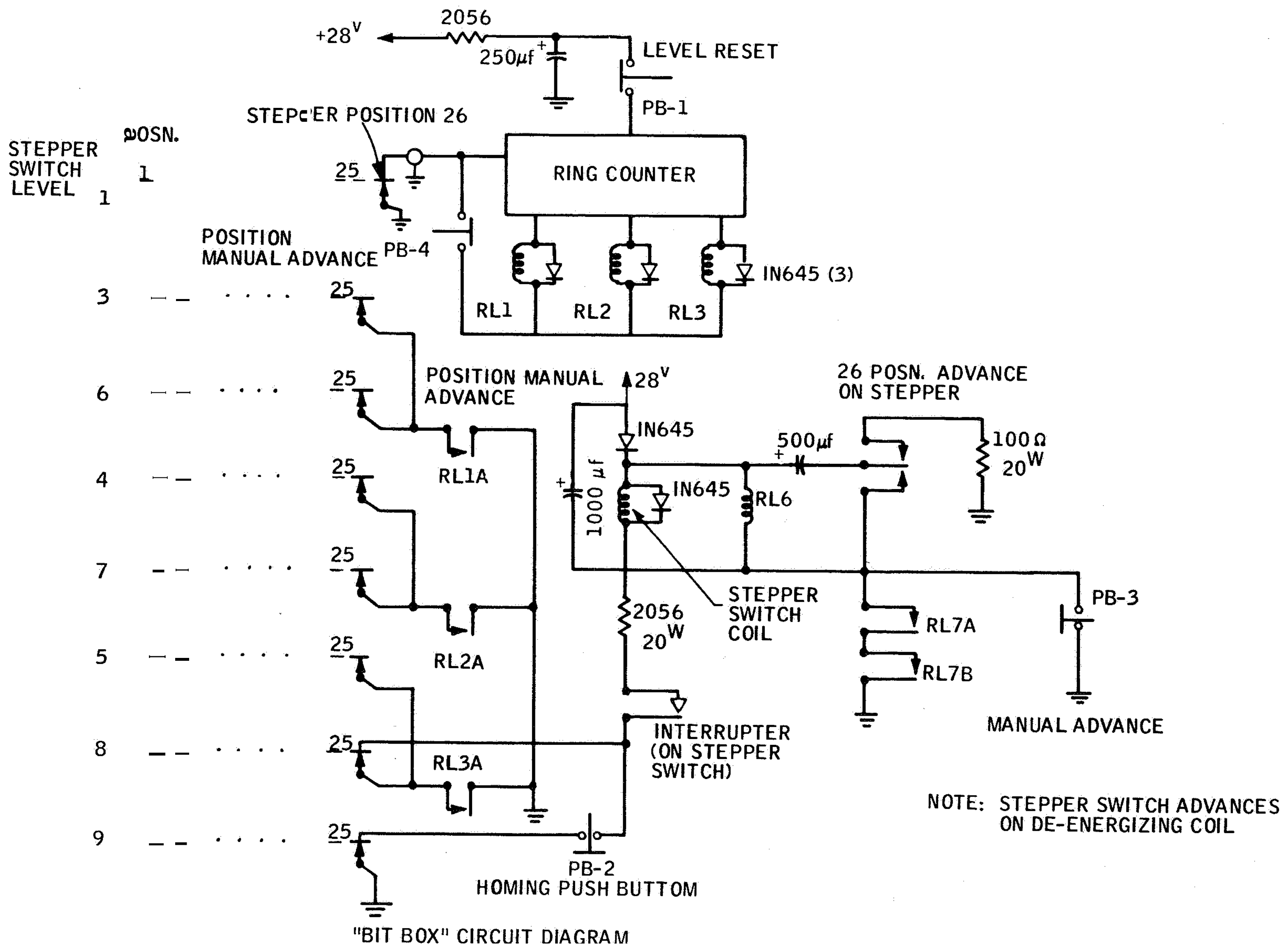
+28V
2056
250µf
LEVEL RESET
PB-1
STEPPER SWITCH LEVEL
POSN.
1
1
STEPPER POSITION 26
25
RING COUNTER
POSITION MANUAL ADVANCE
PB-4
IN645 (3)
RL1
RL2
RL3
3
6
4
7
5
8
9
25
POSITION MANUAL ADVANCE
28V
IN645
26 POSN. ADVANCE ON STEPPER
500µf
100Ω 20W
1000 µf
IN645
RL6
RL1A
RL2A
RL3A
2056 20W
STEPPER SWITCH COIL
RL7A
RL7B
PB-3
MANUAL ADVANCE
INTERRUPTER (ON STEPPER SWITCH)
PB-2
HOMING PUSH BUTTOM
NOTE: STEPPER SWITCH ADVANCES ON DE-ENERGIZING COIL
"BIT BOX" CIRCUIT DIAGRAM

Figure C3. Bit Box Circuit Diagram

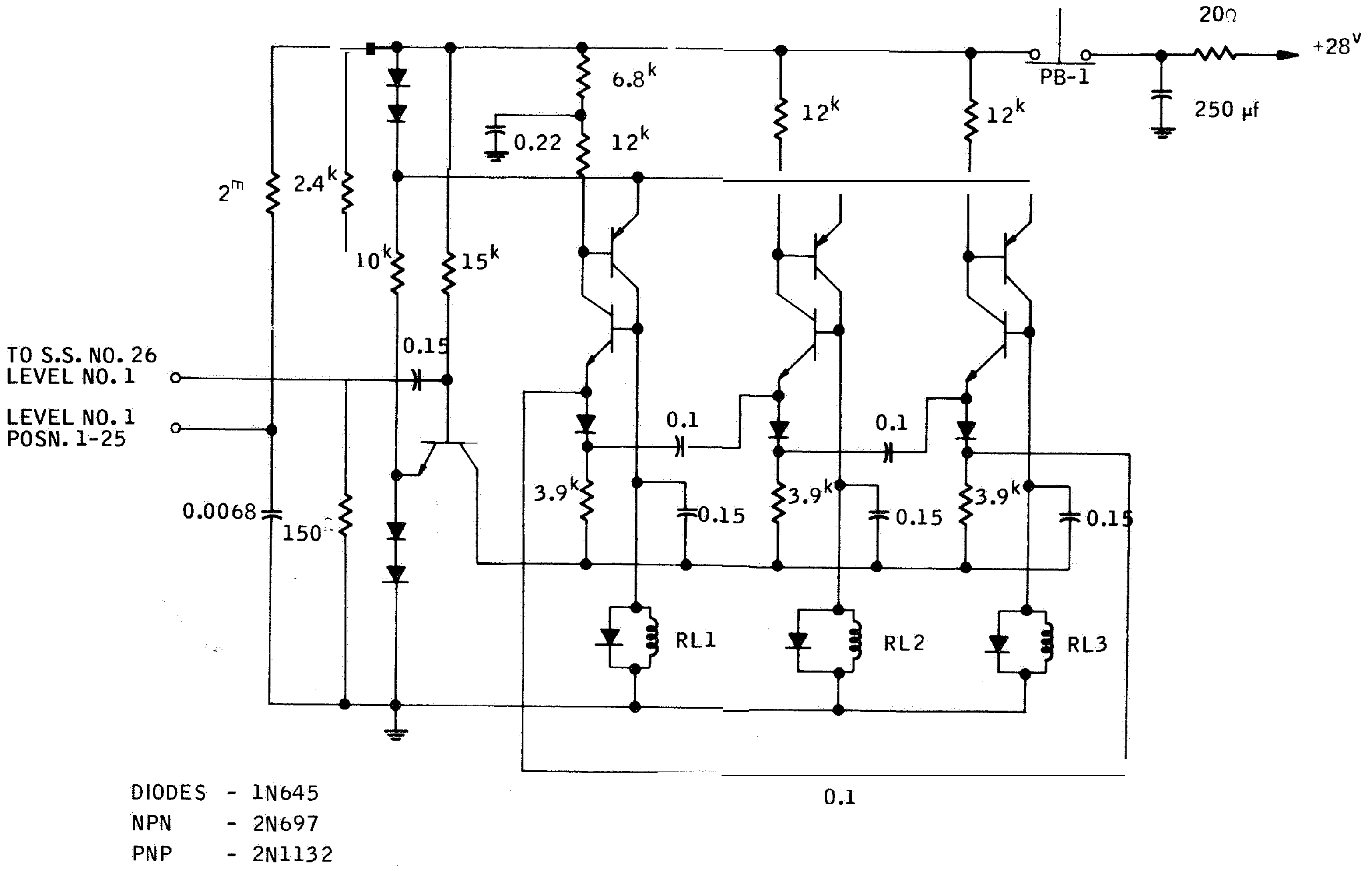
+28^v
20Ω
250 µf
PB-1
6.8^k
12^k
12^k
12^k
0.22
2^E
2.4^k
10^k
15^k
0.15
TO S.S. NO. 26
LEVEL NO. 1
LEVEL NO. 1
POSN. 1-25
0.1
0.1
3.9^k
3.9^k
3.9^k
0.15
0.15
0.15
0.0068
150
RL1
RL2
RL3
0.1
DIODES - 1N645
NPN - 2N697
PNP - 2N1132

Figure C4. Ring C cter

LEVEL 3, 4, 5, ARE FOR RIGHT LAMPS } FACING BOX
LEVEL 6, 7, ARE FOR LEFT LAMPS }

| | | | | | | | | | | | | | | | | | | | | | | | | | |
|---|---|---|---|---|---|---|---|---|---|---|---|---|---|---|---|---|---|---|---|---|---|---|---|---|---|
| POSITION | 1 | 2 | 3 | 4 | | 6 | | 8 | | 10 | | 12 | | 14 | | 16 | | 18 | | 20 | | 22 | | 24 | | 26 |
| NUMBER | 1 | | 3 | | 5 | | 7 | | [illegible] | | 11 | | 13 | | 15 | | 17 | | 19 | | 21 | | 23 | | 25 | |
| LEVEL 6 | 1 | 3 | 5 | 4 | 1 | 2 | 2 | 5 | [illegible] | 1 | 3 | 3 | 4 | 6 | 5 | 9 | 6 | 4 | 2 | 1 | 3 | 5 | 6 | 9 | 8 | |
| LEVEL 3 | 9 | 8 | 5 | 8 | 1 | 1 | 9 | 6 | [illegible] | 2 | 1 | 9 | 9 | 8 | 8 | 4 | 9 | 1 | 2 | 3 | 2 | 1 | 4 | 3 | 1 | |
| POSITION | 1 | 2 | | 4 | | 6 | | 8 | | 10 | | 12 | | 14 | | 16 | | 18 | | 20 | | 22 | | 24 | 25 | |
| NUMBER | 26 | 27 | | 29 | 30 | | 32 | | 34 | | 36 | | 38 | | 40 | | 42 | | 44 | | 46 | | 48 | 49 | 50 | |
| LEVEL 7 | 5 | 3 | 9 | 2 | 1 | 4 | 8 | 5 | | 6 | 8 | 4 | 9 | 2 | 1 | 3 | 6 | 8 | 8 | 5 | 8 | 4 | 9 | 2 | 1 | |
| LEVEL 4 | 9 | 3 | 8 | 3 | 4 | 2 | 9 | 2 | - | 5 | 4 | 3 | 2 | 4 | 5 | 4 | 1 | 8 | 2 | 3 | 6 | 4 | 6 | 5 | 6 | |
| POSITION | 1 | 2 | | 4 | | 6 | | 8 | | 10 | | 12 | | 14 | | 16 | | 18 | | 20 | | 22 | | 24 | | 26 |
| NUMBER | 51 | | 53 | | 55 | | 57 | | 59 | | 61 | | 63 | 64 | ——— HOME ———→ | | | | | | | | | | | |
| LEVEL 8 | 3 | 9 | 5 | 6 | 8 | 6 | 4 | 8 | 2 | 1 | 4 | 3 | 2 | 9 | | | | | | | | | | | | |
| LEVEL 5 | 5 | 5 | 4 | 6 | 3 | 2 | 5 | 5 | 6 | 8 | 6 | 6 | 8 | 9 | | | | | | | | | | | | |

Figure C5. Nixie Light Presentation Sequence

- Manual Advance Push Button PB-3 -- This push button controls the advance of the stepper switch. Pressing down and releasing effects a one position advance on the stepper switch,

- Position Manual Advance Button PB-4 -- This switch controls the stepper switch level (through the ring counter) while maintaining the stepper switch position, For example, if the stepper switch is on levels 6 and 3 at position 14, then pressing PB-4 advances the stepper switch to levels 7 and 4 at position 14 (see Figure C5).

Figure C4 is a circuit diagram of the ring counter, which switches levels on the stepper switch on receiving a pulse from position 26 of level 1. If the stepper. switch is on levels 8 and 5 at position 14 (i,e,, after a total of 64 numbers), the switch homes to position 1 on 6, 3.